2016

The Influence of Cholesterol-Related Membrane Fluidity on the Shear Stress Control of Neutrophil Adhesion and Its Implications in Hypercholesterolemia

Michael L. Akenhead
University of Kentucky, mak227@g.uky.edu
Digital Object Identifier: http://dx.doi.org/10.13023/ETD.2016.287

www.manaraa.com

STUDENT AGREEMENT:

I represent that my thesis or dissertation and abstract are my original work. Proper attribution has been given to all outside sources. I understand that I am solely responsible for obtaining any needed copyright permissions. I have obtained needed written permission statement(s) from the owner(s) of each third-party copyrighted matter to be included in my work, allowing electronic distribution (if such use is not permitted by the fair use doctrine) which will be submitted to UKnowledge as Additional File.

I hereby grant to The University of Kentucky and its agents the irrevocable, non-exclusive, and royalty-free license to archive and make accessible my work in whole or in part in all forms of media, now or hereafter known. I agree that the document mentioned above may be made available immediately for worldwide access unless an embargo applies.

I retain all other ownership rights to the copyright of my work. I also retain the right to use in future works (such as articles or books) all or part of my work. I understand that I am free to register the copyright to my work.

REVIEW, APPROVAL AND ACCEPTANCE

The document mentioned above has been reviewed and accepted by the student's advisor, on behalf of the advisory committee, and by the Director of Graduate Studies (DGS), on behalf of the program; we verify that this is the final, approved version of the student's thesis including all changes required by the advisory committee. The undersigned agree to abide by the statements above.

<div align="right">

Michael L. Akenhead, Student

Dr. Hainsworth Y. Shin, Major Professor

Dr. Abhijit R. Patwardhan, Director of Graduate Studies

</div>

THE INFLUENCE OF CHOLESTEROL-RELATED MEMBRANE FLUIDITY ON
THE SHEAR STRESS CONTROL OF NEUTROPHIL ADHESION AND ITS
IMPLICATIONS IN HYPERCHOLESTEROLEMIA

DISSERTATION

A dissertation submitted in partial fulfillment of the requirements for the degree of
Doctor of Philosophy in the College of Engineering at the University of Kentucky

By

Michael L. Akenhead

Lexington, Kentucky

Co-Directors: Dr. Hainsworth Shin, Assistant professor of Biomedical Engineering
and   Dr. Abhijit Patwardhan, Professor of Biomedical Engineering

Lexington, Kentucky

ABSTRACT OF DISSERTATION

THE INFLUENCE OF CHOLESTEROL-RELATED MEMBRANE FLUIDITY ON THE SHEAR STRESS CONTROL OF NEUTROPHIL ADHESION AND ITS IMPLICATIONS IN HYPERCHOLESTEROLEMIA

Hypercholesterolemia is a significant risk factor in the development of cardiovascular disease and is associated with chronic leukocyte adhesion in the microvasculature. While the underlying mechanisms behind this have yet to be determined, it may be possible that hypercholesterolemia impairs the fluid shear stress (FSS) inactivation of neutrophils through the rigidifying effect of cholesterol on membrane fluidity. FSS restricts surface expression of CD18 integrins through cathepsin B (ctsB) proteolysis, which minimizes neutrophil adhesivity. If hypercholesterolemia blocks FSS mechanotransduction, then the inhibition of CD18 cleavage may link pathologic blood cholesterol elevations with dysregulated neutrophil adhesion. We hypothesized that elevated cholesterol contributes to dysregulated neutrophil adhesion by impairing ctsB FSS-induced CD18 cleavage through membrane fluidity changes.

In the first part of this study, we demonstrated that FSS-induced CD18 cleavage is a robust response of neutrophils and involves selective cleavage of macrophage 1-antigen (Mac1) through ctsB proteolysis. The second part of this study confirmed that ctsB regulates neutrophil adhesion through its proteolytic actions on Mac1, an important integrin involved in adhesion and chemotaxis. Specifically, ctsB accelerated neutrophil motility through an effect on Mac1 integrins during pseudopod retraction. Furthermore, by using a flow-based assay to quantify the mechanoregulation of neutrophil adhesivity, we demonstrated that FSS-induced ctsB release promoted neutrophil detachment from platelet-coated substrates and unstimulated endothelium. For the third part of this study, we linked cholesterol-related membrane fluidity changes with the ability of FSS to restrict neutrophil adhesion through Mac1. We also determined that pathologic cholesterol elevations associated with hypercholesterolemia could block FSS-induced Mac1 cleavage and were linked to disrupted tissue blood flow. This was accomplished using low-density lipoprotein receptor deficient (LDLR$^{-/-}$) mice fed a high-fat diet.

Ultimately, the results provided in the present study confirmed that cholesterol-related changes in membrane fluidity blocked the ability of ctsB to regulate neutrophil adhesion through FSS-induced Mac1 cleavage. This implicates an impaired neutrophil FSS mechanotransduction response in the dysregulation of neutrophil adhesion associated with

hypercholesterolemia. Since dysregulated adhesion may be one of the earliest upstream features of cardiovascular disease associated with hypercholesterolemia, the present study provides a foundation for identifying a new mechanobiological factor in the pathobiology of microcirculatory dysfunction.

Keywords: Mechanotransduction, Fluid Shear Stress,
Integrin, Hypercholesterolemia, Inflammation

Michael L. Akenhead
Student's Signature

July 13, 2016
Date

THE INFLUENCE OF CHOLESTEROL-RELATED MEMBRANE FLUIDITY ON
THE SHEAR STRESS CONTROL OF NEUTROPHIL ADHESION AND ITS
IMPLICATIONS IN HYPERCHOLESTEROLEMIA

By

Michael Akenhead

Hainsworth Y. Shin
_____
Co-Director of Dissertation

Abhijit R. Patwardhan
_____
Co-Director of Dissertation

Abhijit R. Patwardhan
_____
Director of Graduate Studies

July 13, 2016
_____
Date

DEDICATION

I dedicate this dissertation to my parents, Linda and Robert Akenhead, and my brother, Matthew Akenhead, for all the encouragement they provided me over the years. Your unwavering support inspired me to do my best, through thick and thin.

ACKNOWLEDGEMENTS

TABLE OF CONTENTS

LIST OF TABLES

LIST OF FIGURES

CHAPTER 1: INTRODUCTION

Cardiovascular disease is one of the leading causes of death for adults, with over 1.5 million cases each year in the United States [1]. By studying the upstream risk factors, it may be possible to reduce the lethality of cardiovascular disease and prevent death. Hypertension and hypercholesterolemia represent two diseases associated with cardiovascular disease [2,3]. Patients with these conditions are likely to exhibit chronic inflammation in the blood and microvascular dysfunction, two risk factors linked to the development of lethal cardiovascular disease [4-6]. Historically, increased numbers of activated leukocytes in the blood and microcirculation are associated with cardiovascular disease [7-10], suggesting that dysregulated leukocyte activity may contribute toward cardiovascular pathogenesis.

Neutrophils, the most numerous leukocyte subtype in the blood under physiological conditions, are among the first responders of the acute inflammatory response [11]. These cells are highly sensitive to stimuli, and can rapidly activate in the presence of as little as 10 – 100 bacterial peptides [12]. Due to this high sensitivity and their vast destructive potential, it is possible that the neutrophils are highly susceptible to pathogenic factors and, thus, serve as one of the earliest contributors to the onset of chronic inflammation. This possibility is conceivable since tight regulation of neutrophil activity is essential to maintain the body in a non-inflamed state. Failure to do so may result in sustained neutrophil activation which contributes to lethal tissue injury [13] via an autodigestive process, where dysregulated release of cytokines (which activate more inflammatory cells) and biodegradative agents (e.g., reactive oxygen species, proteases, etc.) cause damage to healthy vasculature [14]. Alternatively, sustained neutrophil activation in the blood may

1

damage tissues indirectly by impacting blood rheology and impairing tissue perfusion [15]. Finally, progression of a chronic inflammatory state in the circulation could initiate from a combination of both processes [16].

Although neutrophil inactivity is predicated on the absence of inflammatory stimuli, several cellular and molecular mechanisms are in place to ensure that these cells remain inactivated under physiologic conditions [17,18]. Recent evidence established fluid shear stress (FSS) mechanotransduction as one potential regulatory mechanism [19]. Whether neutrophils are adherent or freely-floating, their activity is minimized by exposure to FSS typical of the physiologic bloodstream, ensuring their circulation as rounded, inactivated cells [20-22]. FSS inactivates neutrophils by minimizing pseudopod activity and restricting their surface expression levels of CD18 integrins via a cleavage process involving the release of lysosomal cysteine protease, cathepsin B (ctsB) [23]. These FSS responses are thought to be important aspects of neutrophil regulation since their impairment has been implicated as a potential contributor to pathological elevations in peripheral vascular resistance [24,25].

To determine how neutrophil FSS mechanotransduction may become impaired and contribute to microvascular pathogenesis, recent studies from our lab focused on the cholesterol-related membrane fluidity of the cells [26,27]. This focus on cell membrane fluidity was predicated on the principle that changing cell membrane mechanical properties may alter the ability of FSSes to induce conformational (i.e., structural) activity in putative mechanosensors on the neutrophil surface. Considering that cholesterol is an important lipid regulator of the membrane fluidity of mammalian cells [28], changes in membrane cholesterol content may conceivably alter cell sensitivity to physical stimuli.

2

One scenario for which the cholesterol-related membrane properties may change and lead to dysregulation of the neutrophils is hypercholesterolemia. Pathological blood cholesterol elevations that occur during hypercholesterolemia are associated with chronic leukocyte activation in the blood and microcirculation as well as microvascular dysfunction [29]. By using pseudopod retraction to estimate FSS mechanosensitivity, cholesterol-related changes in membrane fluidity were demonstrated to impair neutrophil mechanotransduction and to be linked with the onset of microvascular dysfunction due to hypercholesterolemia [26,27]. However, it remained to be determined how the impaired neutrophil responsiveness to FSS, which was quantified by using pseudopod retraction as a surrogate marker, manifested into microvascular dysfunction. The present study focused on the possibility that an impaired ability of FSS to limit neutrophil CD18 surface expression may explain the connection between hypercholesterolemia, dysregulated neutrophil adhesion, and dysregulated microvascular function. For these purposes, the present study tested the hypothesis that *pathological blood cholesterol elevations dysregulate neutrophil adhesion by reducing membrane fluidity and impairing FSS-induced ctsB release which blocks CD18 cleavage.*

To address this hypothesis, the following specific aims were carried out:

1) Link ctsB release with reduced expression of neutrophil adhesion molecules.

2) Show that ctsB activity minimizes neutrophil adhesion under shear exposure.

3) Verify that neutrophil adhesion and detachment under flow is affected by cholesterol-related changes in membrane fluidity.

4) Demonstrate that extracellular cholesterol elevations, similar to that of hypercholesterolemia *in vivo,* block FSS regulation of neutrophil adhesion.

3

CHAPTER 2: BACKGROUND

2.1 The Potential Impact of Neutrophil Activation on Blood Flow

As the most numerous leukocytes in the body, the neutrophils are second only to the red blood cells (RBCs) in their impact on microvascular flow. Under physiologic conditions, inactivated neutrophils patrol the circulation as spherical, non-adhesive cells. This state enables their passive deformation through the microcirculation, ensuring that they have a minimal impact on blood flow while inactivated [30]. Once activated, however, neutrophils are capable of influencing blood rheology through changes to their cellular geometry and adhesivity (Fig. 2.1).
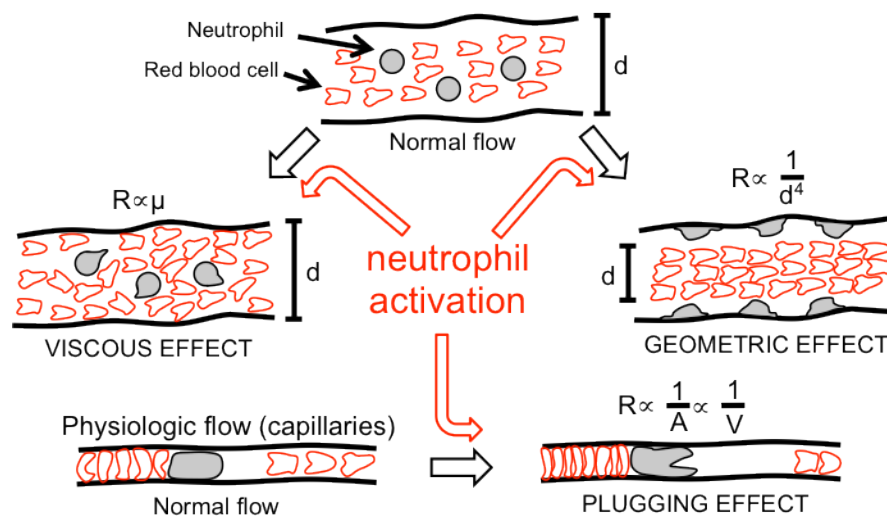
Figure 2.1. The effects of neutrophil activation on microvascular blood flow.
Blood flow through non-capillary vessels can be impaired by neutrophil activation. Activated neutrophils may project pseudopods which elevate the viscosity of blood. Alternatively, activated neutrophils may adhere to the endothelium and reduce the apparent diameter of the vessel. In both cases, resistance to flow is elevated due to the changes in viscosity or diameter. In the case of the capillaries, activated neutrophils have been demonstrated to plug capillaries. This restricts blood flow and elevates the resistance to flow.

Neutrophils activate in response to stimulation with inflammatory agonists, such as formyl-methionyl-leucyl-phenylalanine (fMLP) or platelet-activating factor (PAF) [15]. The most visible change that accompanies neutrophil activation is the extension of pseudopods, causing the cell to adopt an irregular geometry [13]. In addition to projecting pseudopods, neutrophils also upregulate their expression of CD18 cell-cell adhesion molecules when stimulated with inflammatory agonists [31]. In these ways, neutrophil activation may potentially impact blood rheology and flow within the microcirculation as described in the following sections.

2.1.1 The rheological effects of activated neutrophils on microvascular flow

Activated neutrophils in the blood are capable of physically influencing microvascular flow and thus affecting peripheral resistance. This influence may be roughly inferred from the Hagen-Poiseuille approximation in the following forms:

$$\Omega \propto \mu/A_c \text{ (microvessel network)}$$

or

$$\Omega \propto \mu/D^4 \text{ (single vessels)}$$

where Ω is microvessel resistance, μ is cell suspension viscosity, A_c is total cross-sectional area to flow, and D is vessel diameter. This relationship exemplifies how changes in either the blood apparent viscosity or the microvasculature geometry may affect flow resistance.

In microvascular networks, inactivated neutrophils with diameters of 12–15 μm are capable of deforming and squeezing through capillaries with diameters of 5–10 μm [32,33]. However, activated neutrophils express F-actin enriched pseudopods and are far less deformable, which may lead to capillary plugging (Fig. 2.1, Plugging Effect) [34]. A

5

significant degree of capillary plugging in microvascular networks, which would manifest as a reduction in the total cross-sectional area to flow of capillary beds, would lead to increased peripheral resistance. Because the capillaries make up the greatest total cross sectional area in the body [35], a significant degree of capillary plugging can have a great effect on flow resistance.

Activated neutrophils may also have an effect on microvascular flow within the non-capillary microcirculation. Presumably, the presence of pseudopod projections on neutrophils causes them to adopt irregular, non-spherical shapes that increase their tumbling behavior in the linear velocity gradient of the blood flow field within vessels. This enhanced tumbling may increase the number of collisions they experience with other cell types, including the numerous RBCs in the surrounding environment [36,37]. As RBCs are displaced laterally toward the low viscosity cell-free plasma layer located near the vessel wall [38], the apparent viscosity of the blood is elevated (Fig. 2.1, Viscous Effect). According to the Hagen-Poiseuille approximation, this means flow resistance is increased in response to activated neutrophils, due to pseudopod-induced elevations in the apparent viscosity of blood in the non-capillary microvasculature (10 – 300 μm in diameter [39]) which make up a large percentage of microvessels in the microcirculation. This potential influence of cell activation and viscosity on flow resistance was supported by *in vivo* evidence, where interactions between activated leukocytes and RBCs in blood-like cell suspensions elevated both apparent viscosity and flow resistance [40].

It may also be possible for activated neutrophils to alter microvascular resistance by adhering to the non-capillary microvasculature, particularly the venules. Upregulation of CD18 integrins on activated neutrophils causes these cells to become much more

6

adhesive than their inactivated counterparts. Consequently, the apparent diameter of a microvessel may decrease if significant numbers of rolling and migrating neutrophils are present on the microvascular walls (Fig. 2.1, Geometric Effect). According to the Hagen-Poiseuille approximation, it may be possible that a reduction in apparent diameter would elevate microvascular resistance, due to the inverse 4th power relationship between resistance and diameter. In support of this, studies have shown that inflammatory stimulation can promote leukocyte adhesion and migration in the capillaries and non-capillary microvessels, with an enhancing effect on microvascular resistance [41].

2.1.2 The effects of activated neutrophils on endothelial cell functions

It is important to note that the previously described mechanisms have focused on the rheological effects of neutrophil activation alone. However, neutrophils may also affect microvascular flow by biologically modifying the activity of other cells. For example, their binding may influence the activity of endothelial cells responsible for regulating blood flow through the release of signaling molecules (i.e., nitric oxide, prostacyclin, thromboxane, endothelin) [42]. Endothelial signaling in response to changes in the intravascular environment can lead to the dilation or constriction of vascular smooth muscle, altering the microvascular resistance to blood flow [42,43]. Alternatively, signaling molecules can change the permeability of the endothelium, leading to a net transfer in fluid from the venules to the interstitial tissues which may alter interstitial pressures and physically interfere with the function of neighboring arterioles [44,45].

It is difficult for circulating neutrophils to affect endothelial cell activity, due to the extracellular fluid containing antioxidants and protease inhibitors which limit leukocyte

7

cytotoxicity under physiologic conditions [46]. However, the recruitment/adhesion of neutrophils to endothelial cells creates a sequestered "microenvironment" which enables neutrophil oxidants and proteases to overwhelm these restrictive factors [47,48]. This enables adhesive neutrophils to exert their full cytotoxic effects, which are capable of altering the activity of endothelial cells [14,49]. Importantly, the secretion of endothelial products and the permeability of endothelial cells may be altered by adhesive neutrophils [50,51]. This suggests that sustained neutrophil adhesion to the microvascular wall may lead to dysregulated endothelial cell activity in the microvasculature (Fig. 2.2). The impaired secretion of endothelial productions responsible for vasomotor control, for example, would affect microvascular flow resistance [52], leading to disrupted tissue blood flow and microvascular dysfunction. Additionally, increased endothelial permeability may have paracrine or systemic effects, where the surrounding cells are affected by cytokine release [53,54]. These surrounding cells would then activate and secrete more cytokines, promoting a chronic inflammatory state that sustains dysregulated neutrophil and endothelial cell activity.

In summary, dysregulated neutrophil activity may disrupt tissue blood flow either directly through a physical effect or indirectly through actions on endothelial cells of the microvasculature. This possibility implicates the neutrophils as a critical feature of microvascular blood flow rheology. It also suggests that dysregulation of the neutrophils may contribute to microvascular dysfunction and downstream lethal pathologies due to factors that affect their responsiveness to FSS (e.g., hypercholesterolemia).
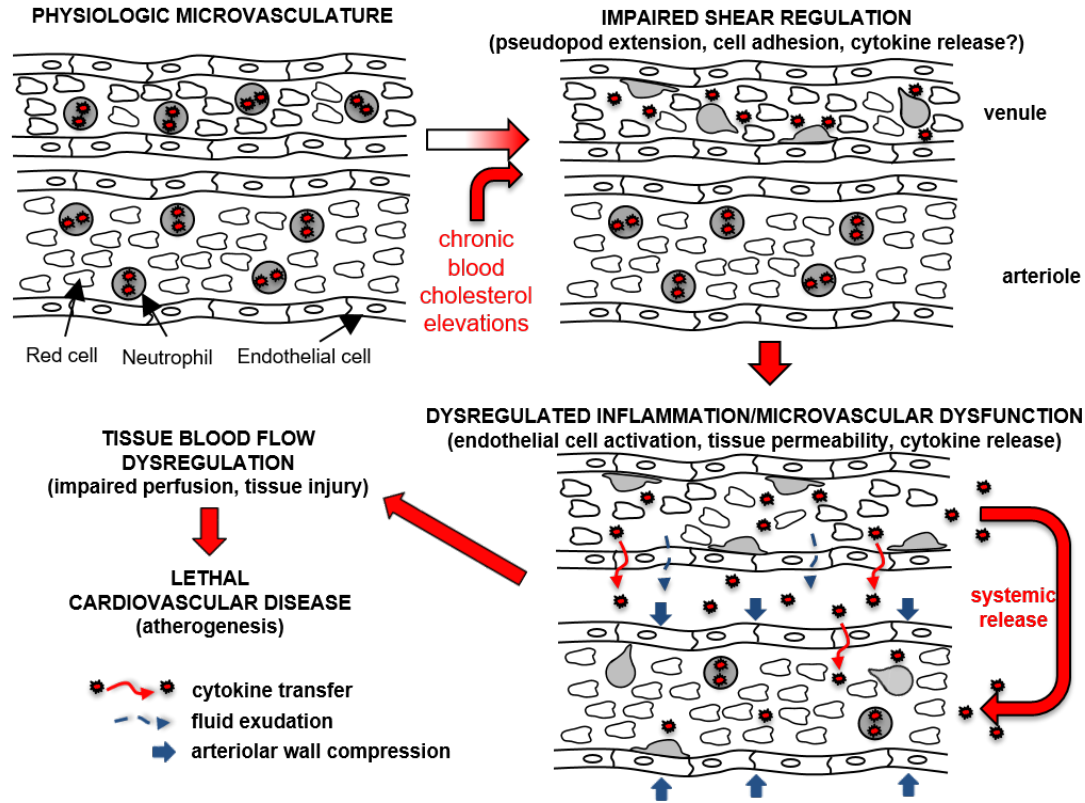
Figure 2.2. The proposed impact of neutrophil activation on hemodynamic resistance and blood flow regulation in microvessels.
Flow resistance may be altered by the effects of activated neutrophils on endothelial cells. This may manifest as either dysregulated cytokine release or increased tissue permeability, both of which contribute to microvascular dysfunction. Ultimately, sustained neutrophil and endothelial cell activation promote a chronic inflammatory state that can lead to lethal cardiovascular disease. The impact of the neutrophils here is focused on blood flow in the non-capillary vessels.

2.2 Control of Neutrophil Activity by Fluid Shear Stress Mechanotransduction

2.2.1 Fluid shear stress induces retraction of neutrophil pseudopod projections

A growing body of evidence points to the mechanotransduction of hemodynamic FSS (i.e., $1 - 10$ dyn/cm^2) [41] as a potential control mechanism in the blood for the purpose of restricting leukocyte activity under physiological conditions, when their recruitment is not needed [19,21,23]. FSS-induced pseudopod retraction represents one of the most overt evidence in support of the ability of fluid flow mechanotransduction to promote neutrophil deactivation. Within $1 - 2$ minutes of being exposed to FSS ($1 - 2$ dyn/cm^2) using a

micropipette, neutrophils migrating on glass substrates retract F-actin enriched pseudopods and adopt a rounded morphology [21]. It appears as though FSS exposure interferes with the ability of neutrophils to project pseudopods, since the F-actin content of neutrophils will rapidly decrease in parallel with their pseudopod retraction response [55]. FSS has also been demonstrated to reduce the phagocytic behavior of neutrophils, which relies on the formation of pseudopods [56]. These observations support the ability of shear to mechanobiologically restrict or limit pseudopod activity.

2.2.2 Fluid shear stress induces cleavage of CD18 by cathepsin B release

FSS downregulates the expression of intact CD18 adhesion molecules that mediate firm adhesive interactions with substrates [23]. CD18 is the common β_2 polypeptide subunit for a family of heterodimeric integrins [57]. Of the four CD18 subtypes, the two most numerous on the neutrophil surface are lymphocyte function-associated antigen 1 (LFA1; CD11a/CD18) and macrophage-1 antigen (Mac1; CD11b/CD18). LFA1 is typically associated with loose capture interactions which promote neutrophil arrest during inflammatory recruitment, and Mac1 supports the firm adherence of neutrophils to venular walls, either directly on endothelium or via platelet bridges [58].

Reportedly, FSS-induced downregulation of CD18 expression involves proteolytic cleavage of excess amounts of these integrins off the neutrophil surface. During *in vitro* studies after harvest from fresh blood, reintroducing neutrophils to venular-level shear stress ($1.5 - 5$ dyn/cm^2) for as short as 5 minutes cleaves approximately $20 - 30\%$ of cell surface-associated CD18 integrins. This shedding process involves the FSS-induced release of lysosomal cysteine protease ctsB at the cell surface [23]. Previous studies

10

identified the role of ctsB through the use of broad-spectrum protease inhibitors. Blocking the activity of several different protease families, such as serine or aspartyl proteases, did not prevent the FSS-induced cleavage of CD18 integrins. However, blocking the activity of cysteine proteases inhibited FSS-induced CD18 cleavage [23]. This inhibition was also observed when ctsB activity was selectively blocked; however, selectively blocking other cysteine proteases had no effect on FSS-induced CD18 cleavage.

Recently, our lab demonstrated that CD18 cleavage by neutrophils exposed to FSS is specific for Mac1 and occurs in parallel with their reduced binding to platelets and fibrinogen [59]. This suggested that Mac1 cleavage serves to reduce or prevent neutrophil adhesion under flow. However, the underlying mechanism, including the protease responsible for cleaving the CD11b subunits of Mac1, remained to be elucidated. Furthermore, because Mac1 plays a role in firm adhesion, it remained to be demonstrated whether ctsB-induced Mac1 cleavage restricted neutrophil binding to unstimulated endothelium under flow.

2.2.3 Agonist stimulation overrides fluid shear stress mechanotransduction

Inactivation of neutrophils by FSS mechanotransduction occurs even in the presence of low amounts of inflammatory agonists. Mild stimulation of neutrophils with < 1 µM fMLP or < 10 µM PAF does not compromise their ability to retract pseudopods when exposed to FSS [19-21,27,60]. In contrast, stimulation of neutrophils with these same agonists above their critical thresholds abolishes FSS-induced pseudopod retraction [20]. Intuitively, this dose-dependent relationship between agonist stimulation and impairment of neutrophil deactivation under FSS makes sense. It is consistent with the likelihood that

11

inflammatory agonists are capable of overriding the FSS-induced deactivation of neutrophils, such as during acute inflammation when they are needed to respond to infection or tissue injury.

Interestingly, deactivation of neutrophils under FSS exposure is linked with their surface expression of G protein-coupled receptors (GPCRs) such as the formyl peptide receptor (i.e., fMLP receptor) [61]. The desensitization of FPR by fMLP ligand binding is typically associated with receptor internalization [62]. However FPR is reportedly internalized into perinuclear compartments under shear exposure [63]. It has been demonstrated that the shear-induced internalization of FPR causes neutrophils to resist activation in response to low concentrations of fMLP [64]. This is in line with the inactivation of neutrophils by FSS exposure in the presence of low quantities of inflammatory agonists. Furthermore, it is possible that stimulation with agonists, such as fMLP, above a threshold level, prevents FSS-induced GPCR internalization, and thus, the neutrophils activate in spite of the local flow environment.

Overall, FSS mechanotransduction serves to maintain neutrophils in an inactivated state. However, under some circumstances it is possible for neutrophils to become unresponsive to FSS exposure. In the event that the FSS mechanotransduction response becomes impaired, the dysregulation of neutrophil activity may have detrimental effects on microvascular physiology.

2.3 Consequences of Impaired Neutrophil Fluid Shear Stress Mechanotransduction

To date, there is an accumulation of evidence suggesting that, under physiologic conditions, FSS serves to minimize the activity of neutrophils in the bloodstream unless there is sufficient agonist stimulation to override this control mechanism. However, it is also possible that FSS mechanotransduction becomes compromised due to the onset of pathological conditions. Presumably, this impairment in the FSS mechanotransduction response results in dysregulated neutrophil activation that eventually drives a chronic inflammatory phenotype in the body.

Neutrophils promote an inflammatory phenotype by releasing cytokines and cell agonists that not only promote tissue injury, but also recruit other leukocytes [65,66]. As a result, the dysregulated activity (i.e., sustained activation) of neutrophils and other leukocytes can damage host tissue and promote the development of chronic inflammation, a common denominator for a wide variety of lethal pathologies (e.g., microvascular dysfunction, cardiovascular disease, diabetes, cancer, etc.) [67,68]. Since neutrophils are among the first leukocytes recruited during inflammation, their sustained activity due to impairment of regulatory mechanisms may be one of the earliest upstream factors driving the dysregulation of microvascular flow associated with chronic inflammation (Fig. 2.3). In line with this, past studies have linked an impaired FSS mechanotransduction response with dysregulated neutrophil activity and microvascular dysfunction.
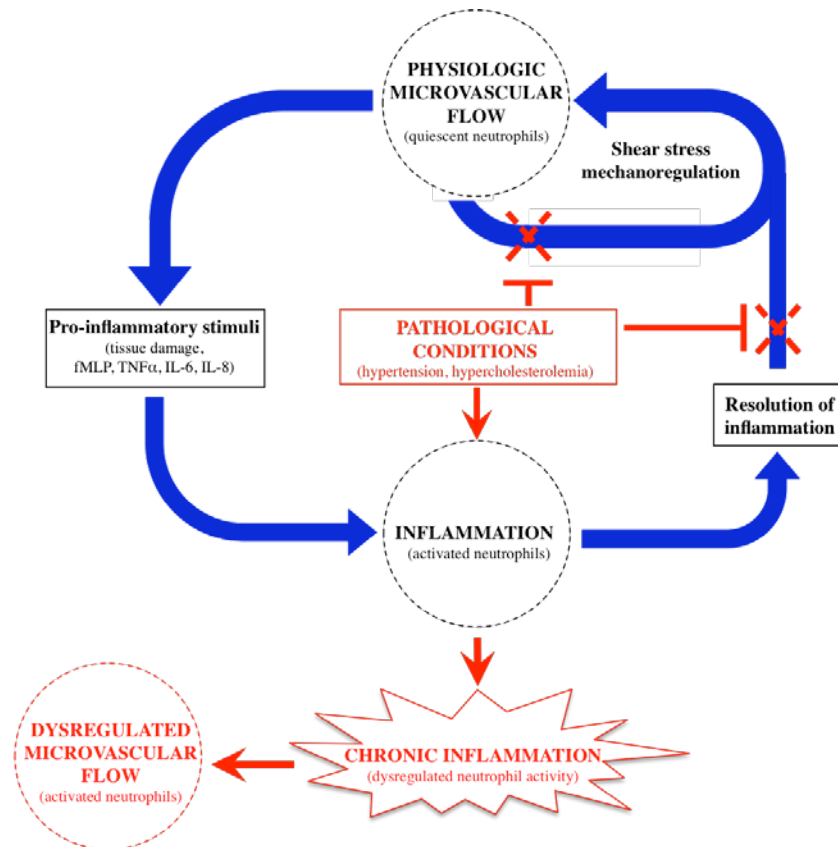
Figure 2.3. The potential impact of impaired neutrophil fluid shear stress mechanotransduction on microvascular rheology.
The regulation of neutrophil activity under physiologic conditions, represented by the blue arrows, ensures neutrophils remain quiescent under non-inflamed conditions. This is accomplished, in part, due to the inactivation of neutrophils by FSS mechanotransduction. Exposure to pro-inflammatory stimuli temporarily overrides the FSS mechanotransduction response and activates neutrophils, leading to inflammation. When inflammation is resolved and agonist levels subside, neutrophils become responsive to FSS mechanotransduction once more and are inactivated. Impairment of FSS mechanotransduction by pathologic conditions, represented by the red arrows, can lead to sustained neutrophil activation in the blood. This, combined with the elevated expression of pro-inflammatory cytokines, promotes a chronic inflammatory state. The accumulation of activated neutrophils during chronic inflammation is thought to contribute to microvascular dysfunction.

Evidence that impaired neutrophil mechanosensitivity contributes to microvascular dysfunction has been reported for rats exhibiting a chronically inflamed phenotype as a result of spontaneous hypertension [24,25,69]. Spontaneously hypertensive rats (SHRs) were found to have significantly elevated hemodynamic resistance due to the sustained

levels of chronically activated neutrophils [25]. The neutrophils from SHRs were found to be unresponsive to FSS exposure. Unlike wild type (WT) neutrophils which retracted pseudopods in the presence of shear, SHR neutrophils lacked a functioning pseudopod retraction response. The persistent presence of pseudopods on SHR neutrophils in the bloodstream were reported to contribute to the elevations in microvascular resistance associated with hypertension [70,71].

It should be noted that spherical leukocytes in the blood might increase apparent viscosity and elevate microvascular flow resistance due to their interactions with RBCs in the flow field [37,72]. This connection may be explained by the presence of pseudopod projections on neutrophils, which enhance their tumbling and exacerbate their impact on surrounding RBC motion, ultimately elevating both apparent viscosity and microvascular resistance to a higher degree than if cellular projections were not present. Recently, we reported that mixed suspensions of activated leukocytes and hematocrit elevate the flow resistance of non-capillary microvascular mimics to a greater degree than similar suspensions with inactivated leukocytes alone (Fig. A.1 and Fig. A.2, Appendix A) [73]. However, although pseudopod extensions had a significant effect on microvascular flow resistance *in vitro*, the magnitude of these flow resistance elevations may not be biologically relevant to induce pathology *in vivo*.

Further evidence regarding impaired neutrophil mechanosensitivity and its putative involvement in microcirculatory pathogenesis came from previous studies from our lab using a hypercholesterolemia murine model. Hypercholesterolemia induces a chronic inflammatory phenotype within the microcirculation, which drives downstream microvascular dysfunction. When neutrophils were taken from the hypercholesterolemic

mice and exposed to shear, these cells were found to have impaired FSS mechanosensitivity; specifically, they were deficient in their pseudopod retraction response to shear exposure [27]. Furthermore, this impaired FSS pseudopod retraction response was correlated with disrupted tissue blood flow autoregulation (i.e., microvascular dysfunction) [26], implicating a link between dysregulated neutrophil activity and microvascular dysfunction. Combined, these observations suggested that the pathologic cholesterol elevations associated with hypercholesterolemia played a role in the impairment of neutrophil FSS mechanosensitivity.

2.4 Hypercholesterolemia-Associated Dysregulation of Neutrophil Adhesion

2.4.1 Dysregulated neutrophil adhesion is a key feature of hypercholesterolemia

Hypercholesterolemia is associated with chronically inflamed blood typified by elevations in the number of activated neutrophils in the microcirculation [74]. One of the first features to manifest during hypercholesterolemia appears to be sustained neutrophil adhesion in the blood and microcirculation. The formation of leukocyte-platelet aggregates, for example, is reportedly enhanced in hypercholesterolemic mice [75]. Additionally, neutrophils also exhibit increased adhesivity to endothelium in hypercholesterolemic rabbits [76]. This enhanced adhesion may be due to the increased Mac1 expression reported for neutrophils subjected to a hypercholesterolemic environment [77]. Sustained neutrophil adhesion, in turn, may drive endothelial cell dysfunction [74,78], leading to tissue blood flow dysregulation and microvascular dysfunction.

Many factors potentially contribute to the reported dysregulation in neutrophil adhesion during hypercholesterolemia. For example, superoxide production by neutrophils

16

positively correlates with plasma cholesterol levels [79]. The enhanced production of superoxide, in turn, reduces the bioavailability of nitric oxide (NO), a mediator of neutrophil adhesion [80]. Notably, impaired NO production by endothelial cells supports dysregulated neutrophil adhesion [81]. This means a combination of enhanced superoxide production and reduced NO availability may promote dysregulated neutrophil adhesion and sustain the chronic inflammatory phenotype observed during hypercholesterolemia. Interestingly, reduced NO levels in the blood have been linked to an impaired neutrophil FSS response [20], suggesting that neutrophil activity may become dysregulated. However, NO production may also be limited independently of neutrophils due to endothelial cell dysfunction [82], which further promotes adhesion and a chronic inflammatory phenotype.

2.4.2 Dysregulated neutrophils impair the post-occlusive reactive hyperemia response in hypercholesterolemic mice

Once adhered, neutrophils may contribute to microvascular dysfunction by dysregulating tissue blood flow. Conceivably, accumulation of chronically activated neutrophils dysregulates microvascular blood flow and disrupts vascular perfusion, leading to lethal tissue injury [83]. Research from our own lab involving neutrophil shear regulation during tissue blood flow autoregulation in response to post-occlusive reactive hyperemia (poRH) further supports this possibility [26].

The poRH response represents a transient overshoot in blood flow during recovery of microvascular tissues in response to a brief period of blood stasis, which elicits ischemia in downstream tissues [74,84]. PoRH is commonly used to assess the health state of microvascular function (e.g., tissue blood flow autoregulation). After the initiation of

17

reperfusion, the blood flow overshoot prior to its return to baseline is believed to occur due to initial vasodilation of blood vessels, enabling the rapid transport of blood to oxygen-starved tissues [85]. Once blood flow has been restored and tissues are reoxygenated, vasoconstriction reduces flow back to pre-stasis levels. While it is believed that endothelial cell functions (e.g., NO release) are involved in regulating blood flow during poRH [84], some studies suggest that factors outside the endothelial cells also play a role [86].

Our prior research focused on the contributions of neutrophils to the impaired poRH response observed during hypercholesterolemia [26,27]. In particular, we found that an impaired poRH response was positively correlated with an impaired pseudopod retraction response to FSS (our surrogate index of shear sensitivity) and elevated cholesterol levels. As such, an impaired FSS response may represent one of the earliest contributing factors toward microvascular dysfunction associated with hypercholesterolemia by promoting tissue blood flow dysregulation. However, the mitigating event linking dysregulated neutrophil activity with hypercholesterolemia remained unclear.

One possible explanation for the impaired blood flow response to poRH observed for hypercholesterolemic mice may be related to dysregulated neutrophil adhesion [74-76]. Neutrophils in a hypercholesterolemic environment exhibit an upregulated expression of adhesion integrins [77]. This upregulated expression may be linked with an impaired FSS mechanotransduction response. Similarly to FSS-induced pseudopod retraction, FSS-induced CD18 cleavage may also be impaired by pathological blood cholesterol elevations. This impairment may be the central link, which connects hypercholesterolemia, microvascular dysfunction, and dysregulated neutrophil adhesion. However, the mechanistic basis for this dysregulation remains to be demonstrated.

2.5 The Role of the Cell Membrane in Fluid Shear Stress Mechanosensitivity

Because blood borne cells, including the neutrophils, are likely to experience large fluctuations in shear stress levels as they circulate through the body [41,87], atypical shear distributions alone are more than likely not the cause of cellular dysfunction. Instead, it is conceivable that the mechanistic basis for the onset of dysregulated neutrophil activity due to hypercholesterolemia, or any pathological condition, arises from changes in the ability of neutrophils to sense and respond to the applied shear stresses (i.e., mechanosensitivity) in their local environment.

The cell membrane, being positioned at the interface between the extracellular and intracellular milieu, is in a strategic position to regulate the mechanosensitivity of many different types of cells, including the neutrophils. In general, the cell membrane is the location for many different classes of membrane-spanning proteins, including various GPCRs, tyrosine kinase receptors, ion channels, and integrins [23,88-94]. Many of these proteins that have regions both inside and outside the cell have been proposed to serve as mechanosensors and/or mechanotransducers for a variety of cells, including endothelial cells, bone cells, and neutrophils [91,92,94].

2.5.1 Evidence of formyl peptide receptors as neutrophil mechanosensors

In the case of neutrophils, FPR has been implicated as a mechanosensor, which drives their downstream responses to shear (e.g., actin depolymerization, pseudopod retraction). Using HL60 derived neutrophilic cells, FPR was demonstrated as an important component of the FSS-induced pseudopod retraction response [92]. In fact, FPR expression alone appeared enough to confer the ability of HL60 cells to exhibit a pseudopod retraction

19

response to FSS. Specifically, while undifferentiated HL60 cells express low levels of FPR and lack the ability to form pseudopods, overexpressing FPR in HL60 cells imparted the ability to form pseudopods that retract under FSS exposure. Moreover, HL60 cells were prevented from retracting pseudopods by using siRNA to silence FPR expression [92].

While the exact involvement of FPR in mechanotransduction processes remains unknown, it appears as though FSS downregulates the surface expression of this receptor [63]. This downregulation does not involve the proteolytic activity of matrix metalloproteinases (MMPs) [64], which are capable of cleaving FPR [69]. Instead, it seems to involve FSS-induced internalization and relocalization of FPR from the surface to a perinuclear compartment, thereby reducing pseudopod activity [63]. It is interesting to note, however, that some FPRs must be present on the cell surface to regulate pseudopod activity, since proteolytic FPR cleavage impairs the FSS-induced retraction response in SHRs [69]. These findings further support the role of FPRs as neutrophil mechanosensors.

2.5.2 Evidence of CD18 integrins as neutrophil mechanosensors

In addition to FPR, the CD18 integrins expressed on neutrophils may also act as mechanosensors. When exposed to FSS, CD18 integrins undergo conformational shifts in their extracellular domains [93]. Reportedly, this structural activity is proposed to facilitate ctsB access to cleavage domains on the CD18 integrins (Fig. 2.4). Simultaneously, it may promote outside-in signaling capable of altering neutrophil activity. There is substantial literature evidence suggesting that CD18 integrins influence cell functions via inside-out as well as outside-in signaling [95,96]. There is also evidence that CD18 integrins play a role in FSS-induced mechanosignaling. For example, neutrophils adhered to substrates

20

through CD18 [97] have a functional pseudopod retraction response to FSS. Neutrophils adherent via β_1 integrins do not. This suggests that integrin specificity plays a role in FSS mechanotransduction responses, further implicating CD18 as a potential mechanosensor.

The reported FSS-induced conformational shifts in CD18 integrins appear to serve as a way for neutrophils to restrict their adhesive capacity. As such, a major consequence of CD18 integrin conformational shifts may be the minimization of neutrophil adhesion. Overall, the collective evidence for neutrophil mechanosensitive receptors, such as FPR and CD18, points to a link between neutrophil shear sensitivity and the expression of these membrane mechanoreceptors.

2.5.3 The cell membrane is involved in the regulation of neutrophil mechanosensitivity

Since the cell membrane acts as the substrate for all transmembrane mechanosensitive proteins, it is conceivable that the mechanical properties of the cell membrane may also be capable of regulating neutrophil responsiveness to FSS. In particular, the fluidity of the cell membrane may affect mechanosensitivity by impacting the shear-related structural activity of transmembrane mechanoreceptors.

Membrane fluidity is a measure of the lipid bilayer microviscosity, which influences the motion and conformational activity of the other phospholipids and resident signaling molecules such as cell surface protein receptors. Membrane fluidity changes may alter the dynamics of membrane protein activity by affecting their intermolecular actions or structural activity. In fact, changes in the membrane fluidity of cells have been reported to influence the number, affinity, lateral mobility, and conformational activity of

membrane receptors [98-101]. These physiological changes in membrane fluidity may arise, in part, due to the actions of cholesterol on the cell membrane (Fig. 2.4)
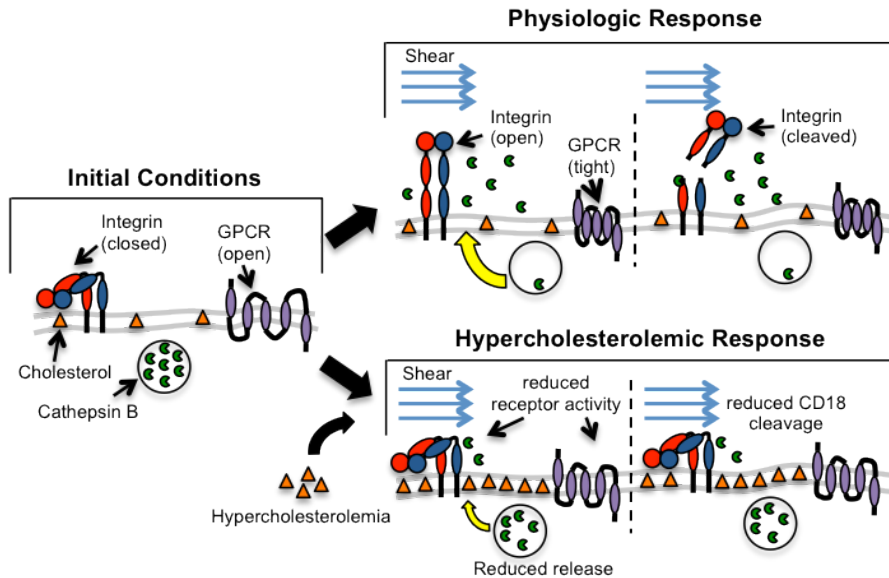
Figure 2.4. Mechanisms by which membrane cholesterol enrichment may impair neutrophil fluid shear stress mechanotransduction.
Pathologic cholesterol elevations can lead to the enrichment of neutrophil membranes with cholesterol. This may alter neutrophil mechanosensitivity by affecting the ability of membrane receptors to response to shear. Alternatively, membrane cholesterol enrichment may interfere with the ability of neutrophils to release lysosomal proteases (such as ctsB) under shear.

Cholesterol is a regulator of membrane fluidity [102] capable of affecting neutrophil mechanosensitivity by altering the fluidity of the cell membrane. When extracellular cholesterol is integrated into the membrane, it causes the membrane to become more rigid and less fluid [103,104]. This has consequences for processes that depend on the fluidity of the cell membrane. For example, membrane cholesterol has been shown to disrupt the signaling of lipid rafts that regulate various neutrophil functions (e.g., chemotaxis/migration, adhesion, etc.) [105]. Furthermore, conformation-dependent receptors, such as GPCRs, reportedly display altered structural activity in response to ligand binding when cellular membrane fluidity is altered [88]. This suggests that, similar

22

to GPCRs, neutrophil FSS mechanosensors may have difficulty adopting changes in conformation under shear exposure due to membrane fluidity changes (Fig. 2.4).

In addition to affecting the conformational activity and signaling of mechanosensitive receptors, cholesterol-related changes in membrane fluidity may also impair the release of bioactive molecules produced within the neutrophil. In support of this, membrane stiffening has been demonstrated to interfere with the release of pro-inflammatory cytokines into the extracellular milieu [106]. This suggests that the transmembrane release of ctsB, which is required to cleave CD18 integrins, may be prevented by membrane fluidity changes associated with cholesterol enrichment (Fig. 2.4).

Taken together, it is conceivable that the actions of hypercholesterolemia on the neutrophil membrane interfere with a critical regulatory mechanism (i.e., FSS mechanotransduction) charged with ensuring neutrophils remain inactivated. In doing so, this may lead to the neutrophils becoming more adhesive, resulting in their sustained retention in the microvasculature with a detrimental impact on the microcirculation. This possibility is the focus of the investigations in the present dissertation.

2.6 Study Rationale

Recently, our lab reported neutrophil mechanosensitivity to be a function of the cholesterol-related fluidity of the cell membrane [27]. We also determined that cholesterol-related impairment of FSS-induced pseudopod retraction was correlated with tissue blood flow dysregulation in hypercholesterolemic mice [26]. However, the pathogenic mechanism that connects impaired FSS sensitivity, neutrophil dysregulation, and microvascular dysfunction due to hypercholesterolemia remains to be determined.

23

The present study explored a new pathogenic mechanism by focusing on how membrane fluidity changes may affect the FSS mechanoregulation of CD18 integrin expression. In doing so, the present study sought to not only determine how ctsB-induced CD18 cleavage regulated neutrophil adhesion to vascular endothelium, but also examine how membrane cholesterol enrichment may impair FSS mechanotransduction and whether it may serve as a potential mechanistic link between dysregulated neutrophil adhesion and microvascular dysfunction, two key features of hypercholesterolemia.

24

CHAPTER 3: CHARACTERIZATION OF THE FLUID SHEAR STRESS-INDUCED CLEAVAGE OF CD18 INTEGRINS BY CATHEPSIN B RELEASE FROM NEUTROPHIL-LIKE CELLS

Neutrophils proteolytically shed the extracellular domains of surface-associated CD18 integrins when exposed to FSS under physiologic conditions [23,59,93]. This occurs through FSS-induced release of the cysteine protease ctsB, which targets CD18 in the ectodomain. However, it is not known which of the CD18 integrin heterodimers (i.e., either LFA1, Mac1, CD11c/CD18, or CD11d/CD18) is cleaved by ctsB.

The present study sought to elucidate further mechanistic insight regarding the role of ctsB in the FSS regulation of CD18 integrin surface expression by neutrophils. Since all of the possible CD18-containing integrins have different roles during leukocyte recruitment and adhesion to the endothelium, the integrin specificity of ctsB was expected to provide a clue as to how FSS-induced CD18 cleavage deactivated the cell.

The present study also sought to verify whether FSS mechanotransduction is a characteristic of the neutrophilic phenotype. HL60-derived neutrophil-like cells (dHL60-NCs) have been used to model neutrophil migration and chemotaxis [107]. Furthermore, dHL60-NCs also exhibit shear sensitivity, as these cells retract pseudopods when exposed to FSS [92,108]. The studies outlined in this section focused on characterizing and verifying that, in response to FSS exposure, dHL60-NCs release ctsB and cleave CD18 integrins similar to primary human neutrophils. The CD18 integrin cleavage responses of human neutrophils and dHL60 cells were compared to also determine if dHL60 cells would serve as a suitable transfection culture model for planned studies.

We exposed human neutrophils and dHL60-NCs to shear using a cone-and-plate viscometer. Using both cells, we analyzed the FSS-induced cleavage response for LFA1 and Mac1 in the presence of protease inhibitors. Additionally, we also analyzed the expression of CD11c on dHL60-NCs. Since dHL60-NCs upregulate CD11a and CD11b after differentiation [109], we wanted to ensure that other CD18 heterodimers were not being upregulated as well. We excluded CD11d from our analyses, as prior studies indicated that expression of this integrin is primarily limited to macrophages [110,111]. Finally, we stimulated cells with different concentrations of fMLP to determine whether inflammatory stimulation overrides FSS-induced CD18 cleavage.

3.1 Methods

3.1.1 Cells

3.1.1a Human neutrophils

Human subject recruitment, informed consent, and phlebotomy were approved by the University of Kentucky Institutional Review Board. Blood samples were harvested from asymptomatic human volunteers into K_2-EDTA-coated vacutainers (Becton-Dickinson) by standard venipuncture, as reported [27]. Neutrophils were then isolated by two-step Histopaque-Percoll gradient centrifugation and resuspended in Hank's balanced salt solution (HBSS) containing calcium and magnesium, as reported [93]. These purified cell suspensions were estimated to contain >90% neutrophils.

3.1.1b HL60-derived neutrophilic cells

HL60 cells (CCL-240; ATCC) were cultured in RPMI-1640 media (Invitrogen) supplemented with 10% fetal bovine serum (FBS; Hyclone) and 1% penicillin/streptomycin/L-glutamine (PSG; Mediatech) under standard incubation conditions (i.e., a humidified, 5% CO_2/95% air environment maintained at 37°C) according to the manufacturer's instructions. To induce a neutrophilic phenotype, HL60 cells (1×10^6 cells/mL) were differentiated in neutrophilic induction media consisting of RPMI-1640 media supplemented with 10% FBS, 1% PSG, and 1.25% dimethyl sulfoxide (DMSO; Sigma-Aldrich). HL60 differentiation proceeded over a period of 5 days as reported [92,108], with fresh neutrophilic induction media being replaced after 3 days. After HL60 cells were completely differentiated into dHL60-NCs, the cells were washed twice in PBS and then allowed to recover in DMSO-free culture medium for 1 hour prior to their use.

3.1.2 Cone-and-plate shear exposure

A custom cone-and-plate viscometer with a cone angle of 1° was used to expose aliquots (1 mL) of human neutrophils or dHL60-NCs to a constant laminar shear stress field of 5 dyn/cm^2 for 10 minutes as previously reported [27]. To achieve the desired shear stress of 5 dyn/cm^2 while assuming a viscosity of ~0.01 P, the cone was set to rotate at a rate of 82 rpm over a 10 minute period (Fig. 3.1). This was determined by using the following equation to calculate the shear stress applied by the cone-and-plate viscometer:

$$\tau = \frac{\mu \times 2\pi\omega}{60 \sin \theta}$$

where τ is shear stress (dyn/cm^2), μ is viscosity (P), ω is the rotational rate of the cone (rpm), and θ is the angle of the cone (degrees).

27
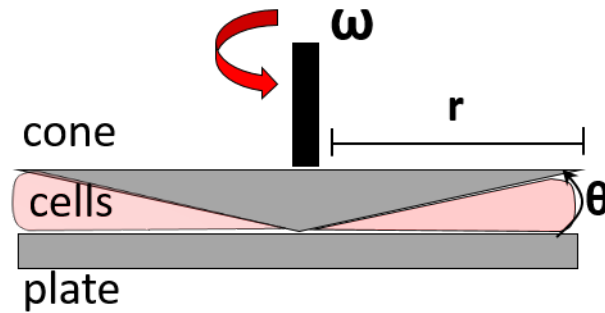
Figure 3.1. Representative diagram of a cone-and-plate viscometer.
By using a cone-and-plate viscometer, cell suspensions can be exposed to a uniform shear stress. The applied shear stress depends on the shallow cone angle, rotational rate, and viscosity of the solution.

Additional chemical treatments were performed on cells prior to, or during, shear exposure to test the involvement of the mechanisms of interest regarding FSS-induced CD18 cleavage. For experiments conducted with protease inhibitors, human neutrophils were pretreated with and without 30 µM E64 (cysteine protease inhibitor), 50 µM CA074-me (ctsB inhibitor) or 5 µM aprotinin (AP; negative control inhibitor) for 5 minutes prior to shear exposure as reported [112]. Similarly, dHL60-NCs were pretreated with 30 µM E64, 5 µM aprotinin, or 1 µM pepstatin (aspartyl protease inhibitor) for 5 minutes, or 50 mM doxycycline (MMP inhibitor) for 30 minutes. For experiments conducted with inflammatory agonists, human neutrophils and dHL60-NCs were pretreated with or without 0.01 – 10 µM fMLP for 10 minutes.

Once human neutrophils or dHL60-NCs were pretreated for the appropriate duration of time, the cells were kept in HBSS with the inhibitory reagents and exposed to shear using the cone-and-plate viscometer. Controls were parallel cell populations maintained under static (i.e., no-FSS), but otherwise similar experimental, conditions. In this case, the cone was held stationary while cells were allowed to incubate on the plate.

Immediately after shear and control experiments, cells were fixed (1% p-formaldehyde in phosphate buffer) for 15 minutes. After fixation, cell populations were washed three times in PBS and prepared for immunofluorescence.

3.1.3 Immunofluorescence

Fixed human neutrophils or dHL60-NCs were resuspended in 1% bovine serum albumin (BSA) in PBS for 30 minutes and subsequently labeled with fluorescent antibodies for one hour using standard immunochemistry. Some cell populations were left unpermeabilized to assess surface expression, while other cell populations were permeabilized to assess intracellular expression by adding 0.1% saponin to the 1% BSA buffer prior to fluorescent antibody labeling. After fluorescent labeling, cell suspensions were washed three times in PBS to remove unbound antibodies and subsequently resuspended in PBS for flow cytometric analyses.

For analysis of surface integrin expression on human neutrophils and dHL60-NCs, FITC-conjugated mouse monoclonal antibody (mAb) to CD18 (clone 6.7), PE-conjugated mouse mAb to CD11a (clone 38), or Alexa Fluor 488-conjugated mouse mAb to CD11b (clone ICRF44) were used to label unpermeabilized cells as reported [59]. Some dHL60-NCs were also labeled with FITC-conjugated mouse mAb to CD11c (clone B-ly6). For analysis of total cellular CD18 levels (i.e., cleaved and uncleaved integrins), permeabilized dHL60-NCs were labeled with goat polyclonal antibody (pAb) against the intracellular domain for CD18 (clone C-20) in conjunction with an Alexa Fluor 488-conjugated donkey anti-goat IgG (i.e., secondary) antibody (Invitrogen). Nonspecific binding was quantified using an Alexa Fluor 488-conjugated mouse IgG1 isotype control (Invitrogen).

29

For analysis of ctsB expression in human neutrophils and dHL60-NCs, cells were labeled with rabbit pAb (clone Ab-3) in conjunction with an Alexa Fluor 488-conjugated goat anti-rabbit IgG (i.e., secondary) antibody (2 mg/mL; Invitrogen). Cells were left unpermeabilized to assess surface ctsB expression, while some cells were permeabilized using 0.1% saponin to assess total ctsB expression. Nonspecific binding was quantified using an Alexa Fluor 488-conjugated mouse IgG1 (Invitrogen) and an Alexa Fluor 488-conjugated goat IgG1 (Santa Cruz Biotechnology).

3.1.4 Flow cytometry

Flow cytometric analyses utilized an LSR II flow cytometer (Becton-Dickinson) interfaced with Becton-Dickinson FACsDiva software, as previously reported [59]. Neutrophil and dHL60-NC populations were gated based on their forward scatter (FSC) and side scatter (SSC) values. The total fluorescence intensity, representing the amount of bound antibodies, was used as the measure of antigen specific expression level. By using the total fluorescence intensity, histograms of antigen-specific fluorescence intensity were generated for each sample using the FCS Express 4 Flow Cytometry software (De Novo Software). Shear-induced changes in the antigen expression levels were normalized to those of their respective controls and expressed as "fold change".

Quantitative data derived from dHL60-NCs and human neutrophils were expressed as mean ± standard error of the mean (SEM) for n ≥ 3 replicates. Statistical analyses were performed using the statistical software program JMP (SAS Institute). One-sample t-tests with $P < 0.05$ were used to identify significant fold changes or percent reductions in experimental treatments compared to a reference value. Comparisons between the means of experimental treatments (i.e. unstimulated cells vs. chemically-pretreated cells) were performed using ANOVA and post-hoc Tukey's test with $P < 0.05$ indicating significance.

3.2 Results

3.2.1 Fluid shear stress-induced cathepsin B release selectively cleaves Mac1 in human neutrophils

Human neutrophils left untreated (UNT) and exposed to FSS (5 dyn/cm^2 for 10 min) with a cone-plate device exhibited reduced binding of antigen-specific antibodies to CD18 and CD11b, but not CD11a integrins relative to time-matched, unsheared controls (Fig. 3.2, A – C). This reduction in CD18 antibody binding was blocked for cells pretreated with CA074, but not AP (our negative control protease), prior to shearing (Fig. 3.2, D). CA074 and AP had no effect on binding of CD11a antibodies to neutrophils after control or FSS experiments (Fig. 3.2, E). Notably, FSS-induced reductions in CD11b antibody binding to neutrophils were mitigated by CA074, but not by AP (Fig. 3.2, F).
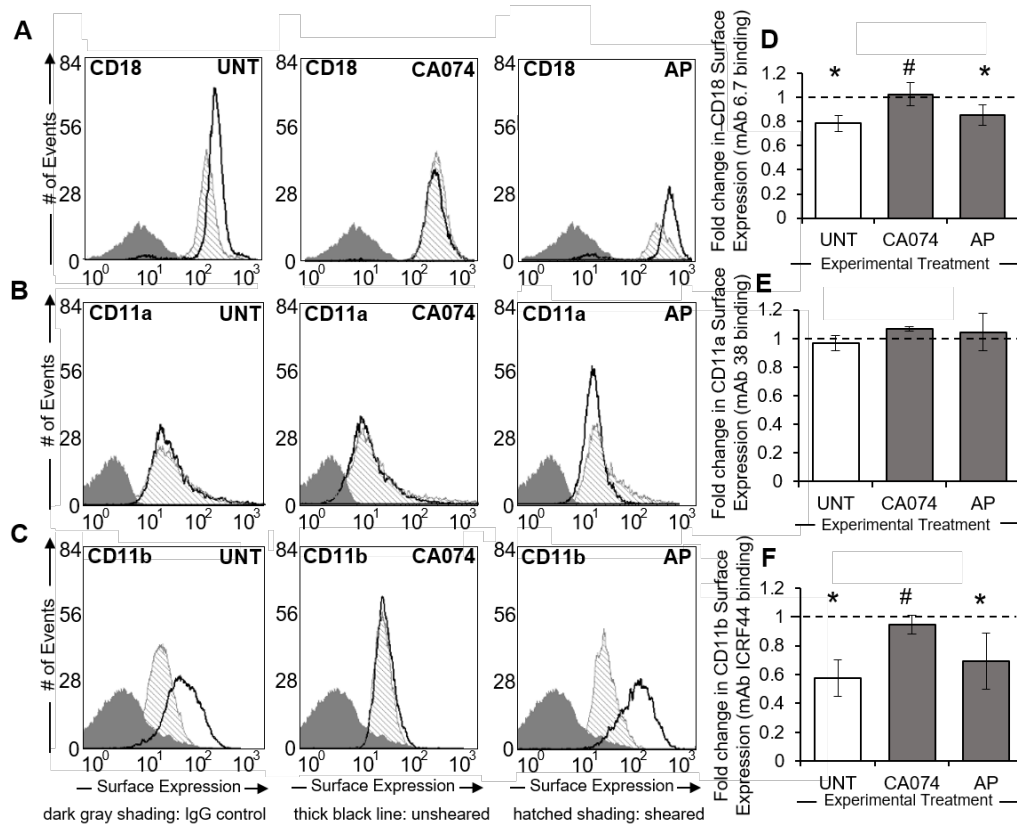
Figure 3.2. The selective cleavage of Mac1 by shear-induced cathepsin B release.
(A-C) Representative flow cytometry histograms depicting the fluorescent intensity of intact CD18 (A), CD11a (B), and CD11b (C) expressed on the surface of neutrophil suspensions maintained under no-flow conditions (thick black line) or subjected to 5 dyn/cm^2 shear stress (hatched shading) using a cone-and-plate viscometer. A negative (IgG) staining control is also displayed in each plot (dark gray shading). Neutrophil suspensions were treated with or without ctsB-specific inhibitor CA074 (50 µM) and serine inhibitor aprotinin (AP; 5 µM). **(D-F)** Based on florescent antibody binding, mean fluorescent intensities of sheared neutrophils were normalized to their respective no-flow controls and plotted as fold change ± SD for CD18 (D), CD11a (E), and CD11b (F) integrins. n = 3 replicates in each group. *P < 0.05 compared to a normalized control value of 1 (dotted line). #P < 0.05 compared to control.

3.2.2 Fluid shear stress induces time-dependent cathepsin B release by human neutrophils

Permeabilized human neutrophils exhibited significantly reduced binding to ctsB antibodies after 2.5 min of FSS exposure when compared to unsheared cells (Fig. 3.3, A). This apparent reduction in total ctsB levels was observed for the duration of the 10 min exposure (Fig. 3.3, C). In contrast, ctsB antibody binding to unpermeabilized human

32

neutrophils remained unchanged after 2.5 and 10 min of FSS exposure (Fig. 3.3, B). While

surface-associated ctsB appeared to be significantly elevated after 5 min of FSS, the

differences in expression levels were minor (Fig. 3.3, D).
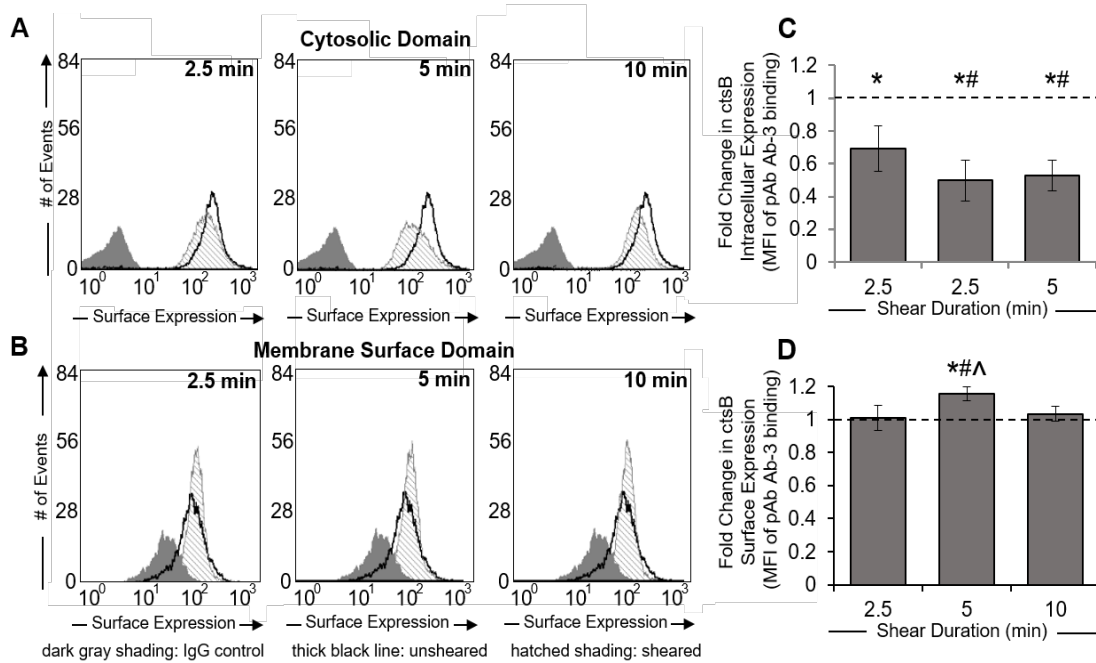
Figure 3.3. Fluid shear stress induces time-dependent cathepsin B release.
(A-B) Representative flow cytometry histograms depicting the fluorescent intensity of ctsB expression within the cytosolic domain (A) or membrane surface domain (B) for neutrophil suspensions maintained under no-flow conditions (thick black line) or exposed to 5 dyn/cm^2 shear stress (hatched shading) using a cone-and-plate viscometer. A negative (IgG) staining control is also displayed in each plot (dark gray shading). Shear duration was gradually increased (2.5, 5, and 10 minutes) to observe the time-dependent effects of shear. **(C-D)** Based on fluorescent antibody binding, mean fluorescence intensities of sheared neutrophils were normalized to their respective no-flow controls and plotted as fold change $\pm$ SD for ctsB cytosolic (C) or membrane surface (D) expression. n = 3 replicates in each group. *P < 0.05 compared to a normalized control value of 1 (dotted line). #P < 0.05 compared to 2.5 minute shear exposure. ^P < 0.05 compared to 10 minute shear exposure.

3.2.3 Exposure to shear induces CD18 cleavage in dHL60-NCs

DHL60-NCs expressed intact CD18 integrins on their surfaces under all conditions

tested in the present study (Fig. 3.4, A) as indicated by their binding affinity to mAb 6.7

relative to that of mouse IgG (negative staining control). Notably, untreated dHL60-NC

populations exposed to 5 dyn/cm^2 FSS, in the absence or presence of 0.01 µM fMLP, exhibited significantly (P < 0.05) reduced binding of mAb 6.7 relative to cells maintained under control (i.e., no-flow), but otherwise similar experimental, conditions. The FSS-induced reductions in cell surface affinity to mAb 6.7 were abrogated when untreated or fMLP-stimulated dHL60-NCs were pretreated and subsequently exposed to shear with the cysteine protease inhibitor E64. In this case, no noticeable shift in fluorescent intensity (indicative of mAb 6.7 binding) was observed between sheared and unsheared samples when the cells were in the presence of E64 (Fig. 3.4, B).
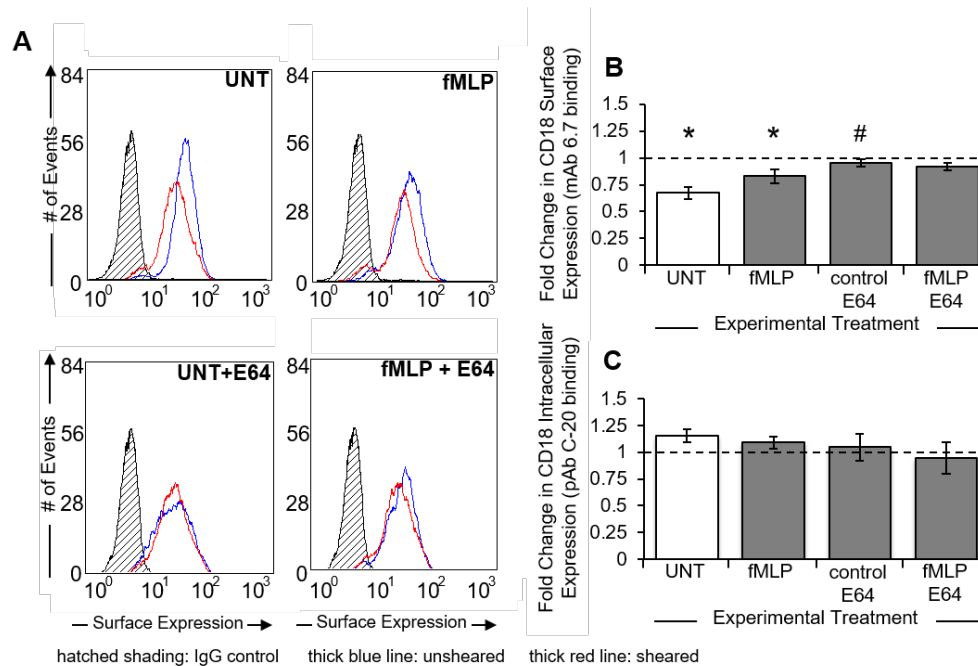
Figure 3.4. Fluid shear stress promotes cleavage of CD18 integrins off the surface of dHL60-NCs.
(A) Representative flow cytometry histograms depicting the fluorescent intensity of CD18 expression on the surface of dHL60-NC suspensions maintained under no-flow conditions (blue line) or exposed to 5 dyn/cm^2 shear stress (red line) using a cone-and-plate viscometer. A negative (IgG) staining control is also displayed in each plot (hatched shading). DHL60-NC suspensions were treated with or without fMLP (0.01 µM) and cysteine inhibitor E64 (30 µM). **(B-C)** Based on fluorescent antibody binding, mean fluorescence intensities of sheared neutrophils were normalized to their respective no-flow controls and plotted as fold change ± SEM for CD18 membrane surface (C) or cytosolic (D) expression. n = 4 replicates in each group. *P < 0.05 compared to a normalized control value of 1 (dotted line). #P < 0.05 compared to control.

www.manaraa.com

Untreated dHL60-NC populations exposed to FSS, whether in the absence or presence of 0.01 µM fMLP, did not exhibit reductions in the binding of pAb C-20 antibody against the cytoplasmic domains of CD18 integrins (Fig. 3.4, C). Similarly, untreated or fMLP-stimulated dHL60-NCs that were pretreated with E64 also did not exhibit a reduction in affinity to pAb C-20 when exposed to FSS. In both cases, the cytoplasmic CD18 integrin expression by dHL60-NCs exposed to FSS remained similar to that expressed by dHL60-NCs maintained under control (i.e., no-flow), but otherwise similar experimental, conditions. Combined, these results provided evidence that shear exposure promotes cleavage of CD18 integrins in the extracellular domain.

3.2.4 Exposure to shear induces CD11a, but not CD11b, cleavage in dHL60-NCs

Under all conditions tested in the present study, dHL60-NCs displayed detectable surface expression levels of intact CD11a (Fig. 3.5, A) and intact CD11b (Fig. 3.5, B) integrins. Specifically, all fluorescent intensities indicative of integrin subtype-specific antibody binding were greater than those of cells stained with isotype-matched mouse IgG negative control proteins.

Notably, the surfaces of dHL60-NCs exposed to FSS, in the absence or presence of fMLP, exhibited reduced binding to mAb 38 antibodies indicative of significant ($P < 0.05$) reductions in surface expression of intact CD11a relative to time-matched, unsheared controls. This FSS-induced reduction in surface affinity for mAb 38 antibodies was attenuated, but not completely blocked, by treatment of either untreated or fMLP-treated cells with E64 prior to and during flow experiments (Fig. 3.5, C).

35

In contrast, untreated and fMLP-treated dHL60-NCs either maintained under control conditions or exposed to FSS exhibited similar binding affinities for mAb ICRF44 directed against the extracellular domain of CD11b (Fig. 3.5, D). Similarly, untreated or fMLP-stimulated dHL60-NCs that were pretreated with E64 and either maintained under control conditions or exposed to FSS also exhibited similar binding affinities for mAb ICRF44 against CD11b. Thus, FSS exposure induced cleavage of CD11a, but not CD11b, integrins by dHL60-NCs.
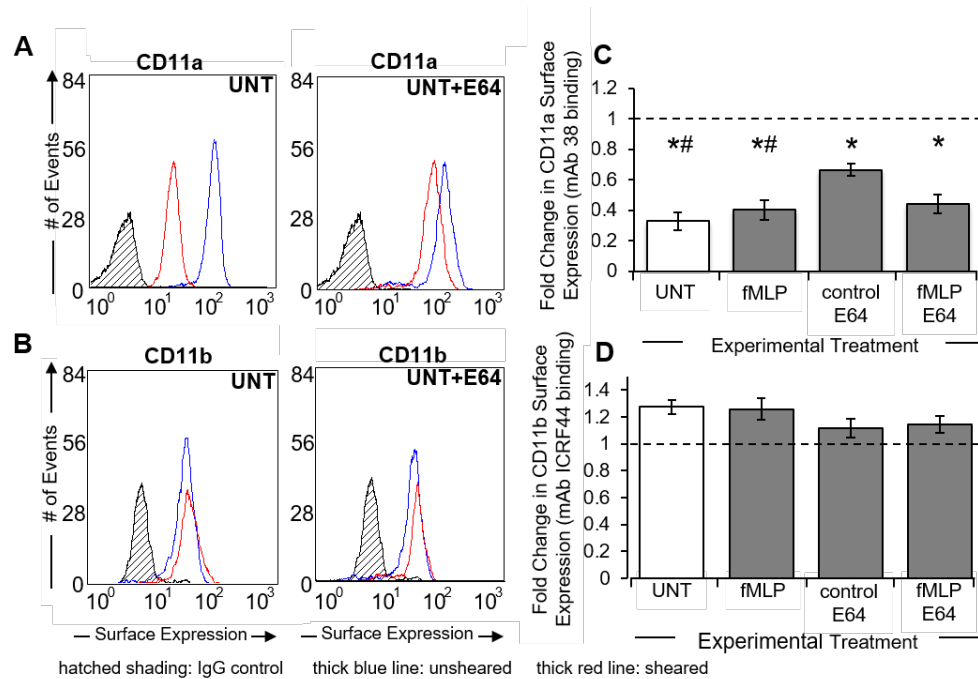
Figure 3.5. Fluid shear stress reduces surface expression of CD11a, but not CD11b, on dHL60-NCs.
(A-B) Representative flow cytometry histograms depicting the fluorescent intensity of CD11a (A) and CD11b (B) expression on the surface of dHL60-NC suspensions maintained under no-flow conditions (blue line) or exposed to 5 dyn/cm^2 shear stress (red line) using a cone-and-plate viscometer. A negative (IgG) staining control is also displayed in each plot (hatched shading). DHL60-NC suspensions were treated with or without fMLP (0.01 µM) and cysteine inhibitor E64 (30 µM). **(C-D)** Based on fluorescent antibody binding, mean fluorescence intensities of sheared dHL60-NCs were normalized to their respective no-flow controls and plotted as fold change ± SEM for CD11a (C) or CD11b (D) expression. n = 4 replicates in each group. *P < 0.05 compared to a normalized control value of 1 (dotted line). #P < 0.05 compared to control + 30 µM E64.

3.2.5 DHL60-NCs do not express the CD11c integrin on their surface

DHL60-NCs are capable of upregulating their expression of CD11a and CD11b integrins during differentiation [109]. We wanted to ensure that other CD18 heterodimers, such as CD11c, were not expressed on dHL60-NCs. As such, we investigated the possibility that CD11c/CD18 integrins were cleaved by dHL60-NCs in response to shear exposure. However, our analyses revealed that dHL60-NCs, either maintained under control conditions or exposed to FSS, did not exhibit detectable surface expression of CD11c integrins. Specifically, there was no detectable difference in the surface binding affinity of unsheared and sheared dHL60-NCs to either mAb B-Ly6 or mIgG negative staining control protein (Fig. 3.6, A). Moreover, treatment of cells with fMLP and/or E64, both with or without FSS exposure, had no effect on the membrane surface expression levels of CD11c integrins (Fig. 3.6, B).
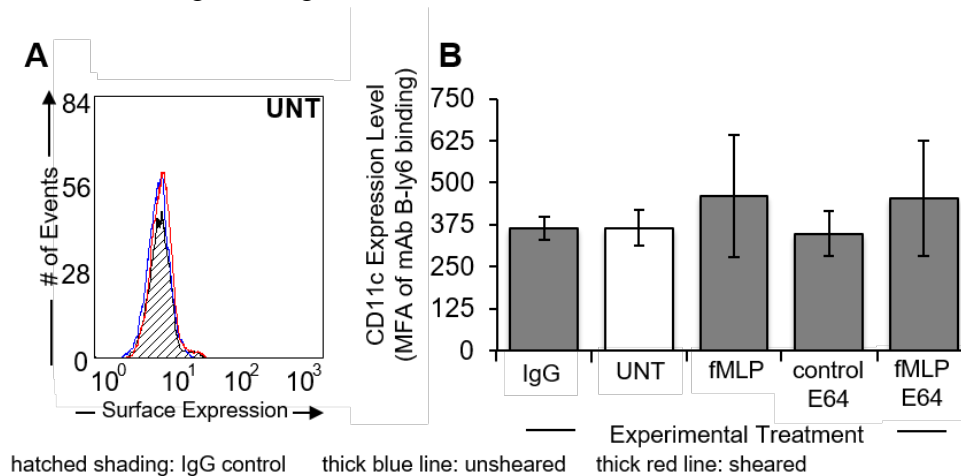
Figure 3.6. DHL60-NCs do not express the CD11c integrin.
(A) Representative flow cytometry histogram depicting the fluorescent intensity of CD11c expression on the surface of dHL60-NC suspensions maintained under no-flow conditions (blue line) or exposed to 5 dyn/cm^2 shear stress (red line) using a cone-and-plate viscometer. A negative (IgG) staining control is also displayed in each plot (hatched shading). DHL60-NC suspensions were treated with or without fMLP (0.01 µM) and cysteine inhibitor E64 (30 µM). **(B)** The mean fluorescence intensities used to quantify binding of mAb B-ly6 to dHL60-NCs were plotted as CD11c expression level ± SEM. n = 3 replicates in each group.

3.2.6 DHL60-NCs display minimal expression of cathepsin B

In comparison to human neutrophils, dHL60-NCs displayed low to minimal surface and cytosolic levels of ctsB (Fig. 3.7, A – B). On average, human neutrophils displayed binding affinities to pAb Ab-3 that were significantly greater than that of the secondary Alexa Fluor 488-conjugated goat anti-rabbit IgG antibody alone, both on their cell surface as well as within their cytoplasm (Fig. 3.7, C). In contrast, the binding affinities of dHL60-NCs to pAb Ab-3, either on the cell surface or within the cytoplasm, were comparable to their binding affinities to the secondary antibody alone (Fig. 3.7, D).
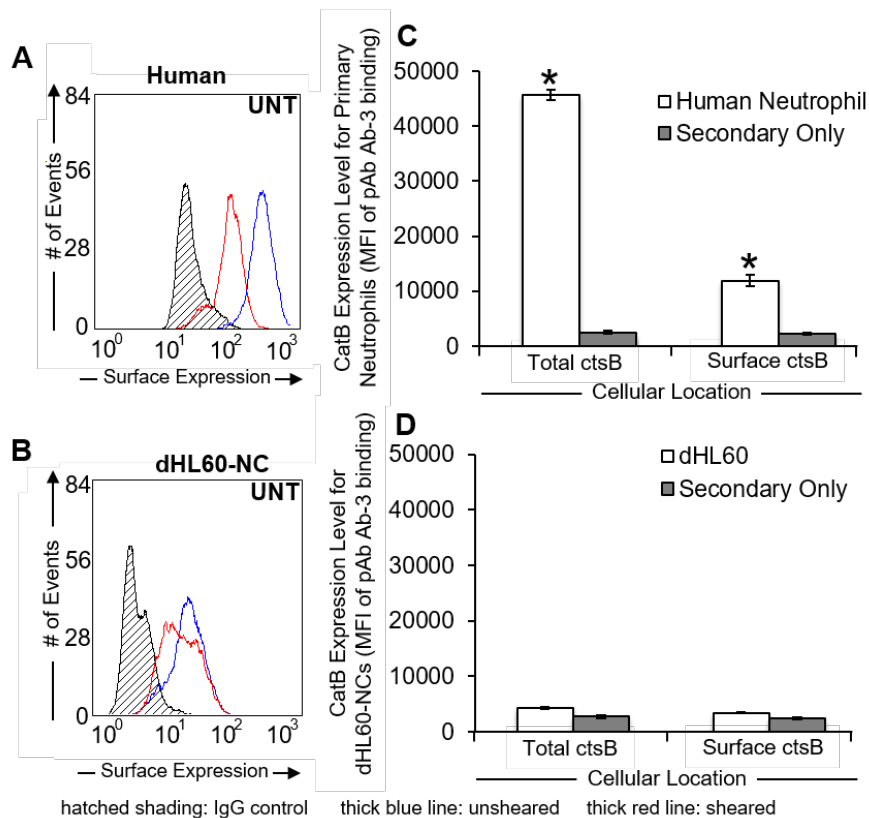
Figure 3.7. Human neutrophils, but not dHL60-NCs, express cathepsin B.
(A-B) Representative flow cytometry histogram depicting the fluorescent intensity of ctsB expression on the surface of human neutrophil (A) or dHL60-NC (B) suspensions maintained under no-flow conditions (blue line) or exposed to 5 dyn/cm^2 shear stress (red line) using a cone-and-plate viscometer. A negative (IgG) staining control is also displayed in each plot (hatched shading). **(C-D)** Based on fluorescent antibody binding, mean fluorescence intensities of sheared cells were normalized to their respective no-flow controls and plotted as ctsB expression level ± SEM for human neutrophils (C) or dHL60-NCs (D). n = 3 replicates in each group. *P < 0.05 compared to secondary antibody.

3.2.7 Shear-induced CD11a/CD18 cleavage may involve multiple proteases, including cysteine proteases, for dHL60-NCs

DHL60-NCs treated with serine and aspartyl protease inhibitors (aprotinin and pepstatin, respectively) prior to, and during, FSS exposure exhibited significant reductions in binding affinities for antibodies directed against the extracellular domains of CD18 and CD11a, relative to their respective time-matched, unsheared controls (Fig. 3.8, A – B). Notably, while doxycycline completely inhibited FSS-induced reductions in dHL60 binding to mAb 6.7 against CD18, it only partially blocked FSS-induced reductions in binding to mAb 38 against CD11a. This same pattern of blocking was observed for E64. Thus, the reduced surface expression of intact CD11a and CD18 integrins by dHL60-NCs exposed to shear occurred independently of aspartyl, serine, and MMP-9 proteases. This implicates a cysteine protease in the FSS-induced reductions of CD11a.
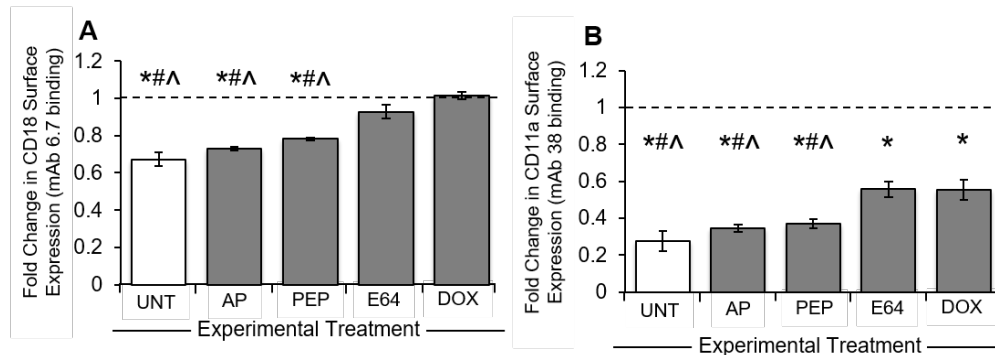
Figure 3.8. Fluid shear stress-induced reductions in CD18 and CD11a surface expression involve cysteine proteases for dHL60-NCs.
(A-B) Mean fluorescence intensities (MFI) used to quantify reductions in CD18 (A) or CD11a (B) expression by dHL60-NCs after exposure to 5 dyn/cm^2 shear stress in the absence (control; white bars) or presence (black bars) of protease inhibitors were normalized to their respective controls and plotted as average fold change ± SEM. The following protease inhibitors were tested: 5 μM aprotinin (AP), 1 μM pepstatin (PEP), 30 μM E64 (cysteine inhibitor), or 50 mM doxycycline (DOX). n = 3 replicates in each group. *$P < 0.05$ compared to a normalized control value of 1 (dotted line). #$P < 0.05$ compared to E64. ^$P < 0.05$ compared to DOX.

3.2.8 Cell agonist fMLP dose-dependently suppresses shear-induced cleavage of CD18 integrins in neutrophil-like cells

Untreated dHL60-NCs, as well as cells stimulated with 0.01 µM fMLP, exhibited significant reductions in CD18 surface expression in response to FSS exposure. However, this response was attenuated, and completely blocked, when stimulated with 1 and 10 µM fMLP, respectively (Fig. 3.9, A). Additionally, CD11a surface expression by dHL60-NCs was significantly reduced after exposure to FSS under all concentrations of fMLP tested (Fig. 3.9, B). The post-shear reduction in CD11a surface expression, however, was attenuated at higher fMLP concentrations (1 and 10 µM).

Similarly to dHL60-NCs, untreated human neutrophils, as well as human neutrophils stimulated with 0.01 µM fMLP, exhibited significant reductions in CD18 surface expression in response to FSS. However, this response was attenuated, and completely blocked, when stimulated with 1 and 10 µM fMLP, respectively (Fig. 3.9, C). In the case of the CD11 subunits, CD11b surface expression by human neutrophils was significantly reduced after exposure to FSS in the presence of 0 – 0.01 µM fMLP (Fig. 3.9, D). The post-shear reduction in CD11b surface expression, however, was attenuated at higher fMLP concentrations (1 and 10 µM). These results suggest that high levels of inflammatory agonists may be capable of overriding the FSS-induced cleavage of CD18 and CD11 integrins.

40
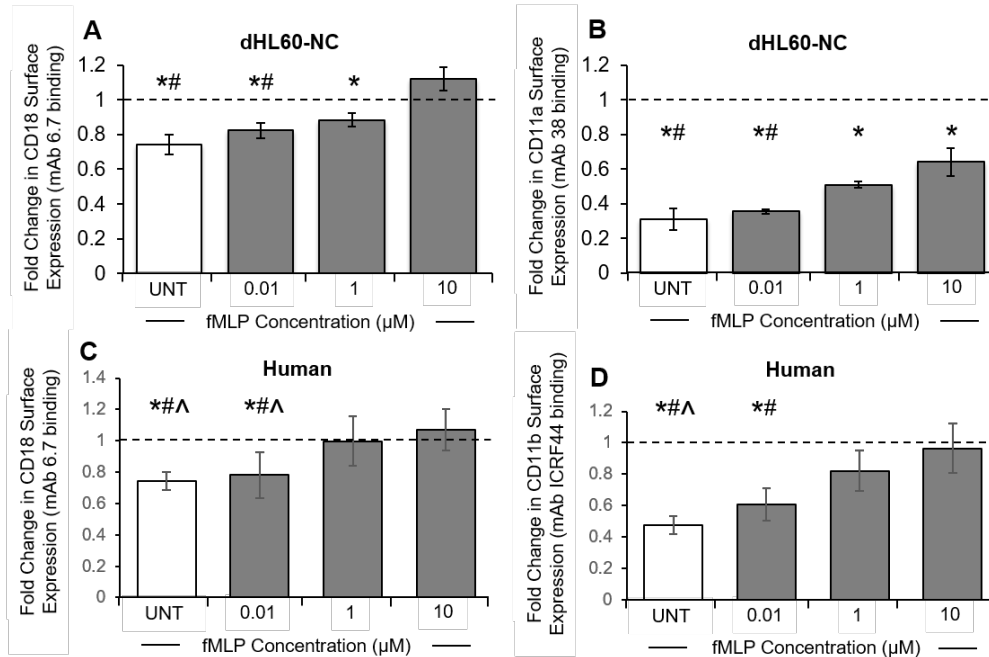
Figure 3.9. The inflammatory agonist fMLP dose-dependently attenuates shear-induced CD18 cleavage in neutrophil-like cells.
(A-B) Mean fluorescence intensities (MFI) used to quantify reductions in CD18 (A) or CD11a (B) expression by dHL60-NCs after exposure to 5 dyn/cm² shear stress in the absence (control; white bars) or presence (black bars) of fMLP were normalized to their respective controls and plotted as average fold change ± SEM. FMLP was used at 0, 0.01, 1, and 10 μM concentrations. **(C-D)** Mean fluorescence intensities (MFI) used to quantify reductions in CD18 (C) or CD11b (D) expression by human neutrophils after exposure to 5 dyn/cm² shear stress in the absence (control; white bars) or presence (black bars) of fMLP were normalized to their respective controls and plotted as average fold change ± SEM. FMLP was used at 0, 0.01, 1, and 10 μM concentrations. n = 3 replicates in each group. *$P < 0.05$ compared to a normalized control value of 1 (dotted line). #$P < 0.05$ compared to 10 μM fMLP. ^$P < 0.05$ compared to 1 μM fMLP.

3.2.9 Summary of findings/interpretations

The results of the present study provided evidence for the following significant findings.

- FSS-induced CD18 cleavage is characteristic of neutrophil-like cells, which suggests this is a key mechanoregulatory control mechanism for neutrophils.

- FSS-induced release of ctsB selectively cleaves Mac1, suggesting FSS mechanotransduction serves to restrict firm neutrophil adhesion.

41

- FSS-induced CD18 cleavage appears to be anti-inflammatory and can be overridden by high levels of inflammatory agonists.

- FSS-induced CD18 cleavage is a characteristic response of neutrophil-like cells to FSS exposure.

- The dHL60-NC culture model may be used as a transfectable cell line for the purpose of mechanistic-based explorations of FSS mechanotransduction for neutrophils.

CHAPTER 4: EVALUATING THE ROLE OF FLUID SHEAR-INDUCED CATHEPSIN B RELEASE IN THE CONTROL OF MAC1-DEPENDENT NEUTROPHIL ADHESION

Because our previous experiments established a role for ctsB in the cleavage of Mac1 under FSS exposure, we wanted to investigate the possibility that this protease regulates Mac1-related neutrophil adhesive processes. *In vivo*, neutrophils firmly adhere to platelets, other leukocytes, and endothelium using Mac1 [12,113,114]. Expression of Mac1 is important, as Mac1-knockout mice are associated with neutrophils that exhibit a markedly reduced adhesive capability, particularly during inflammation [115,116]. Additionally, Mac1-deficient neutrophils exhibit reduced migration rates [117]. Because neutrophil migration involves the projection and retraction of pseudopods which utilize Mac1 for stabilization [117], we sought to determine how ctsB could modulate Mac1-dependent neutrophil pseudopod activity during migration under no-flow conditions. We did so using exogenous ctsB or ctsB inhibitors as well as dHL60-NCs overexpressing ctsB.

Mac1 integrins are also critical for the arrest/firm adhesion of neutrophils to microvasculature under flow conditions [118,119]. Since Mac1 is cleaved under FSS exposure by ctsB release, the experiments in the present study sought to determine how FSS mechanotransduction played a role in the control of Mac1-dependent neutrophil adhesion under flow. To accomplish this, we allowed neutrophils to adhere to platelet and endothelial cell monolayers and exposed them to flow to monitor their detachment as an *in vitro* test of the FSS regulation of neutrophil adhesion. By pretreating neutrophils with ctsB inhibitors, we could evaluate the importance of ctsB in regulating neutrophil adhesion

43

under these flow conditions. Collectively, the goal of the studies described in this chapter was to evaluate the role of ctsB in the control of neutrophil adhesive capacity.

4.1 Methods

4.1.1 Cells

4.1.1a Human neutrophils and platelets

Human neutrophils were purified from whole blood harvested from asymptomatic volunteers as described in section 3.1.1a. Approximately 5 mL of whole blood was also set aside to purify platelets for use in flow-based detachment assays (see section 4.1.3) that were used to quantify the ability of FSS to restrict neutrophil adhesion. Platelets were extracted from plasma by removing erythrocytes and leukocytes through low speed (100xg) centrifugation, washing the supernatant solution in HEPES buffer, and suspending the platelets in Tyrode's buffer, according to detailed procedures [120].

4.1.1b Human cell culture

HL60 cells were cultured as previously described in section 3.1.1b. Differentiation of HL60 cells into dHL60-NCs also occurred as previously described in section 3.1.1b. On day 4 of differentiation, however, dHL60-NCs were transiently transfected with a ctsB-green fluorescent protein (ctsB-GFP) expression vector. Transfections were carried out using a Lonza Nucleofector Electroporator with the preset program T-019 and following the manufacturer's instructions. After transfection, dHL60-NCs were cultured in neutrophilic induction media for the remaining fifth day.

Human umbilical vein endothelial cells (HUVECs; Lifeline Cell Technology) were cultured in VascuLife VEGF media (Lifeline Cell Technology) supplemented with 10% FBS and 1% PSG, according to the manufacturer's instructions. The HUVECs were grown under standard incubation conditions described in section 3.1.1b. HUVECs were passaged approximately every three days to maintain optimal growth. These cells were used for flow-based cell detachment assays (see section 4.1.3) to quantify FSS regulation of neutrophil adhesion.

4.1.2 Pseudopod activity analysis

Glass slides were cleaned prior to experimentation using separate incubations in acetone and 70% ethanol in an ultrasonic cleaner for 15 minutes each. The glass substrates were then treated with 1 N NaOH for 2 hours to generate a hydrophobic surface conducive for cell adhesion and then pre-coated with fetal bovine serum for 10 minutes. For experiments, neutrophils and dHL60-NCs were pretreated for 5 min with and without 1 μM fMLP, 0.5 U/mL ctsB, or 50 μM CA074 and then deposited (at a density of 1×10^6/mL) on the FBS-coated glass slides for 20 min. Non-adherent cells were rinsed with PBS, and the remaining adherent cells were maintained under no-flow conditions in HBSS. Bright field micrographs of neutrophils, as well as bright field and fluorescence images of ctsB-GFP transfected cells, were acquired every 15 s for 10 min using an Olympus IX-71 fluorescence microscope.

To calculate cell centroid displacement rates, ImageJ was used to manually trace individual cells and track the movement of their centroid between consecutive frames

45

[121]. The centroid displacement rate, calculated by the following equation, was used as a surrogate measure of dynamic cell shape changes due to pseudopod activity:

$$\text{Centroid displacement rate (CDR)} = \frac{\sqrt{(x_2 - x_1)^2 + (y_2 - y_1)^2}}{t}$$

where x_1 is the initial x coordinate, x_2 is the final x coordinate, y_1 is the initial y coordinate, y_2 is the final y coordinate, and t is the time between frames (Fig. 4.1, A).
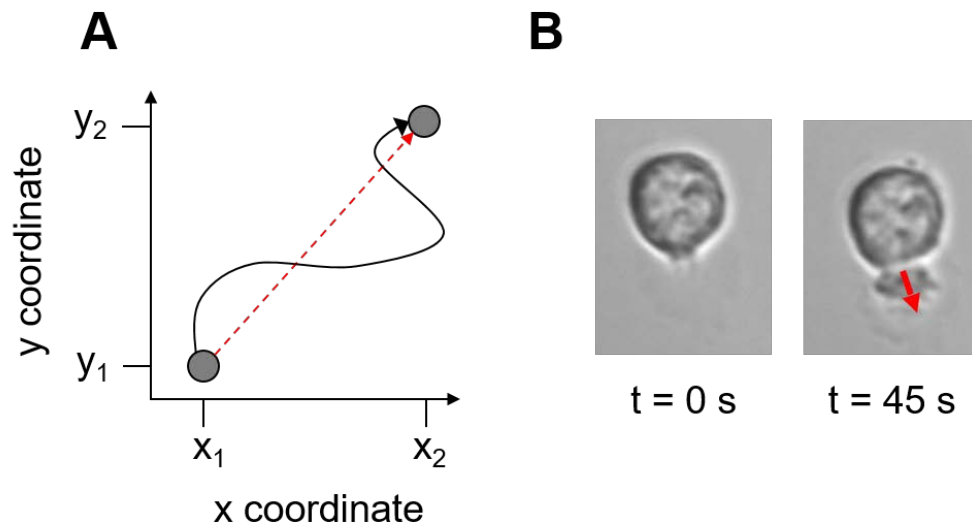
Figure 4.1. Representative images of centroid displacement and pseudopod projection analyses.
(A) The rate of cell migration was calculated as the rate of centroid displacement. The black solid arrow represents the migration path of a neutrophil over a specific duration of time. The red dashed arrow represents the centroid displacement rate (CDR) of the neutrophil over that same duration of time. **(B)** The rate of pseudopod projection or retraction was calculated by dividing the major axis length of a pseudopod by the interval of time necessary to achieve this length. The red arrow represents the major axis length of a pseudopod.

To calculate the rates of pseudopod extension and retraction, ImageJ was used to analyze selected pseudopod projections (Fig. 4.1, B). First, the major axis length of a pseudopod projection was calculated. Then, the duration of time it took for the pseudopod to achieve this length was measured over several consecutive frames. For pseudopod projection, the initial time point was determined to be when a pseudopod emerged from

46

the cell membrane, and the final time point was estimated to be when the same pseudopod achieved its major axis length. For pseudopod retraction, the initial time point was when the pseudopod was at its major axis length, and ended once the pseudopod had fully retracted. The corresponding rate of projection or retraction was then calculated by dividing the maximum pseudopod length by the duration of time.

4.1.3 Neutrophil detachment assay

Detachment assays were conducted using autologous human platelets that had been deposited on cleaned glass slides (described in section 4.1.2) and allowed to spread into a uniform coating for 30 min following previously-reported procedures [122]. A flow channel was assembled by interfacing the platelet-coated slides to a polycarbonate base having inlet and outlet ports (Fig. 4.2). A pre-cut gasket separating these two components formed a 200-µm high parallel plate flow channel. We selected a parallel plate flow chamber for experimental analyses to expose cells to a constant laminar shear stress over a given duration of time. This ensured that cell detachment under FSS exposure would be due to mechanoregulatory processes at our defined shear stress magnitude.

Detachment assays were also conducted using HUVECs seeded (5×10^5/mL) and grown on fibronectin-coated culture surfaces of 17 (l) x 3.8 (w) mm Ibidi microslides ($VI^{0.4}$; 400-µm high channel) for 3 days as reported [123]. The Ibidi microslides offered a sterile culture environment to grow HUVEC monolayers to confluency, and have been used in previous flow-based assays to maintain sterility [123,124]. Furthermore, the dimensions of the Ibidi microslides enabled us to achieve the same shear stress magnitude as our custom parallel plate flow system.

47
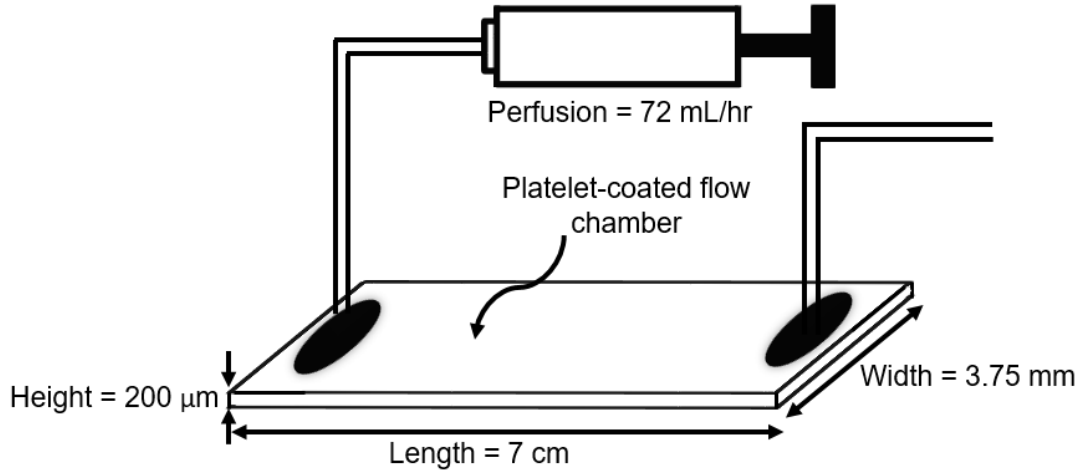
Figure 4.2. Schematic representation of the flow-based detachment assay.
This diagram represents the flow-based detachment assay for platelet-coated glass slides.
HBSS is perfused into the chamber using the syringe pump.

For flow studies, neutrophils (5×10^6/mL) were pretreated with and without 1 µM fMLP, 30 µM E64, 50 µM CA074-me, or 5 µM AP for 5 min and deposited on the platelet or HUVEC monolayers for 10 min, after which the non-adherent cells were rinsed away. A syringe pump was used to perfuse HBSS through the chamber to impose a FSS of 5 dyn/cm^2 on the wall of the channel. The flow rate was adjusted to impose 5 dyn/cm^2 as calculated according to the following equation:

$$\text{Flow rate } (Q) = \frac{\tau_w b h^2}{6\mu}$$

where τ_w is wall shear stress, b is the channel width, h is the channel height, and µ is the perfusate viscosity. Bright field micrographs (100X magnification) of the neutrophils were acquired every 5 s for 10 min, and neutrophil detachment was estimated by normalizing the number of neutrophils visible in each image against that present 30 seconds after flow initiation. We defined this initial time point to be t = 0 to ensure non-adherent cells were rinsed away prior to analyses.

48

Quantitative data derived using human blood-derived neutrophils and dHL60-NCs cells were expressed as mean ± standard deviation (SD) for n ≥ 3 replicates. Statistical analyses were performed using JMP software (SAS Institute). One-sample t-tests with P < 0.05 were used to identify significant fold changes or percent reductions in experimental treatments compared to a reference value. Comparisons between the means of experimental treatments were performed using ANOVA and post-hoc Tukey's test with P < 0.05 indicating significant differences.

4.2 Results

4.2.1 Cathepsin B enhances human neutrophil pseudopod activity

Human neutrophils were treated with exogenous ctsB in order to determine how Mac1-dependent neutrophil migration may be affected by proteolytic cleavage. Compared to untreated human neutrophils, those treated with exogenous ctsB (Fig. 4.3, A) displayed significantly elevated cell centroid displacement rates consistent with increased pseudopod activity (Fig. 4.3, B). The observed ctsB-mediated increases in pseudopod activity were attenuated by CA074. Notably, ctsB stimulated a greater increase in pseudopod retraction rates (by 2 to 2.5 fold over untreated cells) than in pseudopod extension rates (by approximately 1.5 fold over untreated cells) (Fig. 4.3, C). CA074 attenuated the effects of ctsB. Combined, these data are consistent with ctsB enhancing the pseudopod activity of neutrophils, likely through an effect involving Mac1 cleavage during pseudopod retraction.

49
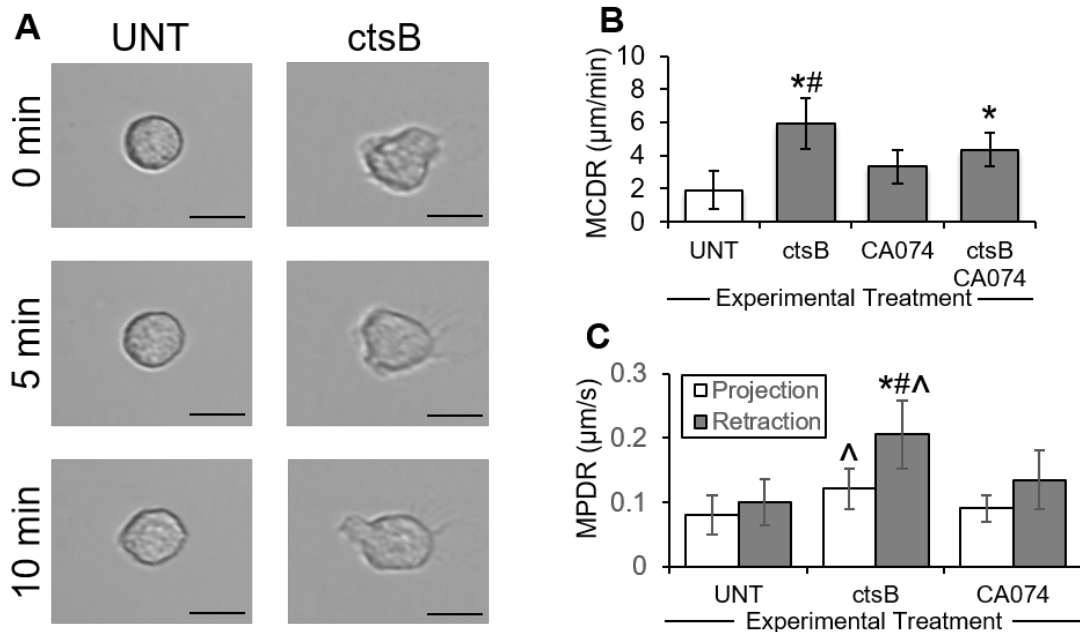
Figure 4.3. The influence of cathepsin B on neutrophil pseudopod activity.
(A) Representative images of migrating neutrophils adhered to glass slides and maintained under no-flow conditions. Untreated neutrophils were quiescent and formed few pseudopods. CtsB-stimulated neutrophils rapidly formed and retracted many pseudopods, some of which are observed in the representative images. **(B)** Neutrophil migration was quantified as mean centroid displacement rate (MCDR) over a 15 seconds and plotted as mean ± SD, based on cell tracings performed using ImageJ software. Neutrophils were treated with or without exogenous ctsB (0.5 u/mL) and ctsB-specific inhibitor CA074 (5 µM). n = 3 replicates in each group. *P < 0.05 compared to control. #P < 0.05 compared to CA074. **(C)** Neutrophil pseudopod activity during migration was quantified as mean pseudopod displacement rate (MPDR) based on manual tracings of projecting (white bars) or retracting (gray bars) pseudopods using ImageJ software. Neutrophils were treated with or without exogenous ctsB (0.5 u/mL) and ctsB-specific inhibitor CA074 (5 µM). n = 3 replicates in each group. *P < 0.05 compared to control (projection). ^P < 0.05 compared to control (retraction). #P < 0.05 compared to CA074 (projection and retraction). Scale bars are 10 µm.

4.2.2 Cathepsin B enhances dHL60-NC pseudopod activity

To further assess the potential influence of ctsB on pseudopod activity, dHL60 neutrophil-like cells were transiently transfected with ctsB-GFP expression plasmids. These cells displayed GFP fluorescence (Fig. 4.4, A), indicating that transfected cells were overexpressing ctsB-GFP. Cells transfected with empty vectors (EV) exhibited no GFP fluorescence (Fig. 4.4, B). The EV transfectants exhibited baseline cell centroid

50

displacement rates (indicative of pseudopod activity levels), while those of ctsB-GFP transfectants were significantly (P < 0.05) higher (Fig. 4.4, C). CA074 mitigated the difference in pseudopod activity between these two populations. These data further support the ability of ctsB to enhance pseudopod activity.
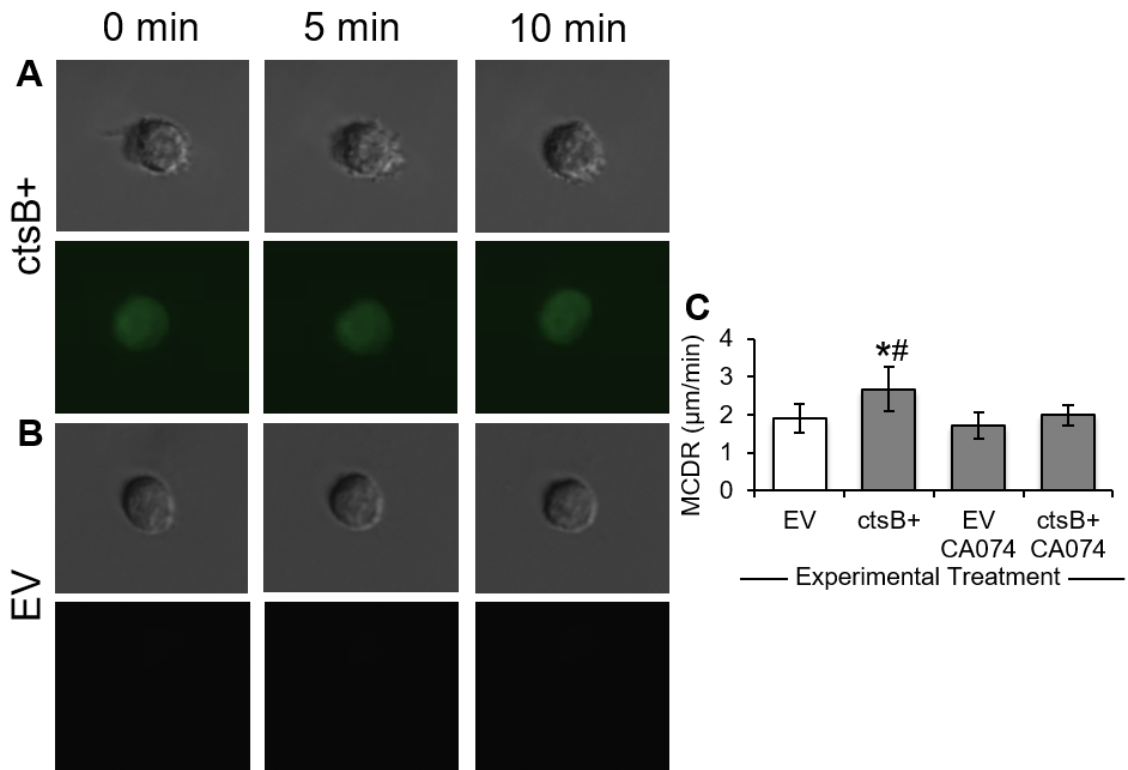
Figure 4.4. The influence of cathepsin B on dHL60-NC pseudopod activity.
(A-B) Representative images of migrating dHL60s that were transiently transfected through electroporation with a ctsB-GFP expression vector (ctsB+) or an empty vector (EV) and maintained under no-flow conditions. **(C)** DHL60 migration was quantified as mean centroid displacement rate (MCDR) over a 15 second time interval and plotted as mean ± SD, based on cell tracings manually performed using ImageJ software. DHL60s transfectants (ctsB+ or EV) were treated with or without ctsB-specific inhibitor CA074 (5 µM). n = 3 replicates in each group. *P < 0.05 compared to control. #P < 0.05 compared to CA074.

4.2.3 Fluid shear stress-induced human neutrophil detachment from substrates involves cathepsin B release

This experiment employed a flow-based cell detachment assay to evaluate the role of FSS in regulating Mac1-dependent neutrophil adhesivity. Untreated human neutrophils

51

pre-adhered to platelet monolayers exhibited time-dependent cell detachment over a 10 min period of FSS exposure (Fig. 4.5, A – B). When human neutrophils were exposed to FSS in the presence of fMLP (above threshold levels known to block neutrophil shear responses [20,112]), little detachment from platelet monolayers was observed (Fig. 4.5, C). Blocking ctsB activity with either E64 or CA074-me also caused human neutrophils to largely remain adherent to platelet monolayers under FSS. In contrast, neutrophils pretreated with irreversible serine protease inhibitor, AP (negative control), detached from platelet layers under FSS exposure in a fashion similar to that of untreated cells.

Similarly, while untreated human neutrophils adhered to HUVEC monolayers exhibited time-dependent cell detachment upon acute exposure to FSS for 10 min, both fMLP (above threshold levels that impair the neutrophil shear responsiveness) and ctsB inhibitors, E64 or CA074-me, blocked this detachment response to FSS (Fig. 4.5, D). On the other hand, pretreatment of cells with AP had no effect on FSS-induced neutrophil detachment. These results implicated the ctsB activity in the FSS-induced regulation of neutrophil adhesion to substrates.

4.2.4 Summary of findings/interpretations

The results of the present study provided evidence for the following significant findings.

- CtsB enhances neutrophil migration rates under no-flow conditions, likely through the cleavage of Mac1 integrins during the uropod retraction phase of neutrophil migration.

- FSS-induced ctsB release serves to restrict neutrophil adhesion to biological substrates through the cleavage of Mac1 integrins under flow conditions.

- Agonist stimulation overrides FSS-induced Mac1 cleavage by promoting neutrophil adhesion under flow conditions, consistent with its role in the recruitment of neutrophils during the acute inflammatory response to infection or tissue damage.
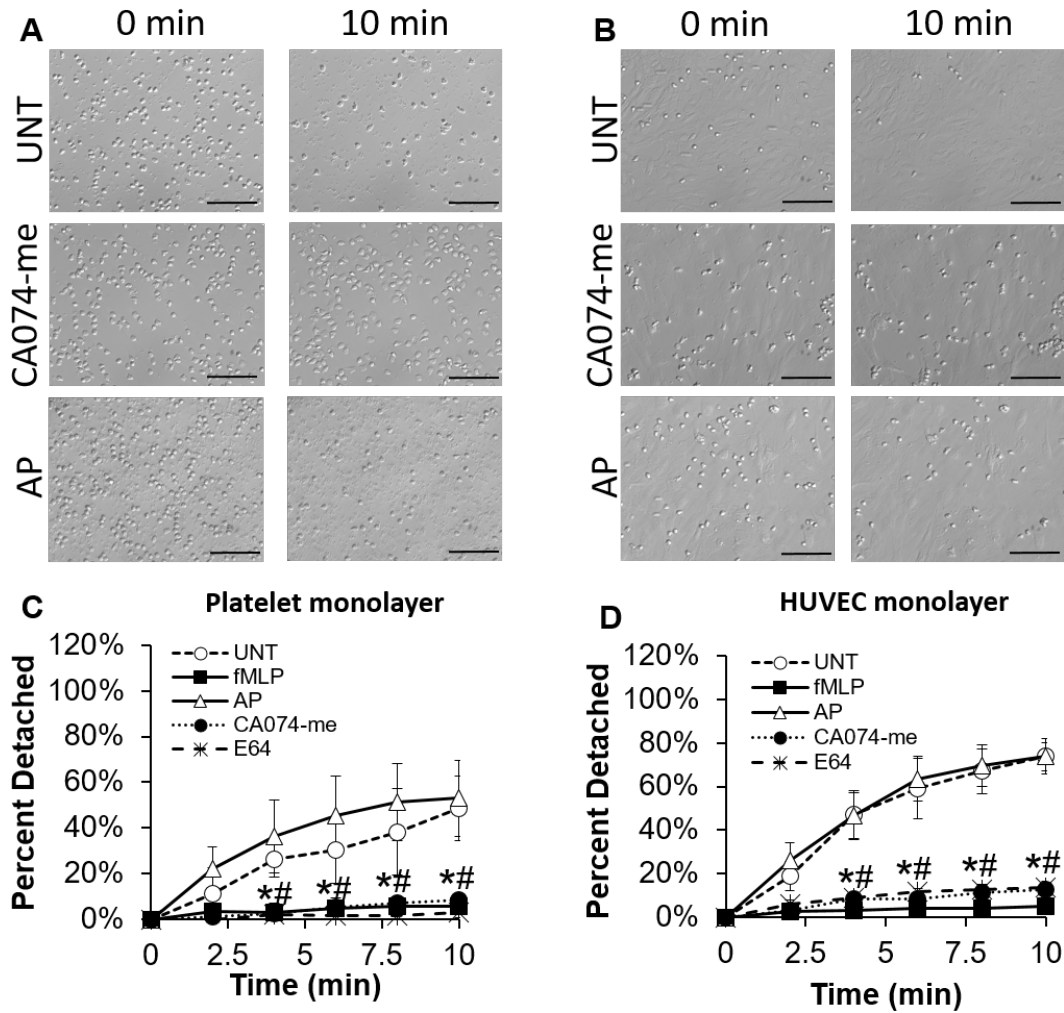
Figure 4.5. The involvement of cathepsin B in the fluid shear stress-induced detachment of neutrophils.
(A-B) Representative images depicting shear-induced neutrophil detachment from platelet (A) or HUVEC (B) monolayers in response to 5 dyn/cm^2 shear stress exposure over a 10 minute period. Neutrophils were treated with or without ctsB-specific inhibitor CA074-me (50 µM) and serine inhibitor aprotinin (AP; 5 µM). **(C-D)** The number of neutrophils remaining adherent to platelet (C) or HUVEC (D) monolayers after 10 minutes of shear exposure was normalized to the initial number of adherent neutrophils prior to shear exposure and plotted as mean ± SD, based on counts manually performed using ImageJ software. Neutrophils were left untreated or pretreated for 5 minutes with inflammatory agonist fMLP (1 µM), serine inhibitor aprotinin (AP; 5 µM), ctsB-specific inhibitor CA074-me (50 µM), or cysteine inhibitor E64 (30 µM). n = 4 replicates in each group. *P < 0.05 compared to control; #P < 0.05 compared to AP. Scale bars are 100 µm.

CHAPTER 5: DETERMINING THE EFFECTS OF EXTRACELLULAR CHOLESTEROL ELEVATIONS ON THE FLUID SHEAR STRESS CONTROL OF MAC1-DEPENDENT NEUTROPHIL ADHESION

Cholesterol is a structural component of lipid bilayers that modulates the membrane fluidity of a cell. As the cell membrane becomes enriched in cholesterol, the membrane becomes more rigid, decreasing its overall fluidity. This has implications for cell functionalities, such as actin polymerization, adhesion, and migration [125,126]. In the event that blood cholesterol rises to pathologic levels, such as during hypercholesterolemia, it is possible that the membranes of blood cells become enriched with cholesterol, which can impair their functions and contribute to microvascular dysfunction [127,128].

Previously, our lab demonstrated that membrane cholesterol enrichment blocks the pseudopod retraction response of neutrophils to FSS, likely through an impact on the membrane fluidity of the cell [27]. Furthermore, we observed that cholesterol-related blockade of pseudopod retraction was linked to dysregulated tissue blood flow, observed as impaired tissue blood flow autoregulation in response to poRH [26]. This implicated impaired neutrophil FSS mechanosensitivity as an early forecaster of microvascular dysfunction. However, it was unclear how a deficit in neutrophil FSS sensitivity, indexed by the ability of fluid flow stimulation to restrict neutrophil activity, contributes to the progression of microvascular dysfunction involving changes in hemodynamic resistance.

Reports in the literature [21], as well as the present dissertation thesis, indicate that the adhesivity of neutrophils appears to be minimized due to FSS regulation. This suggests that a deficit in neutrophil FSS sensitivity may contribute to dysregulated adhesion by impairing this mechanoregulatory control mechanism which involves ctsB-related Mac1

المنارة للاستشارات

www.manaraa.com

cleavage. Notably, dysregulated leukocyte adhesion in the microcirculation is also a feature of hypercholesterolemic pathobiology associated with microvascular dysfunction [77]. Combined, these support the possibility that an impaired FSS mechanosensitivity due to hypercholesterolemia manifests as dysregulation of not only neutrophil pseudopod activity, but also cell adhesion.

The study described in this chapter focused on revealing new mechanistic insight regarding an impairment in the control of neutrophil adhesion by FSS as a putative link between the pathogenesis of hypercholesterolemia, dysregulated neutrophil adhesion in the microcirculation, and microvascular dysfunction. Specifically, we examined the possibility that excess cholesterol in the local environment of the neutrophils due to pathological blood cholesterol elevations attenuates their FSS-induced Mac1 cleavage response, which dysregulates neutrophil adhesion and leads to microvascular dysfunction. For this purpose, we conducted a series of ex vivo human blood studies to explore how cholesterol-related changes to the membrane fluidity of neutrophils could block FSS regulation of Mac1 surface expression and neutrophil adhesion under flow. The present study also used a hypercholesterolemic murine animal model to confirm that pathological blood cholesterol elevations in the *in vivo* setting promotes dysregulation of neutrophil adhesion by FSS and that this dysregulation is potentially related to the onset of dysregulated tissue blood flow indicative of a deficit in the control of the microcirculatory function.

55

5.1 Methods

5.1.1 Cells

      Human subject recruitment, informed consent, and phlebotomy were approved by the University of Kentucky Institutional Review Board. Blood was harvested from asymptomatic volunteers into K_2-EDTA-coated vacutainers (Becton-Dickinson) through the use of standard venipuncture, as previously reported. Human neutrophils were purified from the whole blood samples as described in section 3.1.1a and suspended in HBSS containing calcium and magnesium. Parallel to neutrophil isolation, platelets were also extracted from plasma as reported in section 4.1.1a.

5.1.2 Human neutrophil experimental treatments

      To enhance membrane cholesterol content, human neutrophils suspended in HBSS were treated with 0 – 10 µg/mL cholesterol:MβCD complexes for 15 minutes. After treatment, neutrophils were washed in PBS and resuspended in HBSS to remove excess cholesterol conjugates from the cell suspension. For some experiments, human neutrophils treated with 2 µg/mL cholesterol:MβCD conjugates were subsequently exposed to 0 – 7 mM benzyl alcohol (BnOH) or 0 – 12 mM ethanol (EtOH) for 10 minutes to reverse the effects of cholesterol enrichment.

5.1.3 Cone-and-plate shear exposure

      Human neutrophils in HBSS were exposed to a constant (5 dyn/cm^2) laminar FSS field for 10 min using a custom cone-plate device as described in section 3.1.2.

Experiments were also conducted with cell suspensions enriched with cholesterol:MβCD complexes and treated with or without BnOH or ethanol as described in section 5.1.2. Controls were parallel cell populations maintained under static (no-FSS), but otherwise similar experimental, conditions.

5.1.4 Immunofluorescence

Immediately after cone-and-plate shear exposure, cells were fixed (1% p-formaldehyde in phosphate buffer) and labeled with fluorescent antibodies in 1% BSA in PBS using standard immunocytochemistry described in section 3.1.3. For human neutrophils, FITC-conjugated mouse monoclonal antibody (mAb) to CD18 (clones 6.7) or Alexa Fluor 488-conjugated mouse mAb to CD11b (clone ICRF44) was used to assess surface expression of adhesion integrins. Rabbit polyclonal (pAb) against ctsB (clone Ab-3) and Alexa Fluor 488-conjugated goat pAb (Invitrogen) were also used to assess total ctsB expression by permeabilized cells, respectively, as described in section 3.1.3.

5.1.5 Neutrophil detachment assay

Autologous human platelets were deposited on sterile glass slides cleaned with NaOH and allowed to spread into a uniform coating for 30 min as described in section 4.1.3. To create a flow channel for experimentation, the platelet-coated slides were interfaced with a polycarbonate base with both inlet and outlet ports, as described in section 4.1.3. A pre-cut gasket separating the glass slide and the polycarbonate base formed a 200-µm high parallel plate flow channel.

For flow studies, neutrophils ($5x10^6$/mL) were pretreated for 15 minutes with 2 µg/mL cholesterol:MβCD complexes. After PBS washing to remove excess complexes, neutrophils were treated for 10 minutes with or without 1 – 2 mM BnOH or 7 – 8 mM ethanol. Controls were neutrophils that were left untreated. Cells were then deposited on the platelet monolayers for 10 min, at which time non-adherent cells were rinsed away. A syringe pump was used to impose a FSS of 5 dyn/cm^2 on the wall of the channel by perfusing HBSS through the chamber, as described in section 4.1.3. Bright field micrographs (100X magnification) of the neutrophils were acquired every 5 s over a 10 min period, and neutrophil detachment was estimated by normalizing the number of neutrophils visible in each image against that present 30 seconds after flow initiation. This initial time point was defined to be t = 0 to ensure non-adherent cells were rinsed away prior to analyses.

5.1.6 Animal studies

5.1.6a Mice

All handling procedures were approved by the University of Kentucky Institutional Animal Care and Use Committees. Male low-density lipoprotein receptor-deficient (LDLR$^{-/-}$) mice were purchased from the Jackson Laboratory and acclimated for 1 week prior to use. Starting from 8 weeks of age, mice were fed a high fat diet (HFD) enriched in saturated fat (21% wt/wt fat and 0.15% wt/wt cholesterol; Harland Teklad) for up to 8 weeks to induce hypercholesterolemia. Controls were aged-matched LDLR$^{-/-}$ mice fed a normal diet (ND; regular chow) for the same duration.

The blood flow recovery responses of mice were measured in real-time using Near-Infrared (NIR) Diffuse Correlation Spectroscopy (DCS), a technique developed by our collaborator, Dr. Guoqiang Yu (University of Kentucky) [129,130]. DCS works by directly measuring the motion of RBCs to calculate the rate of blood flow. This technique utilizes a probe that contains a light source and a detector separated by 6 mm to enable detection of relative change of blood flow (rBF) within the muscle tissue [131]. The detector picks up the photons emitted from the light source and, depending on the degree of photon fluctuations, converts the signals into real-time rBF measurements. During blood flow, the RBCs are primarily responsible for the photon fluctuations that are detected. DCS has the advantage of being able to non-invasively measure rBF through deep tissue. The data on rBF for our experiments was displayed in real-time on a computer monitor to evaluate the responses of mice to blood flow occlusion (Fig. 5.1, A).

Prior to experimentation, mice were anesthetized by inhalation of 1% isoflurane (Butler Schein) and the hair on the right hindlimb of each mouse was shaved from the skin. A makeshift noose was fashioned from PVC tubing (0.05'' outer diameter) and loosely wrapped around the proximal end of the right hindlimb so as to not restrict blood flow. Distal to the PVC noose, a foam pad equipped with a DCS probe was super-glued to the right hindlimb (Fig. 5.1, B). DCS measurement of rBF was recorded for 5 minutes to establish a baseline reading. Once the baseline was determined, the PVC noose was tightened until the real-time DCS measurement of rBF was reduced to zero. Data was collected for 5 minutes during occlusion, at which point the PVC noose was released using a high temperature surgical cautery pen to sever the knot and instantaneously reintroduce

59

flow to the target tissue of interest. Data continued to be collected until rBF had recovered to baseline levels. During the procedure, the body temperature of each mouse was maintained at 37°C for the duration of the experiment by using a heating pad. After rBF data had been collected, the mice were euthanized by thoracotomy and exsanguination. Blood was harvested from mice (~750 µL) for use in cone-and-plate shear experiments. A small aliquot of blood (~250 µL) was also set aside for cholesterol measurements.
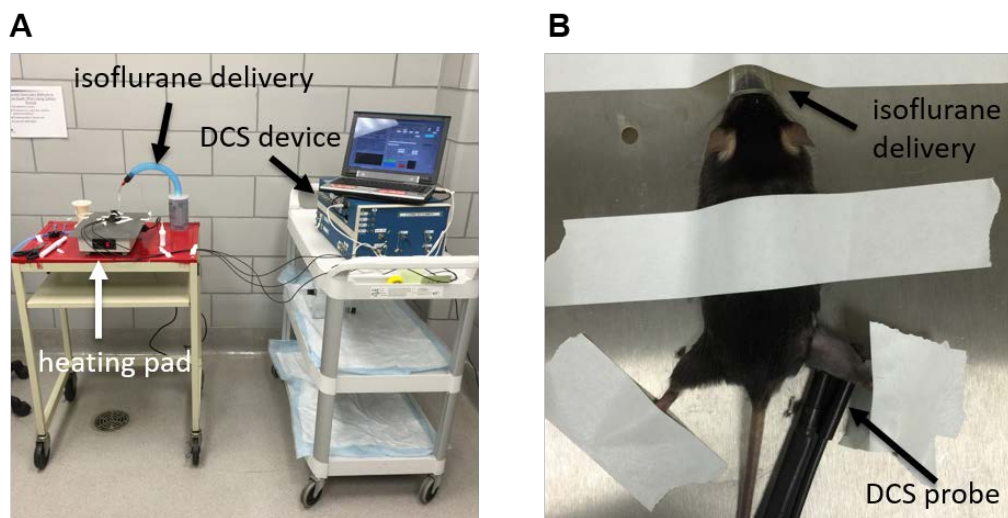
Figure 5.1. Animal study experimental set-up.
(A) Figure depicting the experimental set-up used for murine analyses. The DCS instrumentation is shown to the right, and the heating pad with mouse is shown to the left. (B) Figure depicting the mouse on the heating pad. Tape was used to ensure the mouse remained stationary. The nose of the mouse was placed in a tube delivering 1% isoflurane, visible at the top of the image. The DCS probe is seen attached to the right hindlimb of the mouse.

5.1.6c Analysis of DCS rBF measurements

MATLAB was used to analyze rBF data from LDLR$^{-/-}$ mice (Fig. 5.2). We plotted rBF against time in order to identify the highest rate of blood flow. This peak blood flow was defined to be the greatest rBF value attained after the end of occlusion. In order to reduce the variability due to noise, all rBF values within 10% of the peak blood flow were

60

averaged together and defined as adjusted peak flow (APF). We also calculated the length of time from cuff release to APF, which was reported as tAPF in our analyses.
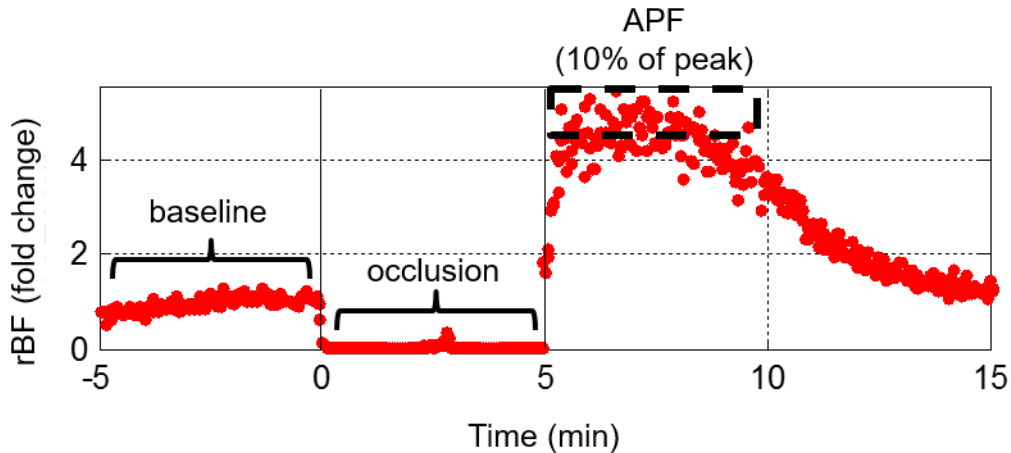
Figure 5.2. Representative image of adjusted peak flow analysis.
This plot is used to identify all rBF values within 10% of the peak blood flow. The values are averaged together and defined as adjusted peak flow (APF). The length of time from cuff release to APF was also calculated and reported as tAPF in our analyses.

<u>5.1.6d Plasma cholesterol quantification</u>

Plasma was harvested from LDLR$^{-/-}$ mice blood aliquots by centrifugation (1000xg, 5 min) and used to quantify the free, total, and esterified cholesterol levels in the mice. The concentration of free cholesterol was estimated by using the Free Cholesterol E kit (Wako) according to the manufacturer's instructions. Absorbance values were measured at 600 nm using a BioTek microplate reader (µQuant). The concentration of total cholesterol was estimated by using the Infinity Cholesterol Reagent (Sigma Aldrich) according to the manufacturer's instructions. Absorbance values were measured at 500 nm using the same BioTek microplate reader. The concentration of esterified cholesterol was estimated from the free and total cholesterol levels using the established relationship [132]:

$$Esterified\ cholesterol = (Total\ cholesterol - Free\ cholesterol) \times 1.67$$

61

Whole mice blood diluted 1:10 (v/v) with HBSS was exposed to a constant (5 dyn/cm^2) laminar FSS field for 10 min using a custom cone-plate device as described in section 3.1.2. Experiments were conducted with no additional treatments. Controls were parallel cell populations maintained under static (no-FSS), but otherwise similar experimental, conditions.

5.1.6f Immunofluorescence

Immediately after cone-and-plate shear exposure, cells were fixed (1% p-formaldehyde in phosphate buffer) and labeled with fluorescent antibodies in 1% BSA in PBS using standard immunocytochemistry described in section 3.1.3. For murine neutrophils, erythrocytes were removed after fixation using RBC lysis buffer (Sigma-Aldrich) followed by PBS washes. Immunofluorescence was carried out using FITC-conjugated rat mAb to CD18 (clone GAME-46), PE-conjugated rat mAb to CD11a (clone M17/4), or FITC-conjugated rat mAb to CD11b (clone M1/70) to assess surface expression of adhesion integrins, as described in section 3.1.3.

5.1.7 Flow cytometry

Flow cytometric analyses utilized an LSR II flow cytometer (Becton-Dickinson) interfaced with Becton-Dickinson FACsDiva software, as previously reported [59]. Neutrophil populations were identified through their FSC, SSC, and CD18 expression as previously described. The total fluorescence intensities representing the amount of bound

antibodies were used as measures of antigen specific expression level. By using the total fluorescence intensities, histograms of antigen-specific fluorescence intensities were generated for each sample using FCS Express 4 Flow Cytometry software (De Novo Software). Shear-induced changes in the antigen expression levels were normalized to those of their respective controls and expressed as "fold change".

5.1.8 Statistics

Quantitative data derived using human or murine neutrophils were expressed as mean $\pm$ SD for n $\geq$ 3 replicates. Statistical analyses were performed using JMP (SAS Institute). One-sample t-tests with $P < 0.05$ were used to identify significant fold changes or percent reductions in experimental treatments compared to a reference value. Comparisons between the means of experimental treatments were performed using ANOVA and post-hoc Tukey's test with $P < 0.05$ indicating significant differences. Linear regression analysis was also performed using JMP to determine the correlation between cholesterol, FSS-induced Mac1 cleavage, APF, and tAPF.

5.2 Results

5.2.1 Membrane cholesterol enrichment blocks the shear-induced Mac1 cleavage response

Human neutrophils exposed to 5 dyn/cm^2 FSS over a 10 min period exhibited reduced expression of CD18 and CD11b integrins relative to time-matched, unsheared controls (Fig. 5.3, A – B). This reduction in integrin expression was dose-dependently blocked for neutrophils pretreated with cholesterol. Notably, neutrophils treated with cholesterol

63

concentrations from 2 – 10 µM did not exhibit significant reductions in CD18 and CD11b integrins after being exposed to FSS (Fig. 5.3, C – D). These results suggested that membrane cholesterol enrichment impaired FSS-induced Mac1 cleavage response.
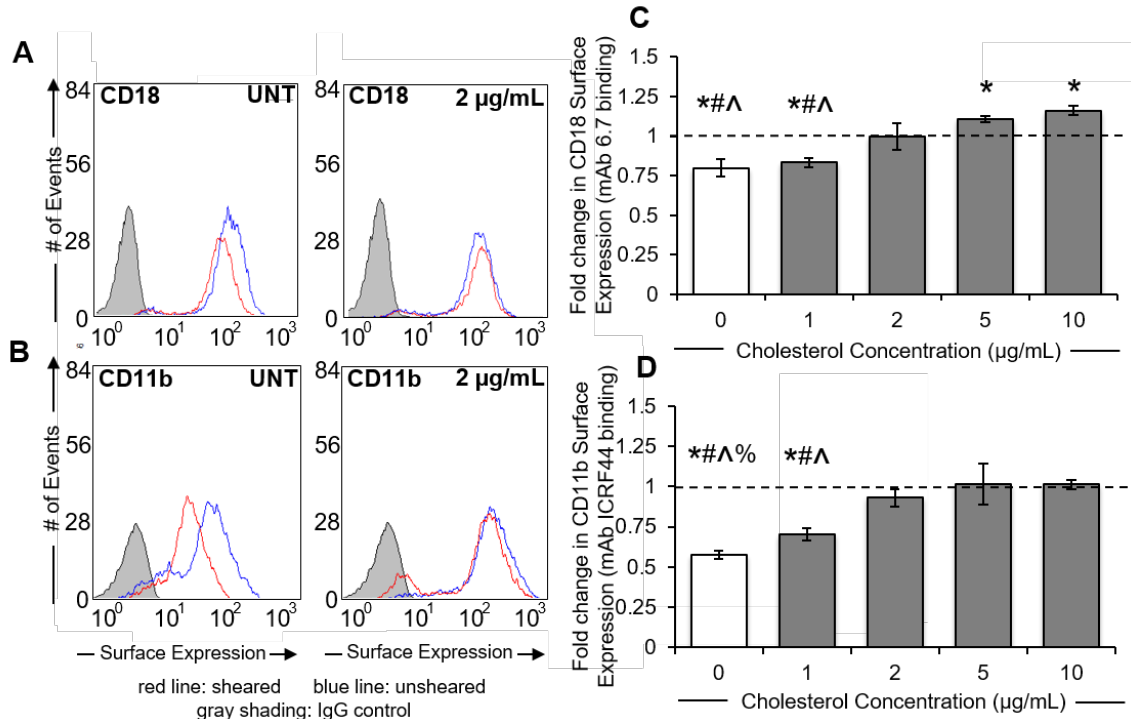
Figure 5.3. Membrane cholesterol enrichment blocks FSS-induced Mac1 cleavage.
(A-B) Representative flow cytometry histograms depicting the fluorescent intensity of intact CD18 (A) and CD11b (B) expressed on the surface of neutrophil suspensions maintained under no-flow conditions (blue line) or subjected to 5 dyn/cm^2 shear stress (red line) using a cone-and-plate viscometer. A negative (IgG) staining control is also displayed in each plot (gray shading). Neutrophil suspensions were treated with 0 – 10 µg/mL cholesterol. **(C-D)** Based on florescent antibody binding, mean fluorescent intensities of sheared neutrophils were normalized to their respective no-flow controls and plotted as fold change ± SEM for CD18 (C) and CD11b (D) integrins. n = 3 replicates in each group. *P < 0.05 compared to a normalized control value of 1 (dotted line). #P < 0.05 compared to 5 µg/mL. ^P < 0.05 compared to 10 µg/mL. %P < 0.05 compared to 2 µg/mL.

5.2.2 Membrane fluidizers reverse cholesterol inhibition of Mac1 cleavage

Human neutrophils pretreated with 2 µg/mL cholesterol and exposed to 5 dyn/cm^2 FSS expressed similar levels of CD18 and CD11b on their surface relative to time-matched, unsheared controls (Fig. 5.4, A – B). BnOH, a membrane fluidizer [133], selectively recovered the ability of FSS exposure to promote a reduction in CD18 and CD11b surface

levels on neutrophils treated with 2 µg/mL cholesterol. Specifically, cholesterol-enriched neutrophils treated with 1 – 2 mM BnOH exhibited reduced CD18 and CD11b expression after FSS exposure, a response similar to that of naïve cells. In contrast, cholesterol-enriched neutrophils treated with 0 – 0.5 mM and 5 – 7 mM BnOH did not exhibit reductions in CD18 and CD11b expression after FSS exposure (Fig. 5.4, C – D). These data provided evidence that the blockade of FSS-induced Mac1 cleavage depends on the membrane fluidity of the cells. Furthermore, there appears to be an optimal membrane fluidity that is conducive for an intact Mac1 cleavage response of neutrophils to FSS.
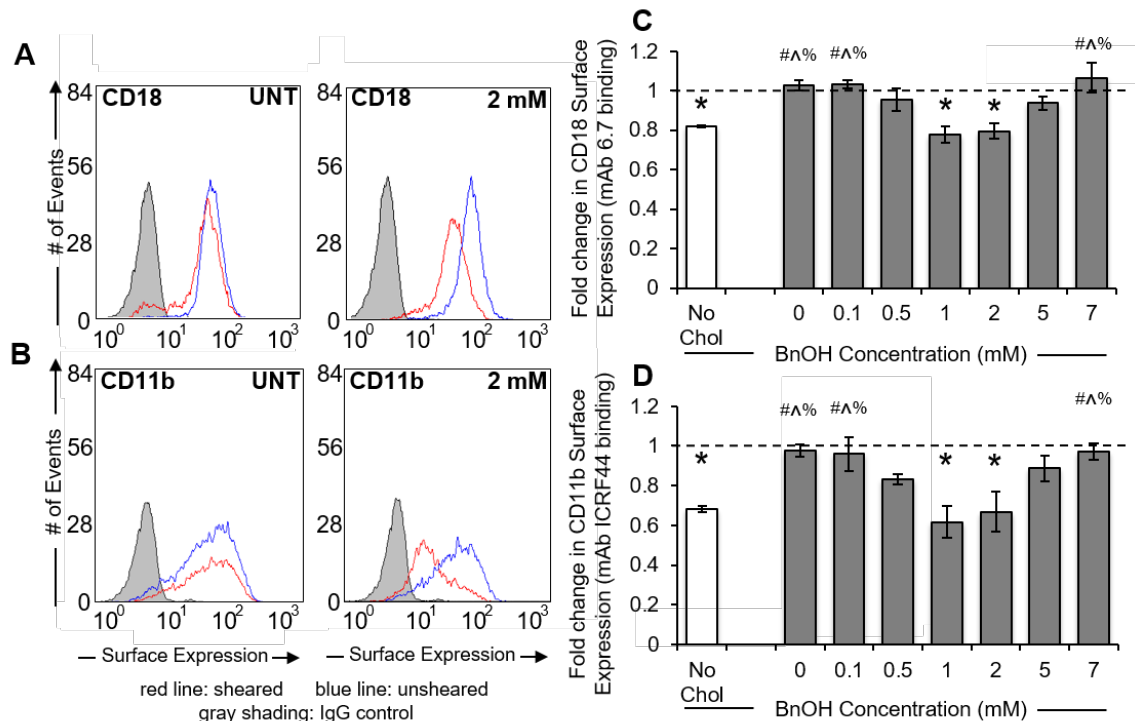
Figure 5.4. Benzyl alcohol reverses the effects of membrane cholesterol enrichment. **(A-B)** Representative flow cytometry histograms depicting the fluorescent intensity of intact CD18 (A) and CD11b (B) expressed on the surface of cholesterol-enriched neutrophil suspensions maintained under no-flow conditions (blue line) or subjected to 5 dyn/cm^2 shear stress (red line) using a cone-and-plate viscometer. A negative (IgG) staining control is also displayed in each plot (gray shading). Neutrophil suspensions were treated with 0 – 7 mM BnOH. **(C-D)** Based on florescent antibody binding, mean fluorescent intensities of sheared neutrophils were normalized to their respective no-flow controls and plotted as fold change ± SEM for CD18 (C) and CD11b (D) integrins. n = 3 replicates in each group. *P < 0.05 compared to a normalized control value of 1 (dotted line). #P < 0.05 compared to 1 mM. ^P < 0.05 compared to 2 mM. %P < 0.05 compared to no chol.

Similarly to BnOH, EtOH, another membrane fluidizing reagent [134], was shown to selectively reverse the blocking effects of membrane cholesterol enrichment on FSS-induced Mac1 cleavage (Fig. 5.5, A – B). Briefly, treatment of cholesterol-enriched neutrophils with 7 – 8 mM EtOH resulted in reduced surface expression of intact CD18 and CD11b integrin subunits on neutrophils after exposure to FSS, similar to that of naïve cells. In contrast, treatment of cholesterol-enriched neutrophils with 0 – 5 mM or 10 – 12 mM EtOH did not exhibit reductions in CD18 and CD11b expression after FSS exposure (Fig. 5.5, C – D). These data further supported the existence of an optimal membrane fluidity level permissive for an intact Mac1 cleavage response of neutrophils to shear.
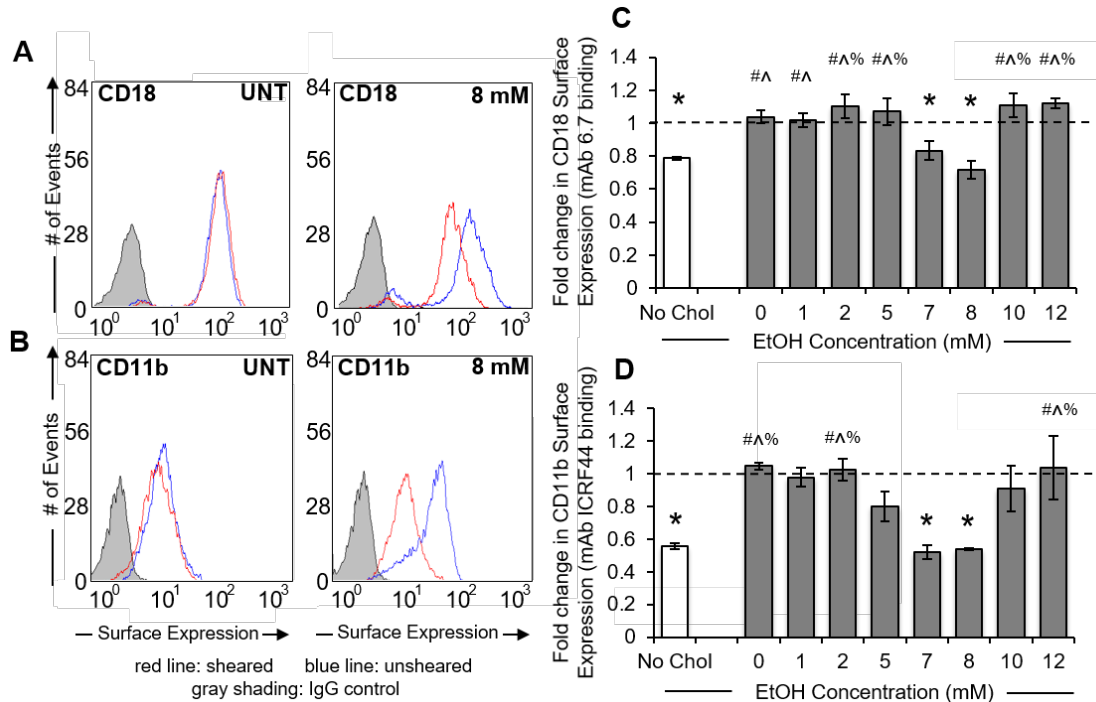
Figure 5.5. Ethanol reverses the effects of membrane cholesterol enrichment.
(A-B) Representative flow cytometry histograms depicting the fluorescent intensity of intact CD18 (A) and CD11b (B) expressed on the surface of cholesterol-enriched neutrophil suspensions maintained under no-flow conditions (blue line) or subjected to 5 dyn/cm^2 shear stress (red line) using a cone-and-plate viscometer. A negative (IgG) staining control is also displayed in each plot (gray shading). Neutrophil suspensions were treated with 0 – 12 mM EtOH. **(C-D)** Based on florescent antibody binding, mean fluorescent intensities of sheared neutrophils were normalized to their respective no-flow controls and plotted as fold change ± SEM for CD18 (C) and CD11b (D) integrins. n = 3 replicates in each group. *$P < 0.05$ compared to a normalized control value of 1 (dotted line). #$P < 0.05$ compared to 7 mM. ^$P < 0.05$ compared to 8 mM. %$P < 0.05$ compared to no chol.

66

5.2.3 Membrane cholesterol enrichment blocks the shear-induced release of cathepsin B

Human neutrophils exposed to 5 dyn/cm^2 FSS over a 10 min period using a cone-plate device exhibited reduced cytosolic levels of ctsB relative to time-matched, unsheared controls (Fig. 5.6, A). This observation suggested that FSS stimulated the release of ctsB into the extracellular milieu. Pretreatment of neutrophils with cholesterol blocked this FSS response. Specifically, neutrophils treated with 2 – 10 µg/mL exogenous cholesterol and either exposed to FSS for 10 min or maintained under static no-flow conditions displayed similar levels of ctsB. Thus, exogenous cholesterol administration dose-dependently blocks FSS-induced ctsB release (Fig. 5.6, B).
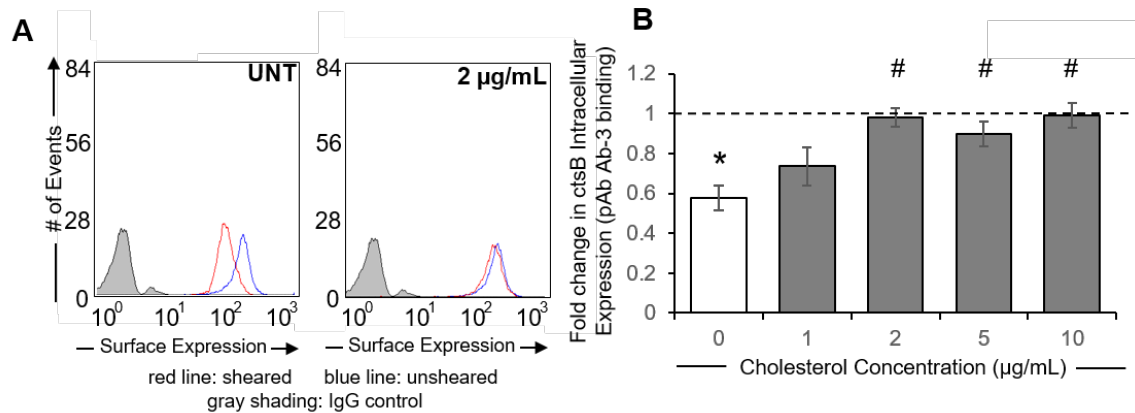
Figure 5.6. Cholesterol enrichment blocks shear-induced release of cathepsin B.
(A) Representative flow cytometry histograms depicting the fluorescent intensity of ctsB expressed in neutrophil suspensions maintained under no-flow conditions (blue line) or subjected to 5 dyn/cm^2 shear stress (red line) using a cone-and-plate viscometer. A negative (IgG) staining control is also displayed in each plot (gray shading). Neutrophil suspensions were treated with 0 – 10 µg/mL cholesterol. **(B)** Based on florescent antibody binding, mean fluorescent intensities of sheared neutrophils were normalized to their respective no-flow controls and plotted as fold change ± SEM for ctsB. n = 3 replicates in each group. *$P < 0.05$ compared to a normalized control value of 1 (dotted line). #$P < 0.05$ compared to 0 mM.

5.2.4 Membrane fluidizers reverse the cholesterol-related inhibition of cathepsin B release

Human neutrophils pretreated with 2 µg/mL cholesterol and exposed to 5 dyn/cm^2 FSS over a 10 min period exhibited similar expression levels of the protease ctsB relative to time-matched, unsheared controls (Fig. 5.7, A). BnOH selectively recovered the ability of FSS exposure to promote a reduction in ctsB expression by neutrophils treated with 2 µg/mL cholesterol. Specifically, treatment of cholesterol-enriched neutrophils with 1 – 2 mM BnOH reduced the expression of ctsB after FSS exposure, a response similar to naïve neutrophils. In contrast, cholesterol-enriched neutrophils treated with 0 – 0.5 mM and 5 – 7 mM BnOH did not exhibit reduced ctsB expression after FSS exposure (Fig. 5.7, B).
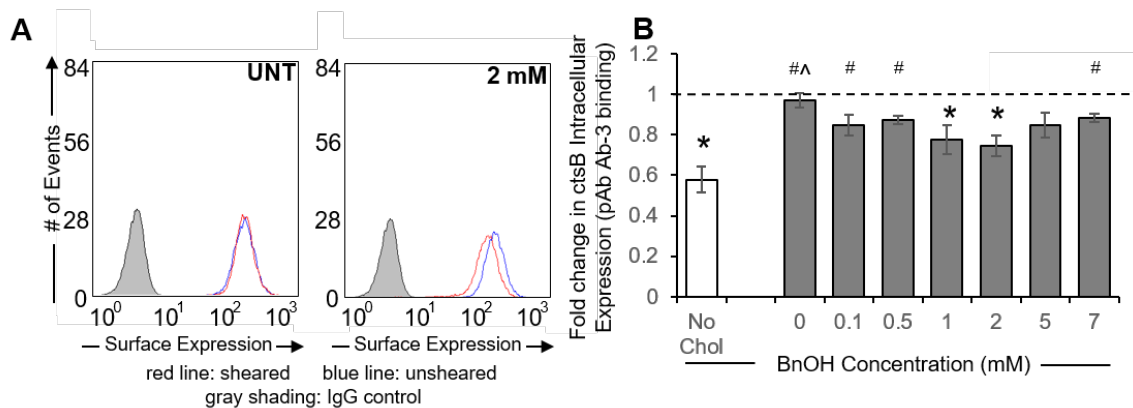
Figure 5.7. Benzyl alcohol recovers the shear-induced release of cathepsin B.
(A) Representative flow cytometry histograms depicting the fluorescent intensity of ctsB expressed in neutrophil suspensions treated with BnOH and maintained under no-flow conditions (blue line) or subjected to 5 dyn/cm^2 shear stress (red line) using a cone-and-plate viscometer. A negative (IgG) staining control is also displayed in each plot (gray shading). Neutrophil suspensions were treated with 0 – 7 mM BnOH. **(B)** Based on florescent antibody binding, mean fluorescent intensities of sheared neutrophils treated with BnOH were normalized to their respective no-flow controls and plotted as fold change ± SEM for ctsB. n = 3 replicates in each group. *P < 0.05 compared to a normalized control value of 1 (dotted line). #P < 0.05 compared to no chol. ^P < 0.05 compared to 2 mM.

Similarly to BnOH, EtOH was also able to selectively reverse the effects of membrane cholesterol enrichment (Fig. 5.8, A). Treatment of cholesterol-enriched neutrophils with 7 – 8 mM EtOH reduced the expression of ctsB after FSS exposure, a response similar to naïve neutrophils. In contrast, cholesterol-enriched neutrophils treated with 0 – 5 mM and 10 – 12 mM EtOH did not exhibit reductions in ctsB expression after FSS exposure (Fig. 5.8, B). Because we previously demonstrated ctsB to be involved in the selective cleavage of Mac1 integrins, these data further support the existence of an optimal membrane fluidity level permissive for an intact Mac1 cleavage response. Notably, the BnOH (1 – 2 mM) and EtOH (7 – 8 mM) concentrations which recover ctsB release also recover Mac1 cleavage, which is in line with the ability of ctsB to cleave Mac1 under shear exposure.
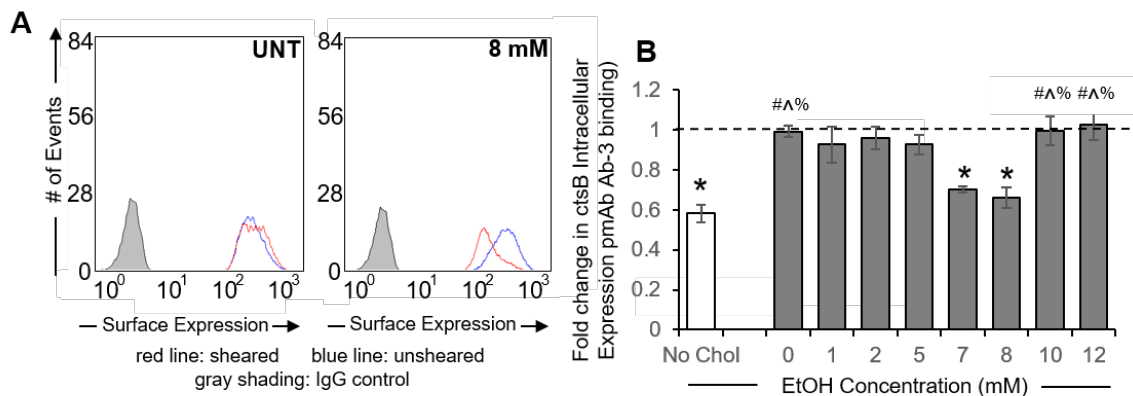
Figure 5.8. Ethanol recovers the shear-induced release of cathepsin B.
(A) Representative flow cytometry histograms depicting the fluorescent intensity of ctsB expressed in neutrophil suspensions treated with EtOH and maintained under no-flow conditions (blue line) or subjected to 5 dyn/cm^2 shear stress (red line) using a cone-and-plate viscometer. A negative (IgG) staining control is also displayed in each plot (gray shading). Neutrophil suspensions were treated with 0 – 12 mM EtOH. **(B)** Based on florescent antibody binding, mean fluorescent intensities of sheared neutrophils treated with EtOH were normalized to their respective no-flow controls and plotted as fold change ± SEM for ctsB. n = 3 replicates in each group. *$P < 0.05$ compared to a normalized control value of 1 (dotted line). #$P < 0.05$ compared to 7 mM. ^$P < 0.05$ compared to 8 mM. %$P < 0.05$ compared to no chol.

5.2.5 *Fluid shear stress-induced regulation of neutrophil adhesion is inhibited by membrane cholesterol enrichment*

This experimental assay, similar to the one described in section 4.1.3, is used as a measure of neutrophil adhesivity. As previously shown, untreated human neutrophils pre-adhered to platelet monolayers exhibited time-dependent cell detachment over a 10 min period of FSS exposure (Fig. 5.9, A). Pretreatment of neutrophils with 2 µg/mL cholesterol prior to incorporation into our cell detachment assay attenuated the ability of FSS exposure to promote their detachment from platelet monolayers (Fig. 5.9, B). This blockade was reversible by treating cells with membrane fluidizers, BnOH or EtOH, at concentrations that we showed to be capable of recovering FSS-induced Mac1 cleavage and ctsB release by neutrophils treated with similar concentrations of exogenous cholesterol. Specifically, neutrophils pretreated with 2 µg/mL cholesterol and subsequently subjected to the flow-based cell detachment assay in the presence of either 2 mM BnOH or 8 mM EtOH exhibited significant detachment from platelet layers under FSS exposure, a response that was similar to that of untreated cells.
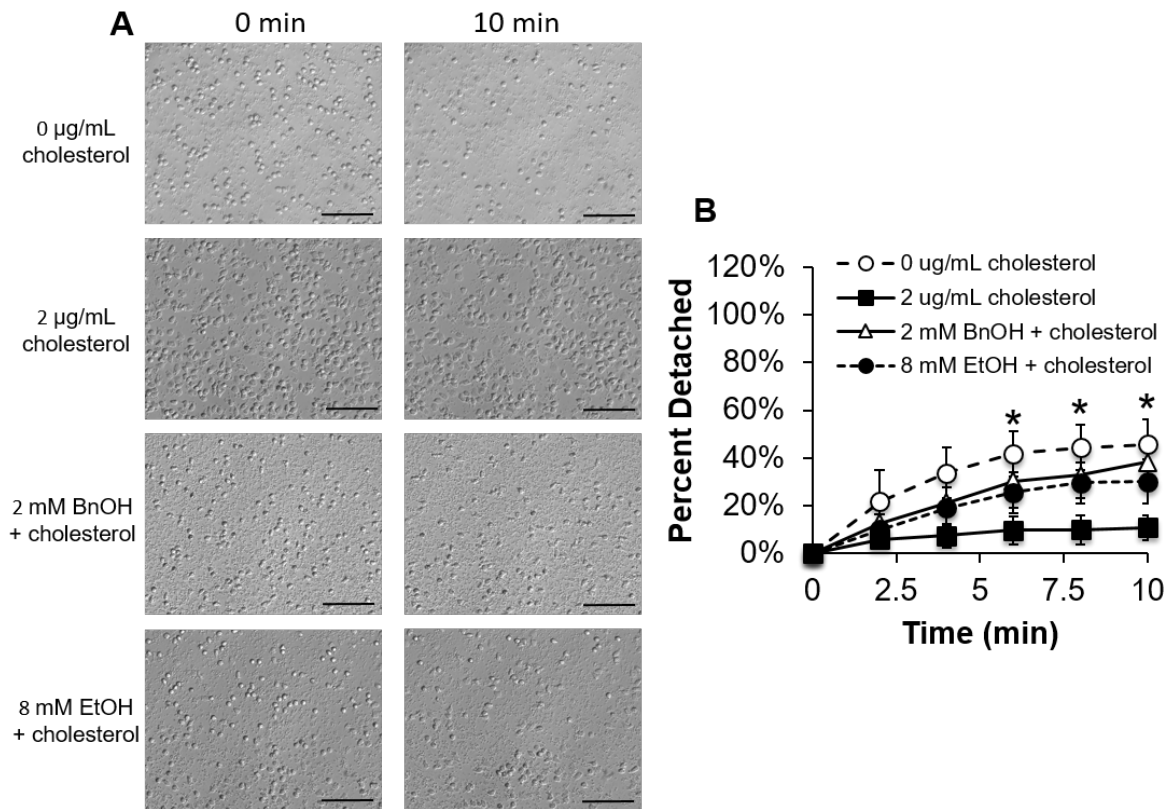
Figure 5.9. Fluid shear stress-mediated regulation of neutrophil adhesion is inhibited by cholesterol enrichment.
(A) Representative images depicting shear-induced neutrophil detachment from platelet monolayers in response to 5 dyn/cm^2 shear stress exposure over a 10 minute period. Neutrophils were left untreated or pretreated with or without 2 µg/mL cholesterol, 2 mM BnOH, or 8 mM EtOH. (B) The number of neutrophils remaining adherent to platelet monolayers after 10 minutes of shear exposure was normalized to the initial number of adherent neutrophils prior to shear exposure and plotted as mean ± SEM, based on counts manually performed using ImageJ software. Neutrophils were left untreated or pretreated with or without 2 µg/mL cholesterol, 2 mM BnOH, or 8 mM EtOH. n = 3 replicates in each group. *P < 0.05 compared to 2 µg/mL cholesterol. Scale bars are 100 µm.

71

5.2.6 Hypercholesterolemia inhibits fluid shear stress-induced Mac1 cleavage

Table 5.1 lists the free, total, and esterified cholesterol concentrations in the blood of male LDLR^{-/-} mice fed a ND or HFD for 6 – 8 weeks. We observed increases in cholesterol levels that were dependent on the diet duration, consistent with the gradual onset of hypercholesterolemia due to high fat intake. The free and total cholesterol levels of 8 week HFD mice were significantly elevated compared to 6 week HFD mice. In addition, the cholesterol levels of LDLR^{-/-} mice fed a HFD were significantly elevated compared to LDLR^{-/-} mice fed a ND, further confirming the onset of hypercholesterolemia in HFD mice. The free and total cholesterol levels of 6 week ND mice, in contrast, were no different than those of 8 week ND mice.

Table 5.1. Cholesterol concentrations in the blood of LDLR^{-/-} mice.

Cholesterol Type	Diet	Cholesterol Concentration (mg/dl)	
		6 weeks	8 weeks
Free	ND	75.8 ± 8.1	69.8 ± 16.5
	HFD	304.0 ± 86.1 *	416.6 ± 60.3 *#
Total	ND	225 ± 27.8	211.8 ± 44.8
	HFD	759.2 ± 78.3 *	829.0 ± 31.8 *#
Esterified	ND	249.2 ± 33.6	237.1 ± 49.6
	HFD	760.1 ± 98.5 *	688.6 ± 70.5 *#

$*P < 0.05$ compared to diet duration-matched LDLR^{-/-} mice fed a normal diet (ND)
$\#P < 0.05$ compared to LDLR^{-/-} mice fed a high fat diet (HFD) for 6 weeks

Murine leukocytes in blood harvested from LDLR^{-/-} mice fed a ND and exposed to 5 dyn/cm^2 FSS for 10 min with a cone-plate device exhibited reduced surface expression of CD18 and CD11b, but not CD11a, integrins relative to time-matched, unsheared controls (Fig. 5.10, A – B). In contrast, FSS exposure had little effect on the surface expression of intact CD18, CD11a, and CD11b integrins on leukocytes in the blood of mice fed a HFD for either 6 weeks or 8 weeks. Leukocytes from the 6 week HFD mice exhibited an

72

attenuated FSS-induced Mac1 cleavage response, while leukocytes from the 8 week HFD

mice exhibited a complete inhibition of FSS-induced Mac1 cleavage.
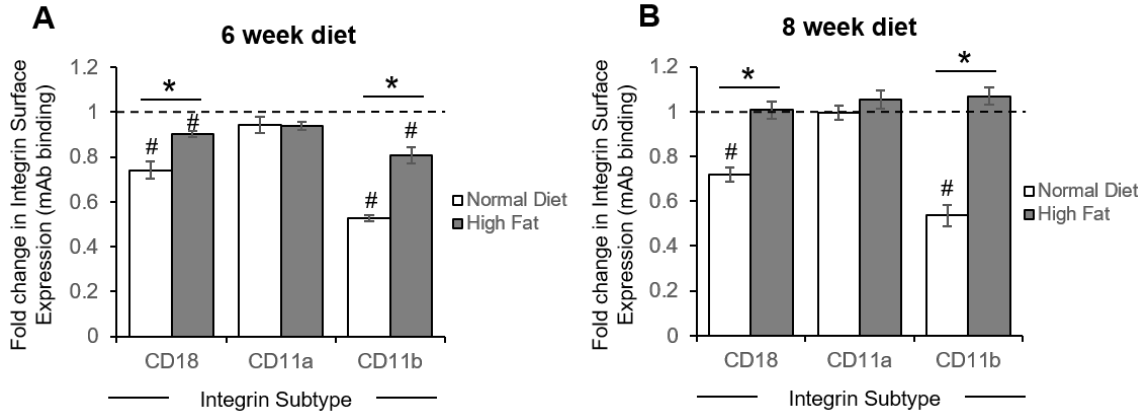
Figure 5.10. Hypercholesterolemia inhibits the fluid shear stress-induced Mac1 cleavage response.
(A-B) Based on florescent antibody binding to neutrophils from mice fed a diet for 6 weeks
(A) or 8 weeks (B), mean fluorescent intensities of sheared neutrophils were normalized to
their respective no-flow controls and plotted as fold change ± SEM for CD18, CD11a, and
CD11b integrins. n = 8 replicates in each group. *P < 0.05 indicates significant differences
between normal diet (ND) and high fat diet (HFD) mice. #P < 0.05 compared to a normalized
control value of 1 (dotted line).

Linear regression analyses indicated that, independent of diet type and duration,

plasma cholesterol concentrations of LDLR$^{-/-}$ mice were positively correlated with the

FSS-related surface expression of CD18 and CD11b, but not CD11a, integrins on

neutrophils (Fig. 5.11, A – B). As cholesterol (free and total) concentrations increased,

the integrin surface expression (CD18 and CD11b) was elevated on neutrophils exposed

to FSS. This data provided confirmation that FSS-induced Mac1 cleavage is affected by

pathologic cholesterol elevations, related to hypercholesterolemia.
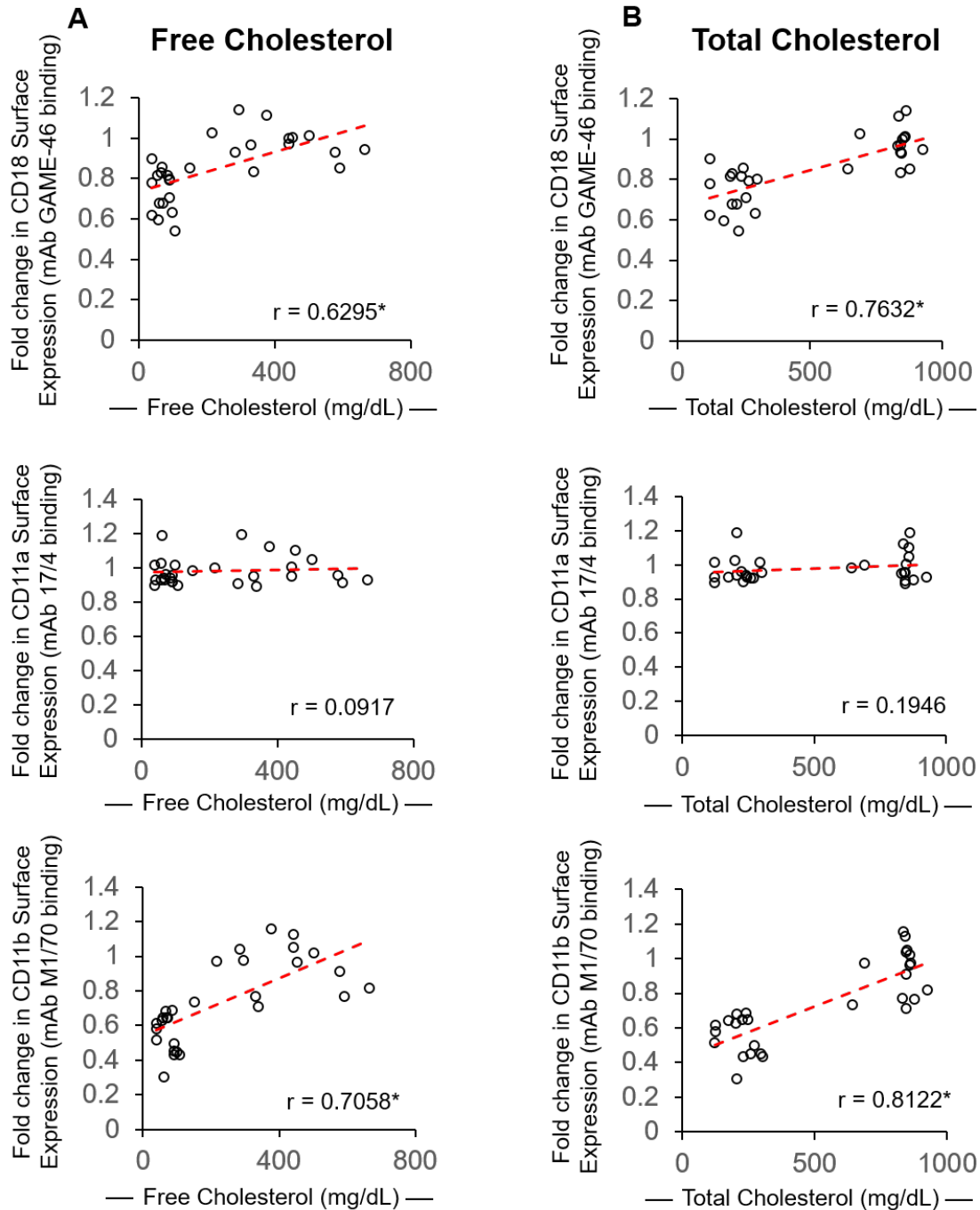
Figure 5.11. Plasma cholesterol concentration is positively correlated with Mac1 expression under fluid shear stress exposure.
(A-B) The free (A) and total (B) cholesterol concentrations of LDLR^{-/-} mice were plotted against the surface expression of CD18, CD11a, and CD11b integrins after exposure to FSS. *P < 0.05 indicates significant correlation between cholesterol concentration and integrin expression.

5.2.7 Cholesterol-related impairment of fluid shear stress-induced Mac1 cleavage is negatively correlated with APF

We used poRH as a measure of evaluating tissue blood flow autoregulation and microvascular function in hypercholesterolemic animals. The rBF curves plotted in MATLAB (Fig. 5.12, A-B) for LDLR$^{-/-}$ mice fed a ND or HFD were similar in response to that of reactive hyperemia reported in humans [129,131]. To evaluate the tissue blood flow response in our mice, we analyzed the peak blood flow attained immediately after cuff occlusion had ended. All rBF data within 10% of the peak blood flow was averaged and reported as APF to reduce noise. Additionally, the duration of time from cuff release to APF was measured and reported as tAPF.
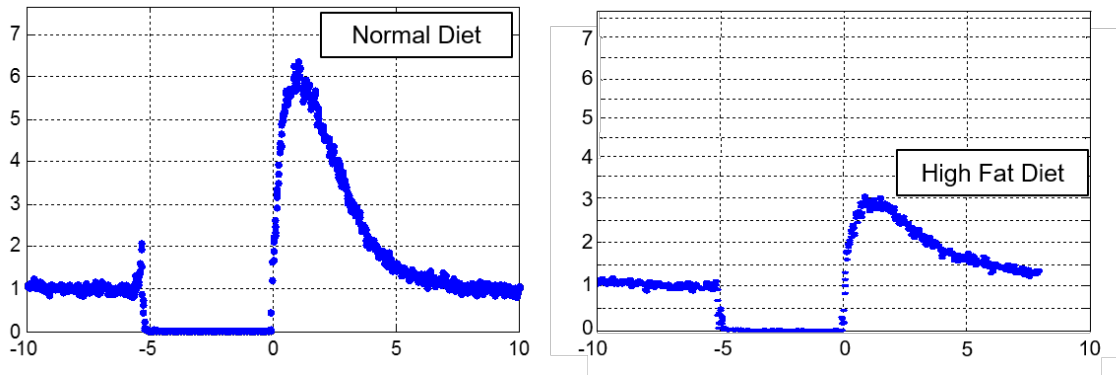
Figure 5.12. Representative images of rBF from normal diet and high fat diet mice. **(A-B)** The ND (A) and HFD (B) rBF curves of LDLR$^{-/-}$ were plotted in MATLAB against time. By using the adjusted peak flow (APF) and length of time to APF (tAPF), we could evaluate the reactive hyperemia of these mice.

On average, the APF of LDLR$^{-/-}$ mice fed a HFD for both the 6 week and 8 week durations appeared to be reduced in comparison to LDLR$^{-/-}$ mice fed a ND (Fig. 5.13, A). However, these diet related changes were not associated with significant difference between ND and HFD mice. Likewise, the tAPF of LDLR$^{-/-}$ mice fed a ND, on average, appeared to be prolonged in comparison to LDLR$^{-/-}$ mice fed a HFD (Fig. 5.13, B) suggesting that tissue blood flow autoregulation in hypercholesterolemic mice may have also been impaired. However, we did not observe a significant difference between ND and HFD mice after 6 and 8 weeks of diet.
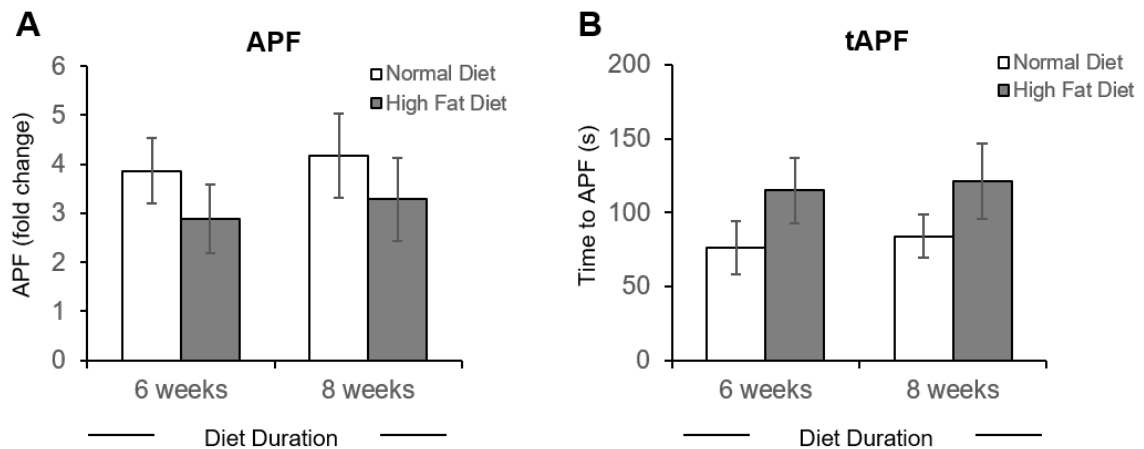
Figure 5.13. The poRH response appears to be disrupted in hypercholesterolemic mice. (A-B) The poRH response of LDLR$^{-/-}$ mice fed a ND or HFD was evaluated and reported as APF (A) and tAPF (B). Bars represent average $\pm$ SEM for APF and tAPF. n = 4 replicates in each group. No significant differences were observed between ND and HFD.

To determine if there was a link between blood cholesterol levels and the tissue blood flow parameters used in the present study, we performed correlation analyses on APF and tAPF independent of diet type or diet duration. Table 5.2 summarizes the results of correlation analyses between plasma cholesterol concentration, FSS-related surface integrin expression, and APF or tAPF. APF was negatively correlated with free and total cholesterol concentrations, indicating that as plasma free or total cholesterol levels in the

blood rose, there was an increase in the degree to which APF was attenuated, which is indicative of an impaired tissue blood flow autoregulation response to poRH.

Additionally, APF was negatively correlated with FSS-related expression of CD18 and CD11b integrins. This indicated that a high expression of Mac1 integrins on neutrophils, likely due to an impaired FSS mechanotransduction response, may contribute to an impaired autoregulation response to poRH in mice. We also observed that tAPF was positively correlated with cholesterol concentrations (free and total), indicating that mice with high plasma cholesterol were likely to have a slow poRH response. However, there was no apparent correlation detected between tAPF and the FSS-related integrin expression of Mac1 or LFA1.

Table 5.2. Correlation analysis of APF.

	FSS-Related Integrin Expression			Cholesterol Concentration	
	CD18	CD11a	CD11b	Free	Total
APF	-0.610*	-0.201	-0.569*	-0.455*	-0.572*
tAPF	0.174	-0.188	0.291	0.472$^{\#}$	0.501$^{\#}$

*P < 0.05 indicates significant correlation with APF
#P < 0.05 indicates significant correlation with tAPF

5.2.8 Summary of data findings/interpretations

The results of the present study provided first evidence for the following significant findings.

- There exists an optimal membrane fluidity permissive of FSS-induced Mac1 cleavage (both ctsB release and Mac1 cleavage)

77

- Extracellular cholesterol elevations block the FSS control of Mac1 surface levels and neutrophil adhesion, likely through effects on membrane fluidity

- Diet-induced hypercholesterolemia is associated with impairment of FSS-induced Mac1 cleavage by neutrophils.

- FSS-induced Mac1 cleavage and plasma free and total cholesterol concentrations are correlated with disrupted tissue blood flow in LDLR$^{-/-}$ mice, suggesting a link between cholesterol-related impairment of neutrophil activity and microvascular dysfunction associated with hypercholesterolemia.

78

CHAPTER 6: DISCUSSION

6.1 First Insight into a Putative Role for Fluid Shear Stress-Induced Cathepsin B Release in the Regulation of Mac1 Surface Expression

6.1.1 Human neutrophil Mac1 expression is regulated by fluid shear stress-induced release of cathepsin B

When exposed to FSS, neutrophils release ctsB, a cysteine protease, to cleave CD18 integrins [23]. Researchers identified the role of ctsB in FSS mechanotransduction through the use of protease inhibitors. There are six main classifications of proteases: cysteine, serine, aspartic, glutamic, threonine, and metalloprotease [135]. Each protease family can be selectively blocked through the use of different inhibitors that are commercially available. Using a panel of protease inhibitors, researchers observed that only a broad-spectrum cysteine protease inhibitor, E64, could block shear-induced CD18 cleavage. The cysteine protease ctsB was later identified after CA074Me, a membrane-permeable inhibitor specific for ctsB [136], was also demonstrated to prevent FSS-induced CD18 cleavage [23]. Later experiments would later implicate the FSS-induced release of ctsB into the extracellular environment through the use of the non-permeable ctsB inhibitor, such as CA074 [93].

While the protease involved in CD18 cleavage had been identified, it was unknown which of the four different CD18 heterodimers, potentially expressed on the neutrophil surface, was targeted for cleavage. Among the four CD18 integrin subtypes, CD11a/CD18 (or LFA1) and CD11b/CD18 (or Mac1) are expressed in high quantities on neutrophils, while very little expression of CD11c/CD18 and CD11d/CD18 is reported [137-139]. This, combined with the important role of LFA1 and Mac1 in neutrophil adhesion and migration [115,140], made it likely that ctsB targeted either CD11a or CD11b, if not both integrins.

79

Previous research in our lab identified that neutrophils selectively cleaved Mac1 integrins on human neutrophils, leaving LFA1 integrins untargeted [59]. This narrowed our focus to the CD18 and CD11b subtypes. But, because the aforementioned research used the broad-spectrum cysteine protease inhibitor, E64, to determine that Mac1 was selectively cleaved due to FSS, it was still unclear if ctsB was capable of cleaving CD11b in addition to CD18.

In the present study, it is apparent that ctsB is involved in the selective cleavage of Mac1 integrins since it can cleave both CD18 and CD11b integrin subunits. CD11a, in contrast, is not cleaved due to FSS-induced ctsB release. It is interesting to point out that FSS exposure reduces CD18 expression by 20 – 30%, and decreases intact CD11b surface levels by up to 50% [59]. This type of proportional relationship would only be possible if neutrophils express similar levels of LFA1 and Mac1, a claim supported by prior analyses of total CD18 subtype expression on neutrophils [141]. Furthermore, these proportional values suggest that during proteolysis of Mac1, CD18 cleavage occurs after CD11b proteolysis. Since FSS exposure does not downregulate LFA1 expression, it is likely that CD11a is somehow able to prevent the cleavage of its partner CD18 subunit. Thus, FSS exposure does not promote cleavage of all the CD18 integrins off the cell surface, only the Mac1-associated ones. It is also possible that CD11a blocks the access of ctsB to CD18, thereby enabling LFA1 to remain on the neutrophil surface in the presence of FSS.

At this point, the reason for why Mac1, but not LFA1 is cleaved under FSS is unknown. One possible explanation may be explained by the specific contributions of LFA1 and Mac1 in recruiting neutrophils to the microvasculature during acute inflammation. LFA1 is typically involved in the early rolling and loose capture stages of neutrophil recruitment to the microvascular wall [58]. In the absence of inflammatory

80

agonist stimulation, LFA1 may remain intact under FSS exposure to enable the neutrophils to still interact with the microvascular endothelium as part of their immune surveillance functionality. Since LFA1 forms loose interactions with the microvasculature [58], this would enable neutrophils to reversibly bind to the vessel wall under FSS exposure but still not commit down the inflammatory cascade if they are not needed. In contrast, Mac1 may be cleaved as a key checkpoint to prevent the commitment of neutrophils along the inflammatory cascade. Since Mac1 supports the firm adherence of neutrophils to the microvasculature [58], cleavage of this integrin would prevent neutrophil adherence to, arrest on, and migration along, the vessel wall and, in turn, maintain neutrophils freely-floating in the bloodstream. Considering that neutrophil binding to the microvasculature may influence endothelial-mediated vasomotor activity and/or affect the cross-sectional area to flow, FSS-induced ctsB release and Mac1 cleavage may preserve microvascular blood flow regulation and reduce apparent viscosity [72,142], thereby minimizing microvascular flow resistance.

In addition to analyzing Mac1 cleavage, we also focused on the release of ctsB under shear exposure. The time-dependent release of ctsB in this study agrees with that reported for CD18 and CD11b cleavage in previous studies [59]. Furthermore, the observed extracellular release of ctsB in a soluble form is also supported by our prior experiments [93]. While the possibility that a lysosomal protease, such as ctsB, is capable of cleaving Mac1 in the extracellular domain is inconsistent with the widespread view that lysosomal proteases typically function optimally in an acidic pH [143] and not a neutral pH outside the cell, evidence supports the extracellular actions of ctsB for many cells. For example, tumor cells and lymphocytes both secrete ctsB, which has been demonstrated to remain

stable and functional at neutral pH for extended periods of time [144-147]. Therefore, it is plausible that ctsB remains functional and able to cleave Mac1 integrins upon its release by neutrophils.

Interestingly, FSS exposure has been shown to increase granular motion in the neutrophil cytosol, which may increase the likelihood of degranulation [21]. This increased granular motion may be linked to the ability of FSS to induce actin depolymerization [55], considering granule exocytosis is dependent on actin remodeling [148,149]. Thus, the FSS-induced increase in granular motion may represent a key aspect of the mechanism that underlies the ability of FSS to promote ctsB release. It should be emphasized that the FSS-induced degranulation of neutrophils is unlikely to be due to mechanical trauma which other investigators reported for neutrophils under flow conditions [150]. The FSS levels used in the present study were well below those used in these earlier studies [150]. Future studies will be required to link FSS-induced degranulation with the release of ctsB at low shear magnitudes.

6.1.2 The shear-induced CD18 cleavage response is characteristic of neutrophils

In addition to confirming the selective cleavage of Mac1 by FSS-induced ctsB release, we also determined whether the ability to regulate Mac1 expression by FSS exposure was characteristic of neutrophils. We selected HL60 promyelocytes for use in our experiments. HL60 cells are capable of differentiating into cells that express a variety of different phenotypes, including neutrophilic [109]. DHL60-NCs approximate human neutrophils after undergoing morphological changes and upregulating their expression of FPR [151] and CD18 integrins on their surface [92,109]. In fact, dHL60-NCs have been

validated as a model for various neutrophil functions, including migration and chemotaxis [107,109,152]. Furthermore, dHL60-NCs can be utilized in transfection experiments and are sustainable in culture for up to one week. This is in contrast to human neutrophils, which are much more difficult to transfect due to their short (i.e., < 24 hour) lifespan once outside the body [153,154].

The results from our experiments involving dHL60-NCs confirmed that the FSS-induced cleavage of CD18 integrins is phenotypic of neutrophils. The total reduction in CD18 expression on the dHL60-NC surface is similar to that observed for human neutrophils exposed to shear [59]. Additionally, FSS-induced CD18 cleavage of dHL60-NCs occurs at an extracellular domain on the integrin, much like with human neutrophils. This was verified due to the similar expression of intracellular CD18 between sheared and unsheared samples. We also used E64, a protease inhibitor incapable of crossing the cell membrane [155-157], to confirm that cysteine proteases are released into the extracellular milieu and cleave CD18 integrins, in line with our human data.

Notably, the specific integrin cleaved under FSS exposure was found to differ between human neutrophils and dHL60-NCs. While human neutrophils cleave Mac1, we observed dHL60-NCs to cleave LFA1. Moreover, E64 prevented shear-induced CD18 cleavage, but only partially blocked cleavage of CD11a subunits. This raised the issue of how shear-induced CD18, but not CD11a, cleavage was blocked in the presence of E64. We ruled out the possibility that our flow cytometric analyses were detecting the cleavage of CD18 dimerized to CD11c, as dHL60-NCs had no detectable expression of this subunit. Instead, it may be possible that different proteases are responsible for cleavage of CD18 and CD11a by dHL60-NCs. Furthermore, since ctsB expression by dHL60-NCs was much

83

lower in comparison to primary neutrophils [158], it is possible that dHL60-NCs express other cysteine proteases capable of cleaving CD18 and CD11a, but not CD11b, integrin subunits under shear exposure. The variance in granule distribution between human neutrophils and HL60s may account for the difference in protease expression for these two cell types [159]. Alternatively, these cell types may also degranulate differently when exposed to shear.

While we did not identify the protease involved in FSS-induced CD11a cleavage for dHL60-NCs, we excluded the involvement of cysteine, serine, and aspartyl proteases. Since we previously observed lymphocytes to exhibit FSS-induced cleavage of CD11a [59], a common mechanism or protease may link the FSS cleavage responses of lymphocytes and dHL60-NCs. We also focused on the involvement of MMPs, as MMP-9 was previously implicated in cleavage of CD18 [160]. However, doxycycline, an antibiotic with broad proteolytic activity against MMP-9 and cysteine proteases, blocked cleavage to the same degree as E64, suggesting that MMP-9 is not involved. However, additional studies are needed to fully rule out this possibility.

Despite the difference in integrin cleavage between human neutrophils and dHL60-NCs, these two cells share a similar FSS mechanotransduction response, i.e., CD18 cleavage. Importantly, we demonstrated that shear-induced CD18 cleavage may be blocked in the presence of threshold concentrations of fMLP. Cleavage of the corresponding CD11 subunit, either CD11b for human neutrophils or CD11a for dHL60-NCs, was also affected by the same threshold concentrations of fMLP. Notably, the threshold ($> 1 \mu M$) of fMLP required to block integrin cleavage was the same as that reported for attenuating the FSS-induced pseudopod retraction response [20].

84

Ultimately, our results pointed toward FSS-induced cleavage of CD18 as a characteristic trait of neutrophil-like cells. We verified that human neutrophils cleave Mac1 through extracellular release of ctsB in response to FSS stimulation. Furthermore, dHL60-NCs cleave CD18 integrins in response to FSS exposure, but were found to express very little ctsB and, instead, cleave CD11a. Despite this discrepancy in the CD18 integrin cleavage response to FSS, the dHL60-NCs would be a useful transfectable culture model to study neutrophil FSS mechanotransduction responses. By transfecting dHL60-NCs to express ctsB, for example, it may be possible to study FSS-induced Mac1 cleavage in these cells as a model for human neutrophils.

Overall, the observations from the studies discussed in this section suggest that CD18 cleavage acts in conjunction with pseudopod retraction under non-inflamed conditions to minimize neutrophil activation when they are not needed. This provided the foundation for future experiments involving the regulation of neutrophil adhesion and migration through FSS-induced ctsB release.

6.2 A Role for Fluid Shear Stress-Induced Cathepsin B Release in the Restriction of Neutrophil Adhesive Functions

6.2.1 The influence of cathepsin B on neutrophil-substrate interactions during migration under no-flow conditions

Originally, it was anticipated that exogenous ctsB would impair the ability of neutrophils to migrate by reducing their adhesive interactions with substrates. Rather than reducing the migration velocity of cells, exogenous ctsB actually enhanced neutrophil motility under no-flow conditions. This observation was in agreement with previous

85

studies [93]. Although this seems counter-intuitive, it is conceivable that ctsB enhances neutrophil motility by altering Mac1-dependent processes involved in the pseudopod projection/retraction dynamics during neutrophil migration.

In essence, neutrophil migration depends on cyclical pseudopod projection and retraction to induce movement in a specific direction [161,162]. The rapid F-actin polymerization and formation of cytoskeletal networks at the "leading edge" of a neutrophil enables lamellipodia to extend from the cell. Once projected, the lamellipodia are filled with cytoplasm to become functioning pseudopods. The presence of adhesive integrins, including Mac1, on the functioning pseudopods enables the neutrophil to adhere to biological substrates and pull itself forward. As the cell body moves forward, the F-actin begins to rapidly depolymerize not long after pseudopod formation, breaking down the cytoskeletal networks that provide structure to the adherent pseudopod [163]. This, in turn, causes the eventual retraction of this pseudopod (referred to as the uropod) at the "trailing edge" of the neutrophil as the cell body continues to advance forward. Ultimately, neutrophil migration rate is dictated by this cyclical formation of lamellipodia and subsequent retraction of uropodia.

In regard to our migration experiments, performed under no-flow conditions, it may be that the addition of exogenous ctsB to migrating neutrophils had an additive effect on their motile function by cleaving the extracellular domains of Mac1. This, in turn, would help to detach uropods and, ultimately, accelerate neutrophil migration. Under flow conditions, it may be possible that exogenous ctsB (i.e., due to FSS-induced ctsB release) cooperates with other cell motility processes, such as calpain-mediated cleavage of intracellular CD18 integrins [164] and Mac1 unbinding kinetics to substrate-bound ligands

[23,26]. This would be in line with the observed increase in pseudopod retraction rates that occurred in the presence of exogenous ctsB under no-flow conditions. Moreover, inhibiting ctsB activity did not have a significant effect on baseline pseudopod retraction and extension rates, further supporting an additive effect of Mac1 cleavage on cell motility.

While we observed large increases in pseudopod retraction rates, we also observed small increases in pseudopod extension rates. It is likely that small increases in pseudopod extension rates for ctsB-stimulated neutrophils were a secondary effect of the large increases in retraction rates. CtsB-enhanced pseudopod retraction, which involves accelerated actin depolymerization, likely promoted an increase in the amount of G-actin monomers in the cytosol. Such an increase in G-actin availability would facilitate the formation of cytoskeletal structures to support new pseudopod projection. However, this scenario is speculative and remains to be confirmed.

It is interesting to note that, while ctsB enhanced pseudopod disengagement through Mac1 cleavage, FSS appears necessary to prevent the formation of new pseudopods on neutrophils. While we observed ctsB to enhance pseudopod retraction, the cells still were able to form new pseudopods. However, under flow conditions, only pseudopod retraction is observed during FSS-induced ctsB release; the cells don't form new pseudopods. This may be due to the contributions of FPR, which is reported to be a neutrophil mechanosensor involved in regulating Rac1 signaling associated with actin dynamics [108].

Briefly, Rac1, a small guanine triphosphase (GTPase) belonging to the Ras protein superfamily [165], initiates cytoskeletal reorganization, actin polymerization, and membrane protrusion when activated [166]. Under FSS exposure in neutrophils, Rac1

activity is significantly decreased, in line with a reduction in pseudopod formation [108]. Notably, FPR expression is necessary for neutrophils to form new pseudopod projections [92]. When neutrophils are exposed to FSS, the expression of FPR on the membrane surface is downregulated through receptor internalization [63]. Since constitutive FPR expression is necessary for pseudopod formation, FPR internalization likely prevents the formation of new pseudopods, potentially by reducing Rac1 activity. This suggests that FSS-induced ctsB release and FSS-induced FPR internalization work in conjunction to retract pseudopods and prevent their formation under flow conditions.

Finally, although dHL60-NCs naturally express a low level of ctsB, we were able to overexpress this protease through transfection and show that both pseudopod activity and neutrophil motility were slightly elevated in the transfected dHL60-NCs in a similar fashion to primary neutrophils. These observations supported the ability of ctsB to influence neutrophil pseudopod activity. Overall, the observations from the present study provided first evidence that release of ctsB is another way by which neutrophils may modulate their migration rates in line with its ability to cleave surface Mac1 integrins.

6.2.2 Fluid shear stress-induced cathepsin B release can restrict neutrophil adhesion through Mac1 cleavage

In addition to its effects on neutrophil motility, we also anticipated that ctsB was involved in directly regulating neutrophil binding/adhesion to biological substrates. Under physiologic conditions, many mechanisms are in place to ensure neutrophils remain freely-floating in the circulation. Some of these regulatory mechanisms are tied to endothelial cell functions. For example, FSS exposure in the physiologic range can induce endothelial cells

to release NO, an anti-inflammatory signaling molecule which can minimize leukocyte adhesion to the endothelium [167]. When exposed to FSS, endothelial cells also downregulate the expression of adhesion molecules that act as receptors for Mac1, further diminishing the ability of leukocytes to adhere under physiologic conditions [167,168].

Much like the endothelial cells, neutrophils appear to also be capable of regulating their own adhesive capabilities. Shedding of Mac1, for example, allows neutrophils in interstitial tissues to detach from extracellular matrix during chemotaxis [169]. Our own lab took this a step further by investigating the involvement of ctsB in neutrophil adhesion to other cells, based on its interactions with Mac1. Previously, the FSS-induced release of ctsB was reported to reduce the binding of neutrophils in suspension to platelets and fibrinogen, a Mac1 ligand [59]. This implicated FSS-induced ctsB release and Mac1 cleavage as a preventative measure against neutrophil adhesion to other cells in the blood. Moreover, these findings suggested that ctsB, in addition to regulating the adhesion of neutrophils in suspension, could also regulate neutrophil adhesion to unstimulated endothelium in the microvasculature, which expresses Mac1 counter-receptors.

The idea for the *ex vivo,* flow-based detachment assay used in the present study came from experiments performed by Moazzam et al [21]. Using intravital microscopy, they found that leukocytes would sediment to, adhere to, and migrate along the microvascular endothelium during transient periods of blood stasis imposed by upstream microvessel occlusion. But when flow was reconstituted, they would detach in a time-dependent fashion and be carried away in the circulation. It should be emphasized that the detachment resembled a mechanobiologically-driven process and not a result of a physical shearing off of the cells.

For our studies, we mimicked this scenario using a microfluidics approach. We studied the ability of FSS exposure to promote the detachment of neutrophils from platelet monolayers as a way to quantify the ability of mechanical stimulus to restrict adhesion. Neutrophils bind to platelets primarily through Mac1 integrins, which allowed us to focus on the role of FSS-induced ctsB release [113]. We also conducted similar studies using HUVECs as a model endothelial cell line. The use of an unstimulated venous endothelial cell line allowed us to more closely approximate the *in vivo* conditions in the microvasculature.

Whether adhered to platelets or unstimulated endothelium, the outcomes of our *ex vivo/in vitro* flow-based analyses confirmed that FSS regulated the adhesive capacity of neutrophils by promoting their detachment from platelets and from endothelial monolayers. Based on our observations, FSS-induced release of ctsB likely served to sever Mac1-dependent neutrophil adhesion. Importantly, FSS was only found to regulate neutrophil adhesion in the absence of agonist stimulation. When stimulated with fMLP concentrations above threshold levels that block FSS-induced pseudopod retraction or CD18 cleavage, the neutrophils remained adherent to substrates even under fluid flow stimulation. This outcome is consistent with the likelihood that an acute inflammatory scenario overrides the FSS mechanotransduction response in order to recruit neutrophils only when they are needed. Taken together, these observations provided evidence that FSS-induced ctsB is a control mechanism that restricts Mac1 dependent adhesion of neutrophils under physiological (i.e., non-inflamed) conditions.

6.3 The Importance of an Optimal Membrane Fluidity in a Functioning Fluid Shear Stress Mechanotransduction Response

6.3.1 An optimal membrane fluidity is permissive of shear-induced Mac1 cleavage

A growing body of evidence, including that presented in this dissertation, indicates that FSS mechanotransduction regulates neutrophil activity under physiologic conditions to keep them quiescent and suspended within the circulation. While inflammatory agonist stimulation is one way the circulation may supersede the neutrophil mechanosensitivity, it is also possible for neutrophils to become unresponsive to FSS under pathological conditions. It is this dysregulation that we believe may contribute to chronic activation, even in the presence of flow. SHRs, for example, are associated with neutrophils that do not retract pseudopods when exposed to shear stress [25]. This is thought to involve the dependence of blood pressure in SHRs on plasma levels of glucocorticoids and the expression of glucocorticoid receptors on the neutrophil membrane [170,171]. Glucocorticoids have been shown to block FSS-induced pseudopod retraction [24]. However, soluble signaling molecules are not the only way to impair cell mechanosensitivity, as changes to the cell membrane itself have also been observed to do this [26,27].

Impaired FSS mechanotransduction responses have previously been demonstrated in our lab for neutrophils in hypercholesterolemic blood [27]. When exposed to shear in a cone-and-plate viscometer, neutrophils from hypercholesterolemic mice are unresponsive to FSS with a deficient pseudopod retraction response to FSS. We reported this to be dependent on the cholesterol-related membrane fluidity of the cell.

Additionally, we found that the degree of impairment in neutrophil mechanosensitivity occurred in a time-dependent fashion (as early as 2 weeks after diet initiation) that tracked with the gradual increases in blood cholesterol levels over the duration of high fat dieting intended to induce hypercholesterolemia in mice [27]. It is likely that, as blood cholesterol concentrations increased over the HFD duration, there was an increased accumulation of cholesterol in the neutrophil membrane. In support of this, hypercholesterolemia reportedly increases the cholesterol concentration of blood cell membranes [104,172]. Conceivably, this gradually increased the degree of impairment in neutrophil mechanosensitivity during the progression of hypercholesterolemia, something previously reported by our laboratory [27] and observed in the present study.

The cholesterol-related impairment of neutrophil FSS mechanosensitivity may also be linked to microvascular dysfunction. Another study performed in our lab found that neutrophils in hypercholesterolemic mice contributed to the dysregulation of tissue blood flow autoregulation in response to poRH, a measure of microvascular function [26]. This suggested that cholesterol-enriched neutrophils with impaired FSS mechanosensitivity is involved in the progression of microvascular dysfunction associated with hypercholesterolemia. However, it was not clear how impaired FSS related pseudopod retraction would manifest into microvascular dysfunction. Since we previously demonstrated that pathologic cholesterol elevations impair FSS mechanosensitivity through an effect on membrane fluidity, it remained possible that membrane cholesterol enrichment would impair FSS-induced Mac1 cleavage. Blocking Mac1 cleavage would disrupt the FSS-induced control of neutrophil adhesion, as we showed using our

detachment assay, potentially contributing to the dysregulated neutrophil adhesion observed during hypercholesterolemia [29,77,173].

In the present study, we identified a dose-dependent inhibitory effect of exogenous cholesterol elevations on FSS-induced cleavage of Mac1 integrins. The threshold concentration of cholesterol that completely blocked this FSS response (> 2 µg/mL) was consistent with the concentration our laboratory previously reported to impair FSS-induced pseudopod retraction (> 1 µg/mL) [27]. Notably, FSS-induced Mac1 cleavage is only partially blocked in cells treated with 1 µg/mL cholesterol. This suggests that, because FSS-induced pseudopod retraction is completely blocked at 1 µg/mL cholesterol, the attenuated Mac1 cleavage keeps enough adhesion integrins intact which are capable of forming membrane-substrate interactions to prevent pseudopod retraction.

After we established 2 µg/mL as the threshold concentration of cholesterol required to impair FSS-induced Mac1 cleavage, we adopted our previously reported strategy involving the membrane fluidizer, BnOH, to recover cholesterol-related blockade of FSS-induced pseudopod retraction [27]. We also used a second compound known to fluidize cell membranes, EtOH. Notably, these membrane fluidizers recovered FSS-induced Mac1 cleavage at concentrations of 1 – 2 mM for BnOH and 7 – 8 mM for EtOH. Importantly, the ability of 1 – 2 mM BnOH to recover FSS-induced Mac1 cleavage was in agreement with that observed previously (1 mM BnOH) to recover FSS-induced pseudopod retraction by neutrophils treated with 2 µg/mL cholesterol [27]. Despite the difference in fluidizer concentrations, the ability of BnOH and EtOH to reverse the cholesterol blockade of FSS-induced Mac1 cleavage provided further evidence supporting the existence of an optimal membrane fluidity level permissive for intact neutrophil FSS sensitivity.

93

While we had linked changes in neutrophil membrane fluidity to the impairment of FSS-induced Mac1 cleavage, the exact mechanistic relationship remains to be elucidated. One possibility is that enriching neutrophil membranes with cholesterol impairs ctsB release. Membrane stiffening has been reported to prevent the release of pro-inflammatory cytokines into the extracellular milieu [106]. Thus, it is plausible that FSS-induced ctsB release is blocked by cholesterol-related changes to membrane fluidity. Our experiments confirmed that FSS-induced ctsB release was blocked at threshold cholesterol concentrations corresponding to those determined in Mac1 cleavage experiments. Importantly, it was possible to reverse the effects of cholesterol impairment by using BnOH and EtOH to recover FSS-induced ctsB release at the same membrane fluidizer concentrations (1 – 2 mM BnOH and 7 – 8 mM EtOH) used to reverse the blockade of FSS-induced Mac1 cleavage by cholesterol.

6.3.2 Cholesterol-related changes in membrane fluidity block fluid shear stress-mediated restriction of neutrophil adhesion

Our next set of experiments focused on the physiologic implications of this impaired mechanotransduction response. In particular, we wanted to determine if cholesterol-related impairment of FSS-induced ctsB release and Mac1 cleavage impairs the ability of FSS to restrict neutrophil adhesion. Using our flow-based detachment assay with platelets as a biological substrate, we demonstrated that neutrophils enriched with cholesterol became unresponsive to FSS exposure and remained adherent to platelet monolayers despite being exposed to flow. These observations are in line with the reported ability of cholesterol to enhance neutrophil tethering and firm arrest to activated

94

endothelium [126], suggesting that cholesterol may, in fact, block the FSS-induced regulation of cell adhesion.

Notably, it was possible to reverse the cholesterol-related impairment of FSS-induced neutrophil detachment from platelet layers using either BnOH or EtOH. More importantly, the concentrations of BnOH and EtOH that recovered FSS-induced detachment by cholesterol-treated neutrophils were the same as those required to recover FSS-induced Mac1 cleavage in similarly-treated cells. These observations, combined with previous results from our laboratory, provided evidence that cholesterol-related changes in membrane fluidity impair FSS-induced ctsB release and Mac1 cleavage, leading to dysregulated neutrophil adhesion under flow. Considering that elevated neutrophil adhesion and activity have been linked with hypercholesterolemia and other downstream cardiovascular pathologies [29,80,174,175], the results presented in this chapter implicated cholesterol-related impairment of FSS-induced Mac1 cleavage as a contributing factor.

6.4 The Contributions of Hypercholesterolemia-Related Impairment of Fluid Shear Stress Mechanotransduction in the Development of Microvascular Dysfunction

6.4.1 Pathologic cholesterol elevations associated with hypercholesterolemia impair fluid shear stress-induced Mac1 cleavage

In order to verify that impairment of the Mac1 cleavage response to FSS may occur in the *in vivo* setting of hypercholesterolemia, we performed studies on neutrophils from LDLR$^{-/-}$ mice. When LDLR$^{-/-}$ mice are fed a HFD, they gradually develop hypercholesterolemia as plasma levels of free and total cholesterol increase over the duration of dieting [176]. We verified this for our study since the LDLR$^{-/-}$ mice on a HFD

95

displayed gradual increases in blood cholesterol levels over the 6- and 8-week durations tested in the present study. Previous studies have shown that leukocytes from humans and animals with pathological blood cholesterol levels have significantly elevated concentrations of membrane cholesterol, with associated reductions in membrane fluidity [172,177]. Overall, this suggests that feeding LDLR$^{-/-}$ mice a HFD was sufficient to: i) induce a hypercholesterolemic state; ii) enrich the neutrophil membrane with cholesterol; and iii) reduce the membrane fluidity of neutrophils.

Neutrophils from LDLR$^{-/-}$ mice fed a ND and exposed to FSS were observed to have an intact Mac1 cleavage response to FSS, similar to that observed for human neutrophils. However, neutrophils from our HFD mice exposed to FSS exhibited an impaired Mac1 cleavage response. While 6 weeks of HFD was sufficient to attenuate FSS-induced Mac1 cleavage, 8 weeks of HFD completely blocked shear-induced Mac1 cleavage. Notably, we also observed that the degree to which FSS-induced Mac1 cleavage was blocked was positively correlated with the plasma cholesterol concentrations (free and total) of LDLR$^{-/-}$ mice. Therefore, it is likely that a gradual impairment of FSS-induced Mac1 cleavage follows gradual increases of plasma cholesterol levels.

The current study is not the first to determine that impairment of FSS mechanotransduction is dependent on the length of time that mice were fed a HFD. Previous studies have reported similar relationships linking diet duration with an impaired FSS-induced pseudopod retraction response [27]. In that study, the mice fed a HFD for as little as 2 weeks exhibited a deficit in their responsiveness to FSS exposure. However, the fraction of neutrophils that retracted pseudopods gradually decreased as HFD progressed. After 8 weeks of HFD, neutrophils from hypercholesterolemic mice appeared to extend

96

pseudopods in response to shear exposure; i.e., a reverse shear response. These past observations, combined with the present study, indicate that FSS mechanotransduction is impaired to a greater degree as membrane cholesterol content increases. Notably, a significant finding of the present study was demonstrating that hypercholesterolemia also impairs FSS control of neutrophil adhesion, which has mechanistic implications in hypercholesterolemia-related pathogenesis.

6.4.2 Cholesterol-related impairment of fluid shear stress-induced Mac1 cleavage is correlated with dysregulated tissue blood flow in hypercholesterolemic mice

Since we demonstrated that cholesterol can impair FSS-induced Mac1 cleavage, we also wanted to determine whether pathologic cholesterol elevations associated with hypercholesterolemia and its detrimental impact on the FSS regulation of Mac1 surface expression contribute to dysregulated tissue blood flow in LDLR$^{-/-}$ mice. Therefore, we analyzed the ability of LDLR$^{-/-}$ mice to recover blood flow in hind limbs after 5 minutes of occlusion, which is similar to poRH in humans [129,131]. The recovery in blood flow was quantified as the peak flow, reported as APF, immediately after cuff removal. We also reported the duration of time after cuff removal (i.e., tissue reperfusion) to reach APF, reported as tAPF.

Hypercholesterolemic mice fed a HFD for 6 and 8 weeks displayed what appeared to be an impaired poRH response, as APF was decreased and tAPF was increased in comparison to ND mice. Since poRH can be used as an estimation of microvascular function and tissue blood flow autoregulation, this suggested that tissue blood flow was disrupted in hypercholesterolemic mice. However, we did not observe a significant

97

different between ND and HFD mice for both APF and tAPF, unlike in previous studies from our lab [26]. This is likely due to the low statistical power in our analyses, as our results were based on data from 4 mice in each group, independent of diet type and diet duration. During earlier studies, the weight of the DCS probe was found to interfere with the rBF data acquired by DCS during poRH. By placing the probe under the mouse leg, rather than on top of the leg, we eliminated the source of error for future experiments. In the future, we would expect at least 7 – 8 mice in each experimental group would be needed to detect significant differences similar to that previously reported for APF and tAPF [26].

We also performed correlation analyses to determine how plasma cholesterol levels were linked with the poRH response in mice, independent of diet type and diet duration. Our correlation analyses found that APF in LDLR$^{-/-}$ mice was negatively correlated with plasma cholesterol levels and, most importantly, this correlation was significant. Thus, elevations in cholesterol appear to have an effect of reducing APF. An interpretation of this outcome may be that pathological cholesterol concentrations associated with hypercholesterolemia contribute to dysregulated tissue blood flow, which is in agreement with prior reports for mice and humans [26,80,128]. Additionally, tAPF was positively correlated with plasma cholesterol levels, indicating that elevations in cholesterol lengthen the amount of time necessary to achieve a complete poRH response. Since poRH can be used to estimate tissue blood flow autoregulation, we can interpret this data to say that blood cholesterol levels are prognostic of an impairment in tissue blood flow autoregulation. This agrees with numerous reports demonstrating a link between blood cholesterol levels and the progression of microvascular dysfunction [178,179].

We also found that APF was negatively correlated with the degree to which FSS-induced Mac1 cleavage was blocked, independent of diet type and duration. These results point to cholesterol-related impairment of FSS-induced Mac1 cleavage as a potential factor that contributes to hypercholesterolemia-related reductions in APF. Specifically, FSS-induced regulation of neutrophil adhesion may be compromised by blocking Mac1 cleavage under FSS exposure, potentially resulting in dysregulated neutrophil adhesion characteristic of the hypercholesterolemic microcirculation [29,77,173]. Notably, dysregulated neutrophil adhesion has been demonstrated to contribute, in part, to the progression of microvascular dysfunction [4,50,128,180-182]. Therefore, it is conceivable that the disrupted tissue blood flow in our studies, which manifested as decreased APF, resulted from the cholesterol-related impairment of FSS regulatory mechanisms.

Overall, the results from our mice study, combined with those from our human neutrophil detachment experiments, implicate the cholesterol-related dysregulation of neutrophil behavior in the progression of microvascular dysfunction associated with the onset and progression of hypercholesterolemia. This relationship between neutrophil adhesion, FSS-induced Mac1 cleavage, and dysregulated tissue blood flow may help design future studies to definitively link an impaired FSS response to the progression of microvascular dysfunction.

CHAPTER 7: CONCLUSIONS

In summary, the evidence provided in this study supports the importance of FSS mechanotransduction in the physiologic control of neutrophil activity. Specifically, this dissertation provided new evidence that cleavage of Mac1 by FSS-induced ctsB release serves to regulate neutrophil adhesion to unstimulated endothelium. By downregulating the expression of Mac1 adhesion integrins, FSS mechanotransduction likely ensures neutrophils remain quiescent and freely-floating in the circulation. We also provided evidence for the existence of an optimal membrane fluidity level permissive of an intact Mac1 cleavage response to flow. Perturbations that alter the membrane fluidity outside this optimal range are expected to impair the physiological regulation of neutrophil activity by FSS, thereby contributing to pathology.

Additionally, we report that cholesterol-related changes in membrane fluidity may lead to impairment of the FSS-related control of neutrophil adhesion by Mac1 cleavage. This has implications during hypercholesterolemia where blood cholesterol elevations, by impairing FSS-induced ctsB release and Mac1 cleavage, may promote dysregulated neutrophil adhesion in the microvasculature and, in doing so, lead to microvascular dysfunction. Ultimately, these results suggest that dysregulated neutrophil adhesion, induced by cholesterol-related impairment of FSS mechanotransduction, may be one of the earliest upstream factors which disrupt tissue blood flow and contribute to microvascular dysfunction, a precursor to lethal vascular disease due to hypercholesterolemia.

Future studies should focus on further elucidating mechanistic aspects of this potential link between dysregulated neutrophil adhesion and microvascular dysfunction. For example, intravital microscopy can be used to monitor neutrophil adhesion to the endothelium under flow conditions in hypercholesterolemic mice. By using a micropipette

100

to first induce blood stasis followed by its removal to reconstitute microvascular flow, it would be possible to determine whether adherent neutrophils in hypercholesterolemic mice respond to shear exposure. Additionally, studies in ctsB-deficient mice can be performed in parallel with those from LDLR$^{-/-}$ mice to determine if a loss of ctsB activity is also linked to dysregulated neutrophil adhesion and microvascular dysfunction *in vivo*. This would suggest that the dysregulated adhesion of cholesterol-enriched neutrophils in hypercholesterolemic mice may be due to a loss in ctsB activity, likely due to membrane fluidity-related impairment of ctsB release. Verification of ctsB release from cholesterol-enriched neutrophils can then be determined using single-molecule tracking with fluorescently labeled ctsB. Finally, it is important to understand the early mechanosignaling events at the mechanosensor and secondary messenger levels to better understand the mechanobiology of neutrophils under FSS exposure. Overall, these studies may contribute toward the development of novel therapeutic treatments that target cholesterol-related pathobiology (e.g., impairment of FSS mechanotransduction in neutrophils) rather than just targeting blood cholesterol levels, a strategy that is still controversial in terms of its efficacy.

A.1 Introduction

Peripheral hemodynamic resistance is affected by activated neutrophils, either through capillary plugging or adhesion to the microvasculature [183,184]. However, neutrophils flowing through the blood in an inactivated state also influence apparent viscosity [72,142], which affects flow resistance. We performed *in vitro* experiments to test whether activated neutrophils could significantly enhance their impact on microvascular flow by altering blood rheology. In this regard, we sought *in vitro* affirmation that sustained neutrophil activation may impact peripheral resistance and downstream tissue perfusion, both of which may contribute to microvascular pathobiology.

The following description of this study is derived with minor modifications from our previously published work:

Akenhead ML, Horrall NM, Rowe D, Sethu P, Shin HY. In Vitro Evaluation of the Link Between Cell Activation State and Its Rheological Impact on the Microscale Flow of Neutrophil Suspensions. ASME. *J Biomech Eng.* 2015;137(9):091003-091003-10.

A.2 Methods

A.2.1 Microfluidics-based microvascular mimics

To evaluate the impact of neutrophil pseudopod activity on flow resistance in microfluidics mimics of non-capillary (i.e., arteriolar/venular) microvessels, we utilized two different experimental configurations. One configuration utilized a polydimethylsiloxane (PDMS) chamber consisting of a single rectangular cross-section microchannel (w: 500 µm; h: 50 µm; l: 20 mm). We also simulated a microvascular

102

network by utilizing a PDMS chamber with twenty 20x50 µm rectangular channels arranged in parallel.

Prior to experimentation, neutrophil suspensions ($1x10^6$ cells/ml) were stimulated with 0 or 10 nM fMLP for 5 min and subsequently fixed in 1% p-formaldehyde. The neutrophil suspensions were perfused through the microfluidic chamber for 3 minutes at flow rates of 1, 1.5, 2, and 5 mL/min in the absence or presence of autologous erythrocytes at 10% hematocrit. During perfusion, we measured the infusion pressure (relative to the atmosphere). For analyses, the baseline pressure reading ($P_{t=0}$) (obtained before the onset of flow) was subtracted from each instantaneous infusion pressure reading (P_t), and used as the instantaneous pressure gradient $\Delta P = P_t - P_{t=0}$. To reduce the impact of noise, we averaged the pressure gradient values recorded over the last 2 min of constant flow (Q) at each flow rate. These averages were then used to quantify the flow resistance (slope of a ΔP vs. Q curve).

A.3 Results

A.3.1 The rheological impact of neutrophil activation is enhanced by the presence of erythrocytes in microscale flows

To simulate flow without plugging through the largest microvessels within the microcirculation, we utilized a single-channel microchamber during experiments. Both activated and inactivated neutrophil suspensions were observed to have similar perfusion pressures during flow through this chamber (Fig. A.1, A). We also simulated microscale flow by utilizing a microvascular network chamber during experiments. Much like the single channel microchamber, both activated and inactivated neutrophil suspensions were

103

observed to have similar perfusion pressures during flow through the microvascular network chamber (Fig. A.1, B). Based on the pressure vs. flow curves generated for each chamber (Fig. A.1, C), activated and inactivated cell suspensions were determined to have a similar impact on flow resistance (Table A.1).
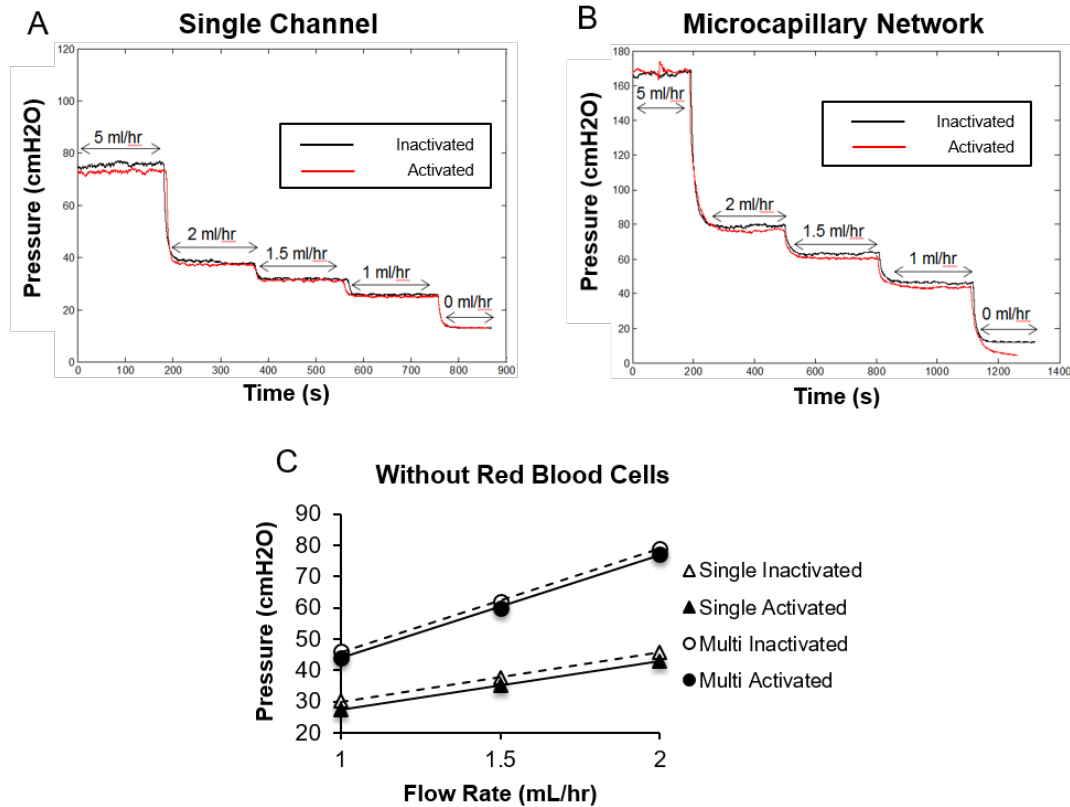
Figure A.1. In the absence of erythrocytes, neutrophil activation does not significantly impact the flow properties of microvascular mimics.
(A-B) Plots of perfusion pressure versus time for a single 500x50 µm channel (A) or a network of twenty 20x50µm microchannels (B) were generated at various flow rates (0, 1, 1.5, 2, and 5 mL/hr) for purified neutrophil suspensions maintained in an inactivated state (solid black line) or activated with 10 nM fMLP (solid red line). **(C)** To determine effects of neutrophil activation on microchannel flow resistance, pressure versus flow curves were generated from the raw data. Pressure values were averaged over the last 2 minutes recorded at each flow rate. From the generated curves, resistance values corresponding to single channel (inactivated, open triangles; activated, solid triangle) or microvascular network (inactivated, open circles; activated, solid circles) were found by computing the slope of each line. Points are mean ± SEM. n = 3.

Table A.1. Summary of flow resistance during neutrophil perfusion.

	Resistance (cmH$_2$O/(mL/hr)		P-value
	Inactivated	Activated	
Single Channel	18.92 ± 6.26	18.65 ± 5.54	P > 0.05
Multi-Network	27.89 ± 3.76	27.9 ± 3.28	P > 0.05

Similar experiments were repeated in the presence of 10% hematocrit to evaluate the contributions of erythrocytes. The perfusion pressure readings obtained from the flow of activated neutrophil populations for both the single-channel microchamber (Fig. A.2, A) and the micronetwork chamber (Fig. A.2, B) appeared to be elevated in comparison to that of inactivated neutrophil populations. In line with this, activated neutrophils in the presence of erythrocytes appeared to increase the slope of the pressure flow curves for both chambers (Fig. A.2, C). Quantitatively, while the baseline resistance to neutrophil perfusion of both chambers was increased by the addition of 10% hematocrit alone, fMLP stimulation, when combined with erythrocytes, significantly (P < 0.05) elevated the flow resistance of both chambers (Table A.2). Notably, the increase in flow resistance of the micronetwork chamber due to neutrophil activation in the presence of hematocrit was significantly (P < 0.05) higher than that of the single-channel microchamber (Table A.3).

105
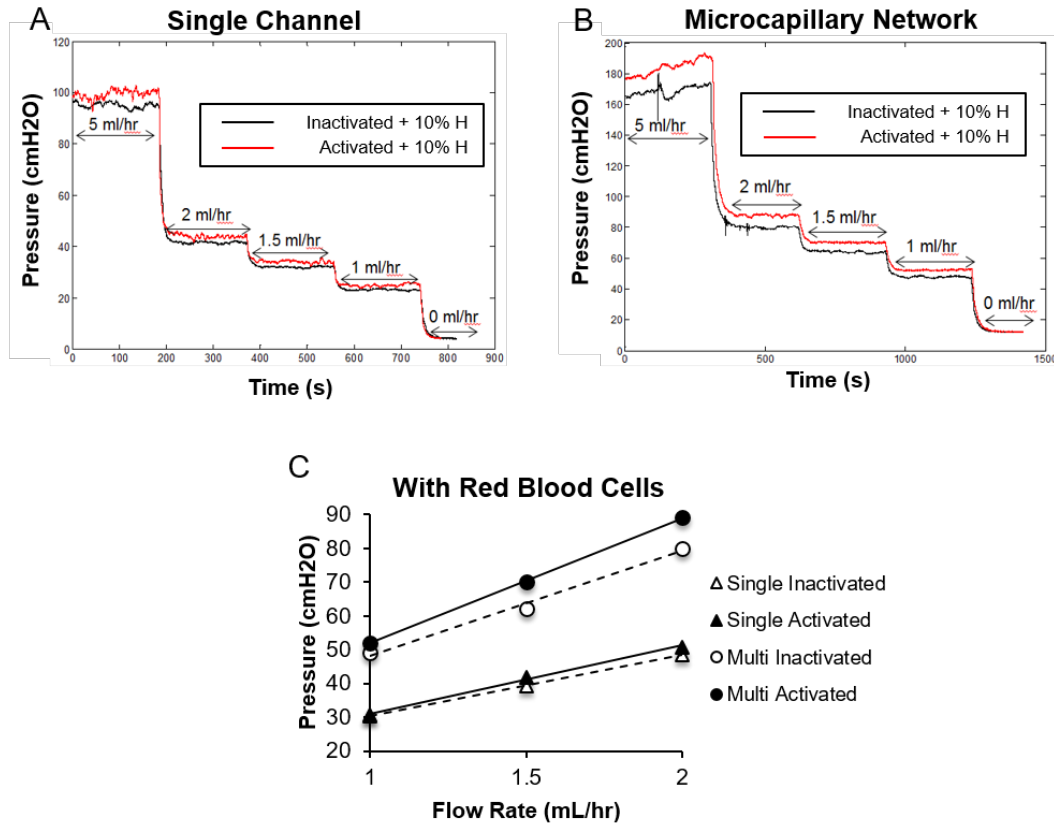
Figure A.2. Suspensions of activated neutrophils and erythrocytes significantly impact the flow properties of microvascular mimics.
(A-B) Plots of perfusion pressure versus time for a single 500x50 µm channel (A) or a network of twenty 20x50µm microchannels (B) were generated at various flow rates (0, 1, 1.5, 2, and 5 mL/hr) for purified neutrophil suspensions maintained in an inactivated state (solid black line) or activated with 10 nM fMLP (solid red line), and subsequently supplemented with 10% hematocrit. **(C)** To determine effects of neutrophil activation on microchannel flow resistance, pressure versus flow curves were generated from the raw data. Pressure values were averaged over the last 2 minutes recorded at each flow rate. From the generated curves, resistance values corresponding to single channel (inactivated, open triangles; activated, solid triangle) or microvascular network (inactivated, open circles; activated, solid circles) were found by computing the slope of each line. Points are mean ± SEM. n = 3.

Table A.2. Summary of flow resistance during neutrophil and erythrocyte perfusion.

	Resistance (cmH$_2$O/(mL/hr)		P-value
	Inactivated	Activated	
Single Channel	21.91 ± 6.87	22.7 ± 7.41	P < 0.05
Multi-Network	31.98 ± 2.21	34.91 ± 3.44	P < 0.05

106

Table A.3. The contributions of erythrocytes in elevating flow resistance.

	Percent Difference		
	0% Hct		10% Hct
Single Channel	1.4%		3.61%*
Multi-Network	0.035%		9.16%*#

*P < 0.05 compared to 0% difference (one-sample t-test)
#P < 0.05 compared to percent difference in single channel (Student's t test)

A.3.2 Summary of findings/interpretations

The results of the present study provided evidence for the following significant findings.

- Neutrophil activation in blood-like cell suspensions enhances the flow resistance of microscale channels of sizes representative of those found for non-capillary microvasculature.

- Hematocrit is an important contributor to the effects of neutrophil activation on the flow resistance of microchannels.

REFERENCES

[1] Ritchey, M. D., Wall, H. K., Gillespie, C., George, M. G., Jamal, A., Division for Heart, D., Stroke Prevention, C. D. C. (2014) Million hearts: prevalence of leading cardiovascular disease risk factors--United States, 2005-2012. *MMWR Morb Mortal Wkly Rep*. **63**(21), 462-467.

[2] Nelson, R. H. (2013) Hyperlipidemia as a risk factor for cardiovascular disease. *Prim Care*. **40**(1), 195-211. doi:10.1016/j.pop.2012.11.003

[3] Weycker, D., Nichols, G. A., O'Keeffe-Rosetti, M., Edelsberg, J., Khan, Z. M., Kaura, S., Oster, G. (2007) Risk-factor clustering and cardiovascular disease risk in hypertensive patients. *Am J Hypertens*. **20**(6), 599-607. doi:10.1016/j.amjhyper.2006.10.013

[4] Granger, D. N. (1999) Ischemia-reperfusion: mechanisms of microvascular dysfunction and the influence of risk factors for cardiovascular disease. *Microcirculation*. **6**(3), 167-178.

[5] Parodi, O., Sambuceti, G. (1996) The role of coronary microvascular dysfunction in the genesis of cardiovascular diseases. *Q J Nucl Med*. **40**(1), 9-16.

[6] Willerson, J. T., Ridker, P. M. (2004) Inflammation as a cardiovascular risk factor. *Circulation*. **109**(21 Suppl 1), II2-10. doi:10.1161/01.CIR.0000129535.04194.38

[7] Horne, B. D., Anderson, J. L., John, J. M., Weaver, A., Bair, T. L., Jensen, K. R., Renlund, D. G., Muhlestein, J. B., Intermountain Heart Collaborative Study, G. (2005) Which white blood cell subtypes predict increased cardiovascular risk? *J Am Coll Cardiol*. **45**(10), 1638-1643. doi:10.1016/j.jacc.2005.02.054

[8] Madjid, M., Awan, I., Willerson, J. T., Casscells, S. W. (2004) Leukocyte count and coronary heart disease: implications for risk assessment. *J Am Coll Cardiol*. **44**(10), 1945-1956. doi:10.1016/j.jacc.2004.07.056

[9] Scalia, R., Appel, J. Z., 3rd, Lefer, A. M. (1998) Leukocyte-endothelium interaction during the early stages of hypercholesterolemia in the rabbit: role of P-selectin, ICAM-1, and VCAM-1. *Arterioscler Thromb Vasc Biol*. **18**(7), 1093-1100.

[10] Tomida, K., Tamai, K., Matsuda, Y., Matsubara, A., Ogura, Y. (2001) Hypercholesterolemia induces leukocyte entrapment in the retinal microcirculation of rats. *Curr Eye Res*. **23**(1), 38-43.

[11] Mayadas, T. N., Cullere, X., Lowell, C. A. (2014) The multifaceted functions of neutrophils. *Annu Rev Pathol*. **9**, 181-218. doi:10.1146/annurev-pathol-020712-164023

[12] Simon, S. I., Goldsmith, H. L. (2002) Leukocyte adhesion dynamics in shear flow. *Ann Biomed Eng*. **30**(3), 315-332.

[13] Schmid-Schonbein, G. W. (2006) Analysis of inflammation. *Annu Rev Biomed Eng*. **8**, 93-131. doi:10.1146/annurev.bioeng.8.061505.095708

[14] Segel, G. B., Halterman, M. W., Lichtman, M. A. (2011) The paradox of the neutrophil's role in tissue injury. *J Leukoc Biol*. **89**(3), 359-372. doi:10.1189/jlb.0910538

[15] Mazzoni, M. C., Schmid-Schonbein, G. W. (1996) Mechanisms and consequences of cell activation in the microcirculation. *Cardiovasc Res*. **32**(4), 709-719.

[16] Schmid-Schonbein, G. W. (2009) 2008 Landis Award lecture. Inflammation and the autodigestion hypothesis. *Microcirculation*. **16**(4), 289-306. doi:10.1080/10739680902801949

[17] Kim, Y. M., Yamazaki, I., Piette, L. H. (1994) The effect of hemoglobin, hematin, and iron on neutrophil inactivation in superoxide generating systems. *Arch Biochem Biophys*. **309**(2), 308-314. doi:10.1006/abbi.1994.1118

[18] Miles, K., Clarke, D. J., Lu, W., Sibinska, Z., Beaumont, P. E., Davidson, D. J., Barr, T. A., Campopiano, D. J., Gray, M. (2009) Dying and necrotic neutrophils are anti-inflammatory secondary to the release of alpha-defensins. *J Immunol*. **183**(3), 2122-2132. doi:10.4049/jimmunol.0804187

[19] Makino, A., Shin, H. Y., Komai, Y., Fukuda, S., Coughlin, M., Sugihara-Seki, M., Schmid-Schonbein, G. W. (2007) Mechanotransduction in leukocyte activation: a review. *Biorheology*. **44**(4), 221-249.

[20] Fukuda, S., Yasu, T., Predescu, D. N., Schmid-Schonbein, G. W. (2000) Mechanisms for regulation of fluid shear stress response in circulating leukocytes. *Circ Res*. **86**(1), E13-18.

[21] Moazzam, F., DeLano, F. A., Zweifach, B. W., Schmid-Schonbein, G. W. (1997) The leukocyte response to fluid stress. *Proc Natl Acad Sci U S A*. **94**(10), 5338-5343.

[22] Shin, H. Y., Zhang, X., Makino, A., Schmid-Schonbein, G. W. (2011) Mechanobiological Evidence for the Control of Neutrophil Activity by Fluid Shear Stress. In: *Mechanobiology Handbook*. CRC Press; 139-175. doi:10.1201/b10780-11

[23] Fukuda, S., Schmid-Schonbein, G. W. (2003) Regulation of CD18 expression on neutrophils in response to fluid shear stress. *Proc Natl Acad Sci U S A*. **100**(23), 13152-13157. doi:10.1073/pnas.2336130100

[24] Fukuda, S., Mitsuoka, H., Schmid-Schonbein, G. W. (2004) Leukocyte fluid shear response in the presence of glucocorticoid. *J Leukoc Biol*. **75**(4), 664-670. doi:10.1189/jlb.1003464

[25] Fukuda, S., Yasu, T., Kobayashi, N., Ikeda, N., Schmid-Schonbein, G. W. (2004) Contribution of fluid shear response in leukocytes to hemodynamic resistance in the spontaneously hypertensive rat. *Circ Res*. **95**(1), 100-108. doi:10.1161/01.RES.0000133677.77465.38

[26] Zhang, X., Cheng, R., Rowe, D., Sethu, P., Daugherty, A., Yu, G., Shin, H. Y. (2014) Shear-sensitive regulation of neutrophil flow behavior and its potential impact on microvascular blood flow dysregulation in hypercholesterolemia. *Arterioscler Thromb Vasc Biol*. **34**(3), 587-593. doi:10.1161/ATVBAHA.113.302868

[27] Zhang, X., Hurng, J., Rateri, D. L., Daugherty, A., Schmid-Schonbein, G. W., Shin, H. Y. (2011) Membrane cholesterol modulates the fluid shear stress response of polymorphonuclear leukocytes via its effects on membrane fluidity. *Am J Physiol Cell Physiol*. **301**(2), C451-460. doi:10.1152/ajpcell.00458.2010

[28] de Meyer, F., Smit, B. (2009) Effect of cholesterol on the structure of a phospholipid bilayer. *Proc Natl Acad Sci U S A*. **106**(10), 3654-3658. doi:10.1073/pnas.0809959106

109

[29] Drechsler, M., Megens, R. T., van Zandvoort, M., Weber, C., Soehnlein, O. (2010) Hyperlipidemia-triggered neutrophilia promotes early atherosclerosis. *Circulation*. **122**(18), 1837-1845. doi:10.1161/CIRCULATIONAHA.110.961714

[30] Hochmuth, R. M., Ting-Beall, H. P., Beaty, B. B., Needham, D., Tran-Son-Tay, R. (1993) Viscosity of passive human neutrophils undergoing small deformations. *Biophys J*. **64**(5), 1596-1601. doi:10.1016/S0006-3495(93)81530-3

[31] Kolaczkowska, E., Kubes, P. (2013) Neutrophil recruitment and function in health and inflammation. *Nat Rev Immunol*. **13**(3), 159-175. doi:10.1038/nri3399

[32] Sutton, D. W., Schmid-Schonbein, G. W. (1992) Elevation of organ resistance due to leukocyte perfusion. *Am J Physiol*. **262**(6 Pt 2), H1646-1650.

[33] Warnke, K. C., Skalak, T. C. (1990) The effects of leukocytes on blood flow in a model skeletal muscle capillary network. *Microvasc Res*. **40**(1), 118-136.

[34] Bathe, M., Shirai, A., Doerschuk, C. M., Kamm, R. D. (2002) Neutrophil transit times through pulmonary capillaries: the effects of capillary geometry and fMLP-stimulation. *Biophys J*. **83**(4), 1917-1933. doi:10.1016/S0006-3495(02)73955-6

[35] Cliff, W. J. (1976) The vessel lumen. In: *Blood Vessels*. Cambridge University Press; New York.

[36] Goldsmith, H. L., Karino, T. (1977) Microscopic considerations: the motions of individual particles. *Annals of the New York Academy of Sciences*. **283**(1), 241-255. doi:10.1111/j.1749-6632.1977.tb41770.x

[37] Helmke, B. P., Bremner, S. N., Zweifach, B. W., Skalak, R., Schmid-Schonbein, G. W. (1997) Mechanisms for increased blood flow resistance due to leukocytes. *Am J Physiol*. **273**(6 Pt 2), H2884-2890.

[38] Fedosov, D. A., Caswell, B., Popel, A. S., Karniadakis, G. E. (2010) Blood flow and cell-free layer in microvessels. *Microcirculation*. **17**(8), 615-628. doi:10.1111/j.1549-8719.2010.00056.x

[39] Secomb, T. W., Pries, A. R. (2013) Blood viscosity in microvessels: experiment and theory. *C R Phys*. **14**(6), 470-478. doi:10.1016/j.crhy.2013.04.002

[40] Pappu, V., Bagchi, P. (2007) Hydrodynamic interaction between erythrocytes and leukocytes affects rheology of blood in microvessels. *Biorheology*. **44**(3), 191-215.

[41] Lipowsky, H. H. (2005) Microvascular rheology and hemodynamics. *Microcirculation*. **12**(1), 5-15. doi:10.1080/10739680590894966

[42] Ooi, B. S., Cohen, D. J., Chang, T. H., Tian, Y., Papademetrious, V. (1998) Stimulation of endothelial cell production of vasoconstrictive substances by hypertensive sera. *Am J Hypertens*. **11**(2), 240-244.

[43] Furchgott, R. F., Cherry, P. D., Zawadzki, J. V., Jothianandan, D. (1984) Endothelial cells as mediators of vasodilation of arteries. *J Cardiovasc Pharmacol*. **6 Suppl 2**, S336-343.

[44] Mehta, D., Malik, A. B. (2006) Signaling mechanisms regulating endothelial permeability. *Physiol Rev*. **86**(1), 279-367. doi:10.1152/physrev.00012.2005

[45] Sukriti, S., Tauseef, M., Yazbeck, P., Mehta, D. (2014) Mechanisms regulating endothelial permeability. *Pulm Circ*. **4**(4), 535-551. doi:10.1086/677356

[46] Halliwell, B., Gutteridge, J. M. (1990) The antioxidants of human extracellular fluids. *Arch Biochem Biophys*. **280**(1), 1-8.

110

[47] Evangelista, V., Piccardoni, P., White, J. G., de Gaetano, G., Cerletti, C. (1993) Cathepsin G-dependent platelet stimulation by activated polymorphonuclear leukocytes and its inhibition by antiproteinases: role of P-selectin-mediated cell-cell adhesion. *Blood*. **81**(11), 2947-2957.

[48] Owen, C. A., Campbell, E. J. (1995) Neutrophil proteinases and matrix degradation. The cell biology of pericellular proteolysis. *Semin Cell Biol*. **6**(6), 367-376.

[49] Dull, R. O., Garcia, J. G. (2002) Leukocyte-induced microvascular permeability: how contractile tweaks lead to leaks. *Circ Res*. **90**(11), 1143-1144.

[50] DiStasi, M. R., Ley, K. (2009) Opening the flood-gates: how neutrophil-endothelial interactions regulate permeability. *Trends Immunol*. **30**(11), 547-556. doi:10.1016/j.it.2009.07.012

[51] Nellore, K., Harris, N. R. (2002) L-arginine and antineutrophil serum enable venular control of capillary perfusion in hypercholesterolemic rats. *Microcirculation*. **9**(6), 477-485. doi:10.1038/sj.mn.7800162

[52] Granger, D. N., Senchenkova, E. Y. (2010) Impaired Vasomotor Responses. In: *Inflammation and the Microcirculation*. Morgan & Claypool Life Sciences; San Rafael, CA.

[53] Sprague, A. H., Khalil, R. A. (2009) Inflammatory cytokines in vascular dysfunction and vascular disease. *Biochem Pharmacol*. **78**(6), 539-552. doi:10.1016/j.bcp.2009.04.029

[54] Tushuizen, M. E., Diamant, M., Sturk, A., Nieuwland, R. (2011) Cell-derived microparticles in the pathogenesis of cardiovascular disease: friend or foe? *Arterioscler Thromb Vasc Biol*. **31**(1), 4-9. doi:10.1161/ATVBAHA.109.200998

[55] Tian, W., Chen, H., Chen, Y., Lei, S., Chen, Y., Bu, H., Wei, Y. (1999) [Changes of F-actin in neutrophils under fluid shear stress]. *Sheng Wu Yi Xue Gong Cheng Xue Za Zhi*. **16**(4), 399-405.

[56] Shive, M. S., Salloum, M. L., Anderson, J. M. (2000) Shear stress-induced apoptosis of adherent neutrophils: a mechanism for persistence of cardiovascular device infections. *Proc Natl Acad Sci U S A*. **97**(12), 6710-6715. doi:10.1073/pnas.110463197

[57] Mazzone, A., Ricevuti, G. (1995) Leukocyte CD11/CD18 integrins: biological and clinical relevance. *Haematologica*. **80**(2), 161-175.

[58] Hentzen, E. R., Neelamegham, S., Kansas, G. S., Benanti, J. A., McIntire, L. V., Smith, C. W., Simon, S. I. (2000) Sequential binding of CD11a/CD18 and CD11b/CD18 defines neutrophil capture and stable adhesion to intercellular adhesion molecule-1. *Blood*. **95**(3), 911-920.

[59] Zhang, X., Zhan, D., Shin, H. Y. (2013) Integrin subtype-dependent CD18 cleavage under shear and its influence on leukocyte-platelet binding. *J Leukoc Biol*. **93**(2), 251-258. doi:10.1189/jlb.0612302

[60] Zhelev, D. V., Alteraifi, A. M., Chodniewicz, D. (2004) Controlled pseudopod extension of human neutrophils stimulated with different chemoattractants. *Biophys J*. **87**(1), 688-695. doi:10.1529/biophysj.103.036699

[61] Migeotte, I., Communi, D., Parmentier, M. (2006) Formyl peptide receptors: a promiscuous subfamily of G protein-coupled receptors controlling immune responses. *Cytokine Growth Factor Rev*. **17**(6), 501-519. doi:10.1016/j.cytogfr.2006.09.009

[62] Ali, H., Richardson, R. M., Haribabu, B., Snyderman, R. (1999) Chemoattractant receptor cross-desensitization. *J Biol Chem*. **274**(10), 6027-6030.

[63] Su, S. S., Schmid-Schonbein, G. W. (2010) Internalization of Formyl Peptide Receptor in Leukocytes Subject to Fluid Stresses. *Cell Mol Bioeng*. **3**(1), 20-29. doi:10.1007/s12195-010-0111-5

[64] Mitchell, M. J., King, M. R. (2012) Shear-induced resistance to neutrophil activation via the formyl peptide receptor. *Biophys J*. **102**(8), 1804-1814. doi:10.1016/j.bpj.2012.03.053

[65] Lawrence, T., Gilroy, D. W. (2007) Chronic inflammation: a failure of resolution? *Int J Exp Pathol*. **88**(2), 85-94. doi:10.1111/j.1365-2613.2006.00507.x

[66] Ryan, S. O., Johnson, J. L., Cobb, B. A. (2013) Neutrophils confer T cell resistance to myeloid-derived suppressor cell-mediated suppression to promote chronic inflammation. *J Immunol*. **190**(10), 5037-5047. doi:10.4049/jimmunol.1203404

[67] Aggarwal, B. B., Shishodia, S., Sandur, S. K., Pandey, M. K., Sethi, G. (2006) Inflammation and cancer: how hot is the link? *Biochem Pharmacol*. **72**(11), 1605-1621. doi:10.1016/j.bcp.2006.06.029

[68] Franceschi, C., Campisi, J. (2014) Chronic inflammation (inflammaging) and its potential contribution to age-associated diseases. *J Gerontol A Biol Sci Med Sci*. **69 Suppl 1**, S4-9. doi:10.1093/gerona/glu057

[69] Chen, A. Y., DeLano, F. A., Valdez, S. R., Ha, J. N., Shin, H. Y., Schmid-Schonbein, G. W. (2010) Receptor cleavage reduces the fluid shear response in neutrophils of the spontaneously hypertensive rat. *Am J Physiol Cell Physiol*. **299**(6), C1441-1449. doi:10.1152/ajpcell.00157.2010

[70] Kanatsuka, H., Lamping, K. G., Eastham, C. L., Marcus, M. L., Dellsperger, K. C. (1991) Coronary microvascular resistance in hypertensive cats. *Circ Res*. **68**(3), 726-733.

[71] Roy, J. W., Mayrovitz, H. N. (1984) Microvascular pressure, flow, and resistance in spontaneously hypertensive rats. *Hypertension*. **6**(6 Pt 1), 877-886.

[72] Helmke, B. P., Sugihara-Seki, M., Skalak, R., Schmid-Schonbein, G. W. (1998) A mechanism for erythrocyte-mediated elevation of apparent viscosity by leukocytes in vivo without adhesion to the endothelium. *Biorheology*. **35**(6), 437-448.

[73] Akenhead, M. L., Horrall, N. M., Rowe, D., Sethu, P., Shin, H. Y. (2015) In Vitro Evaluation of the Link Between Cell Activation State and Its Rheological Impact on the Microscale Flow of Neutrophil Suspensions. *J Biomech Eng*. **137**(9), doi:10.1115/1.4030824

[74] Stokes, K. Y., Granger, D. N. (2005) The microcirculation: a motor for the systemic inflammatory response and large vessel disease induced by hypercholesterolaemia? *J Physiol*. **562**(Pt 3), 647-653. doi:10.1113/jphysiol.2004.079640

[75] Tailor, A., Granger, D. N. (2003) Hypercholesterolemia promotes P-selectin-dependent platelet-endothelial cell adhesion in postcapillary venules. *Arterioscler Thromb Vasc Biol*. **23**(4), 675-680. doi:10.1161/01.ATV.0000056742.97580.79

[76] Lefer, A. M., Ma, X. L. (1993) Decreased basal nitric oxide release in hypercholesterolemia increases neutrophil adherence to rabbit coronary artery endothelium. *Arterioscler Thromb*. **13**(6), 771-776.

112

[77] Stulc, T., Vrablik, M., Kasalova, Z., Marinov, I., Svobodova, H., Ceska, R. (2008) Leukocyte and endothelial adhesion molecules in patients with hypercholesterolemia: the effect of atorvastatin treatment. *Physiol Res*. **57**(2), 185-194.

[78] Granger, D. N., Rodrigues, S. F., Yildirim, A., Senchenkova, E. Y. (2010) Microvascular responses to cardiovascular risk factors. *Microcirculation*. **17**(3), 192-205. doi:10.1111/j.1549-8719.2009.00015.x

[79] Mazor, R., Shurtz-Swirski, R., Farah, R., Kristal, B., Shapiro, G., Dorlechter, F., Cohen-Mazor, M., Meilin, E., Tamara, S., Sela, S. (2008) Primed polymorphonuclear leukocytes constitute a possible link between inflammation and oxidative stress in hyperlipidemic patients. *Atherosclerosis*. **197**(2), 937-943. doi:10.1016/j.atherosclerosis.2007.08.014

[80] Stokes, K. Y., Cooper, D., Tailor, A., Granger, D. N. (2002) Hypercholesterolemia promotes inflammation and microvascular dysfunction: role of nitric oxide and superoxide. *Free Radic Biol Med*. **33**(8), 1026-1036.

[81] Kubes, P., Suzuki, M., Granger, D. N. (1991) Nitric oxide: an endogenous modulator of leukocyte adhesion. *Proc Natl Acad Sci U S A*. **88**(11), 4651-4655.

[82] Liao, J. K. (2013) Linking endothelial dysfunction with endothelial cell activation. *J Clin Invest*. **123**(2), 540-541. doi:10.1172/JCI66843

[83] Maiellaro, K., Taylor, W. R. (2007) The role of the adventitia in vascular inflammation. *Cardiovasc Res*. **75**(4), 640-648. doi:10.1016/j.cardiores.2007.06.023

[84] VanTeeffelen, J. W., Constantinescu, A. A., Vink, H., Spaan, J. A. (2005) Hypercholesterolemia impairs reactive hyperemic vasodilation of 2A but not 3A arterioles in mouse cremaster muscle. *Am J Physiol Heart Circ Physiol*. **289**(1), H447-454. doi:10.1152/ajpheart.01298.2004

[85] Engelke, K. A., Halliwill, J. R., Proctor, D. N., Dietz, N. M., Joyner, M. J. (1996) Contribution of nitric oxide and prostaglandins to reactive hyperemia in human forearm. *J Appl Physiol (1985)*. **81**(4), 1807-1814.

[86] Binggeli, C., Spieker, L. E., Corti, R., Sudano, I., Stojanovic, V., Hayoz, D., Luscher, T. F., Noll, G. (2003) Statins enhance postischemic hyperemia in the skin circulation of hypercholesterolemic patients: a monitoring test of endothelial dysfunction for clinical practice? *J Am Coll Cardiol*. **42**(1), 71-77.

[87] Pohlman, T. H., Harlan, J. M. (2000) Adaptive responses of the endothelium to stress. *J Surg Res*. **89**(1), 85-119. doi:10.1006/jsre.1999.5801

[88] Chachisvilis, M., Zhang, Y. L., Frangos, J. A. (2006) G protein-coupled receptors sense fluid shear stress in endothelial cells. *Proc Natl Acad Sci U S A*. **103**(42), 15463-15468. doi:10.1073/pnas.0607224103

[89] Chen, K. D., Li, Y. S., Kim, M., Li, S., Yuan, S., Chien, S., Shyy, J. Y. (1999) Mechanotransduction in response to shear stress. Roles of receptor tyrosine kinases, integrins, and Shc. *J Biol Chem*. **274**(26), 18393-18400.

[90] Gu, C. X., Juranka, P. F., Morris, C. E. (2001) Stretch-activation and stretch-inactivation of Shaker-IR, a voltage-gated K+ channel. *Biophys J*. **80**(6), 2678-2693. doi:10.1016/S0006-3495(01)76237-6

[91] Lee, H. J., Koh, G. Y. (2003) Shear stress activates Tie2 receptor tyrosine kinase in human endothelial cells. *Biochem Biophys Res Commun*. **304**(2), 399-404.

[92] Makino, A., Prossnitz, E. R., Bunemann, M., Wang, J. M., Yao, W., Schmid-Schonbein, G. W. (2006) G protein-coupled receptors serve as mechanosensors for fluid shear stress in neutrophils. *Am J Physiol Cell Physiol*. **290**(6), C1633-1639. doi:10.1152/ajpcell.00576.2005

[93] Shin, H. Y., Simon, S. I., Schmid-Schonbein, G. W. (2008) Fluid shear-induced activation and cleavage of CD18 during pseudopod retraction by human neutrophils. *J Cell Physiol*. **214**(2), 528-536. doi:10.1002/jcp.21235

[94] Zhang, Y. L., Frangos, J. A., Chachisvilis, M. (2009) Mechanical stimulus alters conformation of type 1 parathyroid hormone receptor in bone cells. *Am J Physiol Cell Physiol*. **296**(6), C1391-1399. doi:10.1152/ajpcell.00549.2008

[95] Abram, C. L., Lowell, C. A. (2009) The ins and outs of leukocyte integrin signaling. *Annu Rev Immunol*. **27**, 339-362. doi:10.1146/annurev.immunol.021908.132554

[96] Lynch, O. T., Giembycz, M. A., Barnes, P. J., Hellewell, P. G., Lindsay, M. A. (1999) 'Outside-in' signalling mechanisms underlying CD11b/CD18-mediated NADPH oxidase activation in human adherent blood eosinophils. *Br J Pharmacol*. **128**(6), 1149-1158. doi:10.1038/sj.bjp.0702892

[97] Marschel, P., Schmid-Schonbein, G. W. (2002) Control of fluid shear response in circulating leukocytes by integrins. *Ann Biomed Eng*. **30**(3), 333-343.

[98] Berlin, R. D., Fera, J. P. (1977) Changes in membrane microviscosity associated with phagocytosis: effects of colchicine. *Proc Natl Acad Sci U S A*. **74**(3), 1072-1076.

[99] Oliver, J. M. (1978) Cell biology of leukocyte abnormalities--membrane and cytoskeletal function in normal and defective cells. A review. *Am J Pathol*. **93**(1), 221-270.

[100] Tomonaga, A., Hirota, M., Snyderman, R. (1983) Effect of membrane fluidizers on the number and affinity of chemotactic factor receptors on human polymorphonuclear leukocytes. *Microbiol Immunol*. **27**(11), 961-972.

[101] Yuli, I., Tomonaga, A., Synderman, R. (1982) Chemoattractant receptor functions in human polymorphonuclear leukocytes are divergently altered by membrane fluidizers. *Proc Natl Acad Sci U S A*. **79**(19), 5906-5910.

[102] Yeagle, P. L. (1991) Modulation of membrane function by cholesterol. *Biochimie*. **73**(10), 1303-1310.

[103] Chabanel, A., Flamm, M., Sung, K. L., Lee, M. M., Schachter, D., Chien, S. (1983) Influence of cholesterol content on red cell membrane viscoelasticity and fluidity. *Biophys J*. **44**(2), 171-176. doi:10.1016/S0006-3495(83)84288-X

[104] Cooper, R. A. (1978) Influence of increased membrane cholesterol on membrane fluidity and cell function in human red blood cells. *J Supramol Struct*. **8**(4), 413-430. doi:10.1002/jss.400080404

[105] Simons, K., Toomre, D. (2000) Lipid rafts and signal transduction. *Nat Rev Mol Cell Biol*. **1**(1), 31-39. doi:10.1038/35036052

[106] Margina, D., Gradinaru, D., Manda, G., Neagoe, I., Ilie, M. (2013) Membranar effects exerted in vitro by polyphenols - quercetin, epigallocatechin gallate and curcumin - on HUVEC and Jurkat cells, relevant for diabetes mellitus. *Food Chem Toxicol*. **61**, 86-93. doi:10.1016/j.fct.2013.02.046

[107] Hauert, A. B., Martinelli, S., Marone, C., Niggli, V. (2002) Differentiated HL-60 cells are a valid model system for the analysis of human neutrophil migration and chemotaxis. *Int J Biochem Cell Biol*. **34**(7), 838-854.

[108] Makino, A., Glogauer, M., Bokoch, G. M., Chien, S., Schmid-Schonbein, G. W. (2005) Control of neutrophil pseudopods by fluid shear: role of Rho family GTPases. *Am J Physiol Cell Physiol*. **288**(4), C863-871. doi:10.1152/ajpcell.00358.2004

[109] Carrigan, S. O., Weppler, A. L., Issekutz, A. C., Stadnyk, A. W. (2005) Neutrophil differentiated HL-60 cells model Mac-1 (CD11b/CD18)-independent neutrophil transepithelial migration. *Immunology*. **115**(1), 108-117. doi:10.1111/j.1365-2567.2005.02131.x

[110] Noti, J. D. (2002) Expression of the myeloid-specific leukocyte integrin gene CD11d during macrophage foam cell differentiation and exposure to lipoproteins. *Int J Mol Med*. **10**(6), 721-727.

[111] Noti, J. D., Johnson, A. K., Dillon, J. D. (2004) The zinc finger transcription factor transforming growth factor beta-inducible early gene-1 confers myeloid-specific activation of the leukocyte integrin CD11d promoter. *J Biol Chem*. **279**(26), 26948-26958. doi:10.1074/jbc.M310634200

[112] Akenhead, M. L., Zhang, X., Shin, H. Y. (2014) Characterization of the shear stress regulation of CD18 surface expression by HL60-derived neutrophil-like cells. *Biomech Model Mechanobiol*. **13**(4), 861-870. doi:10.1007/s10237-013-0541-9

[113] Brown, K. K., Henson, P. M., Maclouf, J., Moyle, M., Ely, J. A., Worthen, G. S. (1998) Neutrophil-platelet adhesion: relative roles of platelet P-selectin and neutrophil beta2 (DC18) integrins. *Am J Respir Cell Mol Biol*. **18**(1), 100-110. doi:10.1165/ajrcmb.18.1.2314

[114] Hu, H., Varon, D., Hjemdahl, P., Savion, N., Schulman, S., Li, N. (2003) Platelet-leukocyte aggregation under shear stress: differential involvement of selectins and integrins. *Thromb Haemost*. **90**(4), 679-687. doi:10.1160/TH03-05-0274

[115] Ding, Z. M., Babensee, J. E., Simon, S. I., Lu, H., Perrard, J. L., Bullard, D. C., Dai, X. Y., Bromley, S. K., Dustin, M. L., Entman, M. L., Smith, C. W., Ballantyne, C. M. (1999) Relative contribution of LFA-1 and Mac-1 to neutrophil adhesion and migration. *J Immunol*. **163**(9), 5029-5038.

[116] van Spriel, A. B., Leusen, J. H., van Egmond, M., Dijkman, H. B., Assmann, K. J., Mayadas, T. N., van de Winkel, J. G. (2001) Mac-1 (CD11b/CD18) is essential for Fc receptor-mediated neutrophil cytotoxicity and immunologic synapse formation. *Blood*. **97**(8), 2478-2486.

[117] Phillipson, M., Heit, B., Colarusso, P., Liu, L., Ballantyne, C. M., Kubes, P. (2006) Intraluminal crawling of neutrophils to emigration sites: a molecularly distinct process from adhesion in the recruitment cascade. *J Exp Med*. **203**(12), 2569-2575. doi:10.1084/jem.20060925

[118] Anderson, D. C., Schmalsteig, F. C., Finegold, M. J., Hughes, B. J., Rothlein, R., Miller, L. J., Kohl, S., Tosi, M. F., Jacobs, R. L., Waldrop, T. C., et al. (1985) The severe and moderate phenotypes of heritable Mac-1, LFA-1 deficiency: their quantitative definition and relation to leukocyte dysfunction and clinical features. *J Infect Dis*. **152**(4), 668-689.

[119] Hogg, N., Stewart, M. P., Scarth, S. L., Newton, R., Shaw, J. M., Law, S. K., Klein, N. (1999) A novel leukocyte adhesion deficiency caused by expressed but nonfunctional beta2 integrins Mac-1 and LFA-1. *J Clin Invest*. **103**(1), 97-106. doi:10.1172/JCI3312

[120] Dhurat, R., Sukesh, M. (2014) Principles and Methods of Preparation of Platelet-Rich Plasma: A Review and Author's Perspective. *J Cutan Aesthet Surg*. **7**(4), 189-197. doi:10.4103/0974-2077.150734

[121] Meijering, E., Dzyubachyk, O., Smal, I. (2012) Methods for cell and particle tracking. *Methods Enzymol*. **504**, 183-200. doi:10.1016/B978-0-12-391857-4.00009-4

[122] Sheikh, S., Nash, G. B. (1996) Continuous activation and deactivation of integrin CD11b/CD18 during de novo expression enables rolling neutrophils to immobilize on platelets. *Blood*. **87**(12), 5040-5050.

[123] Ganguly, A., Zhang, H., Sharma, R., Parsons, S., Patel, K. D. (2012) Isolation of human umbilical vein endothelial cells and their use in the study of neutrophil transmigration under flow conditions. *J Vis Exp*. (66), e4032. doi:10.3791/4032

[124] Jamet, A., Euphrasie, D., Martin, P., Nassif, X. (2013) Identification of genes involved in Neisseria meningitidis colonization. *Infect Immun*. **81**(9), 3375-3381. doi:10.1128/IAI.00421-13

[125] Niggli, V., Meszaros, A. V., Oppliger, C., Tornay, S. (2004) Impact of cholesterol depletion on shape changes, actin reorganization, and signal transduction in neutrophil-like HL-60 cells. *Exp Cell Res*. **296**(2), 358-368. doi:10.1016/j.yexcr.2004.02.015

[126] Oh, H., Mohler, E. R., 3rd, Tian, A., Baumgart, T., Diamond, S. L. (2009) Membrane cholesterol is a biomechanical regulator of neutrophil adhesion. *Arterioscler Thromb Vasc Biol*. **29**(9), 1290-1297. doi:10.1161/ATVBAHA.109.189571

[127] Gauthier, T. W., Scalia, R., Murohara, T., Guo, J. P., Lefer, A. M. (1995) Nitric oxide protects against leukocyte-endothelium interactions in the early stages of hypercholesterolemia. *Arterioscler Thromb Vasc Biol*. **15**(10), 1652-1659.

[128] Stokes, K. Y., Calahan, L., Russell, J. M., Gurwara, S., Granger, D. N. (2006) Role of platelets in hypercholesterolemia-induced leukocyte recruitment and arteriolar dysfunction. *Microcirculation*. **13**(5), 377-388. doi:10.1080/10739680600745877

[129] Yu, G., Durduran, T., Lech, G., Zhou, C., Chance, B., Mohler, E. R., 3rd, Yodh, A. G. (2005) Time-dependent blood flow and oxygenation in human skeletal muscles measured with noninvasive near-infrared diffuse optical spectroscopies. *J Biomed Opt*. **10**(2), 024027. doi:10.1117/1.1884603

[130] Yu, G., Durduran, T., Zhou, C., Wang, H. W., Putt, M. E., Saunders, H. M., Sehgal, C. M., Glatstein, E., Yodh, A. G., Busch, T. M. (2005) Noninvasive monitoring of murine tumor blood flow during and after photodynamic therapy provides early assessment of therapeutic efficacy. *Clin Cancer Res*. **11**(9), 3543-3552. doi:10.1158/1078-0432.CCR-04-2582

[131] Shang, Y., Zhao, Y., Cheng, R., Dong, L., Irwin, D., Yu, G. (2009) Portable optical tissue flow oximeter based on diffuse correlation spectroscopy. *Opt Lett*. **34**(22), 3556-3558. doi:10.1364/OL.34.003556

[132] Galeano, N. F., Milne, R., Marcel, Y. L., Walsh, M. T., Levy, E., Ngu'yen, T. D., Gleeson, A., Arad, Y., Witte, L., Al-Haideri, M., Rumsey, S. C., Deckelbaum, R. J., et al. (1994) Apoprotein B structure and receptor recognition of triglyceride-rich low density lipoprotein (LDL) is modified in small LDL but not in triglyceride-rich LDL of normal size. *J Biol Chem*. **269**(1), 511-519.

[133] Gordon, L. M., Sauerheber, R. D., Esgate, J. A., Dipple, I., Marchmont, R. J., Houslay, M. D. (1980) The increase in bilayer fluidity of rat liver plasma membranes achieved by the local anesthetic benzyl alcohol affects the activity of intrinsic membrane enzymes. *J Biol Chem*. **255**(10), 4519-4527.

[134] Moulin, M., Carpentier, S., Levade, T., Arrigo, A. P. (2007) Potential roles of membrane fluidity and ceramide in hyperthermia and alcohol stimulation of TRAIL apoptosis. *Apoptosis*. **12**(9), 1703-1720. doi:10.1007/s10495-007-0096-2

[135] Lopez-Otin, C., Bond, J. S. (2008) Proteases: multifunctional enzymes in life and disease. *J Biol Chem*. **283**(45), 30433-30437. doi:10.1074/jbc.R800035200

[136] Jane, D. T., Morvay, L. C., Allen, F., Sloane, B. F., Dufresne, M. J. (2002) Selective inhibition of cathepsin B with cell-permeable CA074Me negatively affects L6 rat myoblast differentiation. *Biochem Cell Biol*. **80**(4), 457-465.

[137] Costantini, C., Micheletti, A., Calzetti, F., Perbellini, O., Tamassia, N., Albanesi, C., Vermi, W., Cassatella, M. A. (2011) On the potential involvement of CD11d in co-stimulating the production of interferon-gamma by natural killer cells upon interaction with neutrophils via intercellular adhesion molecule-3. *Haematologica*. **96**(10), 1543-1547. doi:10.3324/haematol.2011.044578

[138] Gahmberg, C. G., Tolvanen, M., Kotovuori, P. (1997) Leukocyte adhesion--structure and function of human leukocyte beta2-integrins and their cellular ligands. *Eur J Biochem*. **245**(2), 215-232.

[139] Sadhu, C., Ting, H. J., Lipsky, B., Hensley, K., Garcia-Martinez, L. F., Simon, S. I., Staunton, D. E. (2007) CD11c/CD18: novel ligands and a role in delayed-type hypersensitivity. *J Leukoc Biol*. **81**(6), 1395-1403. doi:10.1189/jlb.1106680

[140] Root, R. K. (1990) Leukocyte adhesion proteins: their role in neutrophil function. *Trans Am Clin Climatol Assoc*. **101**, 207-224; discussion 224-206.

[141] Diez-Fraile, A., Duchateau, L., Meyer, E., Burvenich, C. (2003) Expression of beta2-integrin on monocytes and blood polymorphonuclear leukocytes in the periparturient period in dairy cows. *Can J Vet Res*. **67**(3), 235-238.

[142] Harris, A. G., Skalak, T. C. (1993) Effects of leukocyte activation on capillary hemodynamics in skeletal muscle. *Am J Physiol*. **264**(3 Pt 2), H909-916.

[143] Bohley, P., Seglen, P. O. (1992) Proteases and proteolysis in the lysosome. *Experientia*. **48**(2), 151-157.

[144] Balaji, K. N., Schaschke, N., Machleidt, W., Catalfamo, M., Henkart, P. A. (2002) Surface cathepsin B protects cytotoxic lymphocytes from self-destruction after degranulation. *J Exp Med*. **196**(4), 493-503.

[145] Frosch, B. A., Berquin, I., Emmert-Buck, M. R., Moin, K., Sloane, B. F. (1999) Molecular regulation, membrane association and secretion of tumor cathepsin B. *APMIS*. **107**(1), 28-37.

[146] Podgorski, I., Sloane, B. F. (2003) Cathepsin B and its role(s) in cancer progression. *Biochem Soc Symp*. (70), 263-276.

117

[147] Roshy, S., Sloane, B. F., Moin, K. (2003) Pericellular cathepsin B and malignant progression. *Cancer Metastasis Rev*. **22**(2-3), 271-286.

[148] Jog, N. R., Rane, M. J., Lominadze, G., Luerman, G. C., Ward, R. A., McLeish, K. R. (2007) The actin cytoskeleton regulates exocytosis of all neutrophil granule subsets. *Am J Physiol Cell Physiol*. **292**(5), C1690-1700. doi:10.1152/ajpcell.00384.2006

[149] Mitchell, T., Lo, A., Logan, M. R., Lacy, P., Eitzen, G. (2008) Primary granule exocytosis in human neutrophils is regulated by Rac-dependent actin remodeling. *Am J Physiol Cell Physiol*. **295**(5), C1354-1365. doi:10.1152/ajpcell.00239.2008

[150] Dewitz, T. S., Hung, T. C., Martin, R. R., McIntire, L. V. (1977) Mechanical trauma in leukocytes. *J Lab Clin Med*. **90**(4), 728-736.

[151] Alemany, R., Meyer zu Heringdorf, D., van Koppen, C. J., Jakobs, K. H. (1999) Formyl peptide receptor signaling in HL-60 cells through sphingosine kinase. *J Biol Chem*. **274**(7), 3994-3999.

[152] Rossy, J., Schlicht, D., Engelhardt, B., Niggli, V. (2009) Flotillins interact with PSGL-1 in neutrophils and, upon stimulation, rapidly organize into membrane domains subsequently accumulating in the uropod. *PLoS One*. **4**(4), e5403. doi:10.1371/journal.pone.0005403

[153] Magalhaes, M. A., Zhu, F., Sarantis, H., Gray-Owen, S. D., Ellen, R. P., Glogauer, M. (2007) Expression and translocation of fluorescent-tagged p21-activated kinase-binding domain and PH domain of protein kinase B during murine neutrophil chemotaxis. *J Leukoc Biol*. **82**(3), 559-566. doi:10.1189/jlb.0207126

[154] Zhao, T., Bokoch, G. M. (2007) Transduction of proteins into intact neutrophils. *Methods Mol Biol*. **412**, 115-123. doi:10.1007/978-1-59745-467-4_9

[155] Dabydeen, S. A., Meneses, P. I. (2009) The role of NH4Cl and cysteine proteases in Human Papillomavirus type 16 infection. *Virol J*. **6**, 109. doi:10.1186/1743-422X-6-109

[156] Moncman, C. L., Wang, K. (1998) Effects of thiol protease inhibitors on myoblast fusion and myofibril assembly in vitro. *Cell Motil Cytoskeleton*. **40**(4), 354-367. doi:10.1002/(SICI)1097-0169(1998)40:4<354::AID-CM4>3.0.CO;2-B

[157] Nowak, N., Lotter, H., Tannich, E., Bruchhaus, I. (2004) Resistance of Entamoeba histolytica to the cysteine proteinase inhibitor E64 is associated with secretion of pro-enzymes and reduced pathogenicity. *J Biol Chem*. **279**(37), 38260-38266. doi:10.1074/jbc.M405308200

[158] Burnett, D., Crocker, J., Vaughan, A. T. (1983) Synthesis of cathepsin B by cells derived from the HL60 promyelocytic leukaemia cell line. *J Cell Physiol*. **115**(3), 249-254. doi:10.1002/jcp.1041150306

[159] Borregaard, N., Cowland, J. B. (1997) Granules of the human neutrophilic polymorphonuclear leukocyte. *Blood*. **89**(10), 3503-3521.

[160] Vaisar, T., Kassim, S. Y., Gomez, I. G., Green, P. S., Hargarten, S., Gough, P. J., Parks, W. C., Wilson, C. L., Raines, E. W., Heinecke, J. W. (2009) MMP-9 sheds the beta2 integrin subunit (CD18) from macrophages. *Mol Cell Proteomics*. **8**(5), 1044-1060. doi:10.1074/mcp.M800449-MCP200

[161] Ballestrem, C., Wehrle-Haller, B., Hinz, B., Imhof, B. A. (2000) Actin-dependent lamellipodia formation and microtubule-dependent tail retraction control-directed cell migration. *Mol Biol Cell*. **11**(9), 2999-3012.

118

[162] Zhang, H., Sun, C., Glogauer, M., Bokoch, G. M. (2009) Human neutrophils coordinate chemotaxis by differential activation of Rac1 and Rac2. *J Immunol*. **183**(4), 2718-2728. doi:10.4049/jimmunol.0900849

[163] Weiner, O. D., Servant, G., Welch, M. D., Mitchison, T. J., Sedat, J. W., Bourne, H. R. (1999) Spatial control of actin polymerization during neutrophil chemotaxis. *Nat Cell Biol*. **1**(2), 75-81. doi:10.1038/10042

[164] Pfaff, M., Du, X., Ginsberg, M. H. (1999) Calpain cleavage of integrin beta cytoplasmic domains. *FEBS Lett*. **460**(1), 17-22.

[165] Tzima, E., Del Pozo, M. A., Kiosses, W. B., Mohamed, S. A., Li, S., Chien, S., Schwartz, M. A. (2002) Activation of Rac1 by shear stress in endothelial cells mediates both cytoskeletal reorganization and effects on gene expression. *EMBO J*. **21**(24), 6791-6800.

[166] Tzima, E. (2006) Role of small GTPases in endothelial cytoskeletal dynamics and the shear stress response. *Circ Res*. **98**(2), 176-185. doi:10.1161/01.RES.0000200162.94463.d7

[167] Berk, B. C., Min, W., Yan, C., Surapisitchat, J., Liu, Y., Hoefen, R. (2002) Atheroprotective Mechanisms Activated by Fluid Shear Stress in Endothelial Cells. *Drug News Perspect*. **15**(3), 133-139.

[168] Traub, O., Berk, B. C. (1998) Laminar shear stress: mechanisms by which endothelial cells transduce an atheroprotective force. *Arterioscler Thromb Vasc Biol*. **18**(5), 677-685.

[169] Zen, K., Guo, Y. L., Li, L. M., Bian, Z., Zhang, C. Y., Liu, Y. (2011) Cleavage of the CD11b extracellular domain by the leukocyte serprocidins is critical for neutrophil detachment during chemotaxis. *Blood*. **117**(18), 4885-4894. doi:10.1182/blood-2010-05-287722

[170] DeLano, F. A., Schmid-Schonbein, G. W. (2004) Enhancement of glucocorticoid and mineralocorticoid receptor density in the microcirculation of the spontaneously hypertensive rat. *Microcirculation*. **11**(1), 69-78.

[171] Sutanto, W., Oitzl, M. S., Rots, N. Y., Schobitz, B., Van den Berg, D. T., Van Dijken, H. H., Mos, J., Cools, A. R., Tilders, F. J., Koolhaas, J. M., et al. (1992) Corticosteroid receptor plasticity in the central nervous system of various rat models. *Endocr Regul*. **26**(3), 111-118.

[172] Day, A. P., Bellavia, S., Jones, O. T., Stansbie, D. (1997) Effect of simvastatin therapy on cell membrane cholesterol content and membrane function as assessed by polymorphonuclear cell NADPH oxidase activity. *Ann Clin Biochem*. **34 (Pt 3)**, 269-275.

[173] Tailor, A., Granger, D. N. (2004) Hypercholesterolemia promotes leukocyte-dependent platelet adhesion in murine postcapillary venules. *Microcirculation*. **11**(7), 597-603. doi:10.1080/10739680490503393

[174] Mori, N., Horie, Y., Gerritsen, M. E., Granger, D. N. (1999) Ischemia-reperfusion induced microvascular responses in LDL-receptor -/- mice. *Am J Physiol*. **276**(5 Pt 2), H1647-1654.

[175] Stokes, K. Y., Clanton, E. C., Russell, J. M., Ross, C. R., Granger, D. N. (2001) NAD(P)H oxidase-derived superoxide mediates hypercholesterolemia-induced leukocyte-endothelial cell adhesion. *Circ Res*. **88**(5), 499-505.

[176] Ishibashi, S., Brown, M. S., Goldstein, J. L., Gerard, R. D., Hammer, R. E., Herz, J. (1993) Hypercholesterolemia in low density lipoprotein receptor knockout mice and its reversal by adenovirus-mediated gene delivery. *J Clin Invest*. **92**(2), 883-893. doi:10.1172/JCI116663

[177] Lichtenstein, I. H., Zaleski, E. M., MacGregor, R. R. (1987) Neutrophil dysfunction in the rabbit model of spur cell anemia. *J Leukoc Biol*. **42**(2), 156-162.

[178] Mangiacapra, F., De Bruyne, B., Peace, A. J., Melikian, N., Wijns, W., Barbato, E. (2012) High cholesterol levels are associated with coronary microvascular dysfunction. *J Cardiovasc Med (Hagerstown)*. **13**(7), 439-442. doi:10.2459/JCM.0b013e328351725a

[179] Stapleton, P. A., Goodwill, A. G., James, M. E., Brock, R. W., Frisbee, J. C. (2010) Hypercholesterolemia and microvascular dysfunction: interventional strategies. *J Inflamm (Lond)*. **7**, 54. doi:10.1186/1476-9255-7-54

[180] Carden, D. L., Smith, J. K., Korthuis, R. J. (1990) Neutrophil-mediated microvascular dysfunction in postischemic canine skeletal muscle. Role of granulocyte adherence. *Circ Res*. **66**(5), 1436-1444.

[181] Granger, D. N., Stokes, K. Y., Shigematsu, T., Cerwinka, W. H., Tailor, A., Krieglstein, C. F. (2001) Splanchnic ischaemia-reperfusion injury: mechanistic insights provided by mutant mice. *Acta Physiol Scand*. **173**(1), 83-91. doi:10.1046/j.1365-201X.2001.00888.x

[182] Kakkar, A. K., Lefer, D. J. (2004) Leukocyte and endothelial adhesion molecule studies in knockout mice. *Curr Opin Pharmacol*. **4**(2), 154-158. doi:10.1016/j.coph.2004.01.003

[183] Schmid-Schonbein, G. W., Usami, S., Skalak, R., Chien, S. (1980) The interaction of leukocytes and erythrocytes in capillary and postcapillary vessels. *Microvasc Res*. **19**(1), 45-70.

[184] Worthen, G. S., Schwab, B., 3rd, Elson, E. L., Downey, G. P. (1989) Mechanics of stimulated neutrophils: cell stiffening induces retention in capillaries. *Science*. **245**(4914), 183-186.

Personal information:

Name: **Michael Laurence Akenhead**

Education:

08/2012 – present	PhD candidate, Department of Biomedical Engineering, University of Kentucky, Lexington, KY
08/2008 – 05/2012	BSE (*Cum Laude*), Biomedical Engineering, Vanderbilt University, Nashville, TN

Previous Internships:

Summer, 2012	Biotrain 2012 summer intern, EGEN Inc. at HudsonAlpha, Huntsville, AL
Summer, 2011	National Nanotechnology Infrastructure Network (NNIN) 2011 summer intern, Washington University in St. Louis, St. Louis, MO
Summer, 2010	National Science Foundation REU 2010 summer intern, The Mayo Clinic, Rochester, MN
Summer 2009	NASA Undergraduate Student Research Program (USRP) 2009 summer intern, John C. Stennis Space Center, Hancock County, MS

Outreach Activities:

2015 – 2016	Supervisor for a high school student as part of a Math and Science Technology Center (MSTC) program for Paul L. Dunbar High School
2014 – 2015	Supervisor to four undergraduate students belonging to two different laboratory research programs
2013 – 2015	Student mentor to engineering student volunteer researchers during each college semester
2013 – 2015	Student mentor to a summer REU engineering student
2013 – 2014	Supervisor for a high school student as part of a Math and Science Technology Center (MSTC) program for Paul L. Dunbar High School
2013	Supervisor for two teachers working on a project for a four-week High School Teachers Fellowship Program

Honors/Certifications:

2015	Most Outstanding Graduate Student, Biomedical Engineering, University of Kentucky
2013	Golden Key Honour Society, University of Kentucky
2013 – 2014	Secretary position, University of Kentucky BMES
2012	Fundamentals of Engineering examination passed
2012	Order of the Engineer, Vanderbilt University
2011	Tau Beta Pi, Vanderbilt University

Awards:

2016 – present	Research Assistantship, University of Kentucky
2013 – 2015	Conference travel support for oral presentations, University of Kentucky
2015 – 2016	Max Steckler Fellowship, University of Kentucky
2014 – 2015	Graduate School Academic Year Fellowship, University of Kentucky
2013 – 2014	Kentucky Opportunity Fellowship, University of Kentucky
2012 – 2013	Integrative Graduate Education and Research Traineeship (IGERT) funding, University of Kentucky

Professional Organizations:

2012 – present	Biomedical Engineering Society, University of Kentucky
2013 – present	American Institute of Chemical Engineers (AIChE), University of Kentucky

Publications:

Peer-Reviewed Journal:

1. Akenhead, M.L; Horrall, N.M; Rowe, D.M; Sethu, P; Shin, H.Y. 2015. "In Vitro Evaluation of the Link Between Cell Activation State and its Rheological Impact on the Microscale Flow of Neutrophil Suspensions." *Journal of Biomechanical Engineering*. 137(9): 1 – 10.

2. Akenhead, M.L; Zhang, X; Shin, H.Y. 2014. "Characterization of the shear stress regulation of CD18 surface expression by HL60-derived neutrophil-like cells." *Biomechanics and Modeling in Mechanobiology*. 13(4): 861 – 870.

123

Book Chapters:

1. Akenhead, M.L; Shin, H.Y. 2015. "The Contribution of Cell Surface Components to the Neutrophil Mechanosensitivity to Shear Stresses." *AIMS Biophysics*. 2(3): 318 – 335.

2. Akenhead, M.L; Zhang, X; Shin, H.Y. 2014. "Impaired Neutrophil Mechanoregulation: a Potential Contributing Factor for Microvascular Dysfunction in Obesity." In: *Studies in Mechanobiology, Tissue Engineering, and Biomaterials: the Mechanobiology of Obesity and Related Diseases*. Gefen, A. and Benayahu, D. (ed.), Springer-Verlag, Berlin, Germany. 16:203 – 232.

Conference Abstracts/Presentations:

1. Akenhead, M.L; Zhao, M; Rateri, D; Daugherty, A; Yu, G; Shin, H.Y. "The effects of extracellular cholesterol elevations and membrane fluidity changes on the fluid shear stress control of Mac1-dependent neutrophil adhesion." Abstract/TALK accepted for presentation at the *11th Annual CCTS Spring Conference* in Lexington, KY (4/2016)

2. Akenhead, M.L; Branham, Z.C; Shin, H.Y. "Linking the Cathepsin B-Mediated Cleavage of Mac-1 Integrins to the Control of Neutrophil Adhesion by Fluid Shear Stress." Abstract/TALK accepted for presentation at the *2015 BMES Annual Meeting* in Tampa, FL (10/2015)

3. Akenhead, M.L; Shin, H.Y. "Investigating the Effects of Hypercholesterolemia on the Anti-Inflammatory Regulation of Neutrophil Mac-1-Dependent Adhesivity by Shear Stress." Abstract/POSTER accepted for presentation at the *2015 Gill Heart Institute Cardiovascular Research Day* in Lexington, KY (10/2015)

4. Akenhead, M.L; Zhang, X; Shin, H.Y. "An Ongoing Investigation to Link Cathepsin B-Mediated Cleavage of Mac-1 Integrins to the Shear-Induced Regulation of Neutrophil Adhesivity." Abstract/POSTER presented at the *10th Annual CCTS Spring Conference* in Lexington, KY (03/2015). Poster was awarded 3rd place out of all posters in the School of Engineering.

5. Akenhead, M.L; Shin, H.Y. "The Role Of Cathepsin B In The Control Of Neutrophil Pseudopod Activity." Abstract/TALK accepted for presentation at the *2014 BMES Annual Meeting* in San Antonio, TX (10/2014)

6. <u>Akenhead, M.L</u>; Shin, H.Y. "Connecting Cathepsin B-Mediated Cleavage of CD18 Integrins to the Regulation of Neutrophil Adhesion by Fluid Shear Stress." Abstract/POSTER presented at the *2014 Gill Heart Institute Cardiovascular Research Day* in Lexington, KY (10/2014)

7. <u>Akenhead, M.L</u>; Zhang, X; Shin, H.Y. "Exploring HL60-Derived Neutrophilic Cells as a Potential Culture Model of Shear Stress Regulated CD18 Surface Expression." Abstract/POSTER presented at the *9th Annual CCTS Spring Conference* in Lexington, KY (03/2014)

8. <u>Akenhead, M.L</u>; Zhang, X; Shin, H.Y. "Evaluating the Use of HL60-Derived Neutrophilic Cells to Examine the Molecular Dynamics of the Regulation of CD18 Surface Expression by Shear Stress Exposure." Abstract/TALK presented at the *2013 AIChE Annual Meeting* in San Francisco, CA (11/2013)

9. <u>Akenhead, M.L</u>; Zhang, X; Shin, H.Y. "Exploring HL60-Derived Neutrophilic Cells as a Potential Culture Model of Shear Stress Regulated CD18 Surface Expression." Abstract/POSTER presented at the *2013 Gill Heart Institute Cardiovascular Research Day* in Lexington, KY (10/2013)

10. <u>Akenhead, M.L</u>; Zhang, X; Horrall, N.M; Shin, H.Y. "Validating the Use of HL60-Derived Neutrophilic Cells to Examine Cathepsin B Release Dynamics Under Shear Stress Exposure." Abstract/POSTER presented at the *8th Annual CCTS Spring Conference* in Lexington, KY (04/2013)

11. <u>Akenhead, M.L</u>. "RNA Amplification and Secretion Technology (RAST) for Secreting shRNA." Abstract/POSTER presented at the *2012 HudsonAlpha Biotrain Poster Session* in Huntsville, AL (08/2012)